

THE SEVERITY OF *CRYPTOCOCCUS NEOFORMANS* INFECTION IN FC GAMMA RECEPTOR  
IIB DEFICIENT MICE



A Dissertation Submitted in Partial Fulfillment of the Requirements  
for the Degree of Doctor of Philosophy in Medical Microbiology  
Medical Microbiology, Interdisciplinary Program  
Graduate School  
Chulalongkorn University  
Academic Year 2018  
Copyright of Chulalongkorn University

ความรุนแรงของการติดเชื้อ *Cryptococcus neoformans* ในหนูทดลองที่ขาดตัวรับ  
ชนิด Fc gamma Receptor IIb



วิทยานิพนธ์นี้เป็นส่วนหนึ่งของการศึกษาตามหลักสูตรปริญญาวิทยาศาสตรดุษฎีบัณฑิต  
สาขาวิชาจุลชีววิทยาทางการแพทย์ สหสาขาวิชาจุลชีววิทยาทางการแพทย์  
บัณฑิตวิทยาลัย จุฬาลงกรณ์มหาวิทยาลัย  
ปีการศึกษา 2561  
ลิขสิทธิ์ของจุฬาลงกรณ์มหาวิทยาลัย

Thesis Title THE SEVERITY OF *CRYPTOCOCCUS NEOFORMANS* INFECTION  
IN FC GAMMA RECEPTOR IIB DEFICIENT MICE

By Miss Saowapha Surawut

Field of Study Medical Microbiology

Thesis Advisor Associate Professor Ariya Chindamporn, Ph.D.

Thesis Co Advisor Associate Professor Tanapat Palaga, Ph.D.  
Assistant Professor Asada Leelahavanichkul, M.D., Ph. D.

---

Accepted by the Graduate School, Chulalongkorn University in Partial Fulfillment  
of the Requirement for the Doctor of Philosophy

..... Dean of the Graduate School  
(Associate Professor Thumnoon Nhujak, Ph.D.)

DISSERTATION COMMITTEE

..... Chairman  
(Professor Nattiya Hirankarn, M.D., Ph. D.)

..... Thesis Advisor  
(Associate Professor Ariya Chindamporn, Ph.D.)

..... Thesis Co-Advisor  
(Associate Professor Tanapat Palaga, Ph.D.)

..... Thesis Co-Advisor  
(Assistant Professor Asada Leelahavanichkul, M.D., Ph. D.)

..... Examiner  
(Rangsim Reantragoon, M.D., Ph. D.)

..... Examiner  
(Assistant Professor Patcharee Ritprajak, D.D.S., Ph.D.)

..... External Examiner  
(Prapaporn Pisitkun, M.D.)

เสาวภา สุราวุธ : ความรุนแรงของการติดเชื้อ *Cryptococcus neoformans* ในหนูทดลองที่ขาดตัวรับ

ชนิด Fc gamma Receptor IIb. (

THE SEVERITY OF *CRYPTOCOCCUS NEOFORMANS* INFECTION IN FC GAMMA RECEPTOR IIB DEFICIENT MICE) อ.ที่

ปรึกษาหลัก : รศ. ดร.อริยา จินตามพร, อ.ที่ปรึกษาร่วม : รศ. ดร.ธนาภัทร ปาลกะ, ผศ. ดร. นพ.อัษฎาศ ลีหวนนิชกุล

*Cryptococcus neoformans* เป็นเชื้อสาเหตุของโรคเยื่อหุ้มสมองอักเสบ (cryptococcal meningitis หรือ cryptococcosis) โดยติดเชื้อจากการหายใจเอาสปอร์เข้าสู่ปอด เชื้อชนิดนี้เป็นเชื้อยีสต์ที่มีแคปซูลล้อมรอบ มีความสามารถในการเพิ่มจำนวนและอยู่รอดได้ภายในเซลล์แมคโครฟาจ รวมถึงการแฝงตัวอยู่ในเซลล์แมคโครฟาจแล้วใช้เป็นพาหะในการเคลื่อนย้ายเชื้อไปสู่อวัยวะเป้าหมายอื่น ๆ เรียกกระบวนการนี้ว่า Trojan horse ดังนั้นเซลล์แมคโครฟาจซึ่งมีความสามารถในการจับกินเชื้อโรคด้วยกระบวนการ phagocytosis จึงมีความสำคัญต่อระบบภูมิคุ้มกันในการก่อโรค cryptococcosis โดยส่วนใหญ่โรคนี้นั้นพบได้ในผู้ที่มีภูมิคุ้มกันร่างกายบกพร่องเช่น ในผู้ป่วยที่ติดเชื้อไวรัสเอดส์และมีจำนวนเซลล์เม็ดเลือดขาวชนิด CD4 T cell ต่ำ ด้วยเหตุนี้ CD4 T cell จึงเป็นเซลล์ระบบภูมิคุ้มกันอีกเซลล์หนึ่งที่มีความสำคัญต่อการเกิดโรคนี้อย่างไรก็ตามมีรายงานพบว่าผู้ที่มีภูมิคุ้มกันปกติก็สามารถที่จะเป็นโรคนี้อีกได้และมีจำนวนรายงานเพิ่มมากขึ้น นอกจากนี้ยังมีรายงานว่า การเกิด polymorphism ในส่วนของยีน Fc gamma receptor IIb มีความเกี่ยวข้องกับความเสี่ยงต่อการเป็นโรค cryptococcosis โดย FcγRIIb เป็นตัวรับส่วน Fc ของ immunoglobulin G ทำหน้าที่ส่งสัญญาณยับยั้งภายในเซลล์ควบคุมกระบวนการทำงานของเซลล์ชนิดนั้นๆ และเนื่องจากแมคโครฟาจเป็นเซลล์ของระบบภูมิคุ้มกันที่มีบทบาทในการควบคุมโรค cryptococcosis เราจึงมีสมมติฐานว่า เซลล์แมคโครฟาจที่สูญเสียการทำงานของ FcγRIIb มีผลต่อการเพิ่มความรุนแรงของโรค cryptococcosis ในการศึกษาครั้งนี้ได้ศึกษาความรุนแรงของโรค โดยฉีด *C. neoformans* ในหนูที่ขาดตัวรับชนิด FcγRIIb (FcγRIIb<sup>-/-</sup>) และในกลุ่มควบคุมซึ่งเป็นหนูปกติ พบว่าหนู FcγRIIb<sup>-/-</sup> มีอัตราการตายสูงกว่าหนูปกติและแสดงความรุนแรงของโรคมกกว่าอย่างมีนัยสำคัญ โดยพบจำนวนเชื้อที่แพร่กระจายในแต่ละอวัยวะมากกว่า อีกทั้งยังแสดงพยาธิสภาพในอวัยวะต่าง ๆ มากกว่าอีกด้วย นอกจากนี้ยังพบสารน้ำ cytokine ชนิด TNF-α และ IL-6 มากกว่าในหนูปกติอย่างมีนัยสำคัญเช่นเดียวกัน โดยเมื่อทำการศึกษาน้ำที่ของเซลล์แมคโครฟาจที่ขาดตัวรับชนิด FcγRIIb (FcγRIIb<sup>-/-</sup> macrophage) ในหลอดทดลอง พบว่า FcγRIIb<sup>-/-</sup> macrophage มีความสามารถในการจับกินเชื้อ *C. neoformans* ได้มากขึ้นเมื่อเทียบกับเซลล์แมคโครฟาจปกติ แต่ความสามารถในการฆ่าเชื้อ ไม่มีความแตกต่างกัน อีกทั้งยังพบว่ามีสารน้ำ cytokine ชนิด TNF-α และ IL-6 ได้มากกว่าเซลล์ปกติด้วย เมื่อทำการศึกษาในหนูทดลองด้วยการฉีดเชื้อ *C. neoformans* เพื่อให้เกิดกระบวนการ phagocytosis ก่อน แล้วจึงทำลายเซลล์แมคโครฟาจด้วยการฉีด clodronate-liposome พบว่าหนู FcγRIIb<sup>-/-</sup> มีการแพร่กระจายของเชื้อลดลง นอกจากนี้ยังพบว่าในหนูปกติที่ถูกฉีดด้วย FcγRIIb<sup>-/-</sup> macrophage ที่ติดเชื้อแล้ว มีการแพร่กระจายของเชื้อไปยังอวัยวะต่าง ๆ มากกว่าหนูปกติที่ถูกฉีดด้วยเซลล์แมคโครฟาจปกติที่ติดเชื้ออย่างมีนัยสำคัญ โดยเมื่อทำการศึกษาประชากรของเซลล์เม็ดเลือดขาวชนิด T cell และการสร้าง IFN-γ พบว่าหนู FcγRIIb<sup>-/-</sup> มีจำนวน CD4 T cell และการสร้าง IFN-γ ไม่น้อยไปกว่าในหนูปกติ จึงสามารถอธิบายได้ว่า การที่หนู FcγRIIb<sup>-/-</sup> มีความรุนแรงของโรค cryptococcosis มากกว่านั้น เนื่องมาจากเซลล์แมคโครฟาจในหนูชนิดนี้มีความสามารถในการจับกินเชื้อ *C. neoformans* ได้มากกว่าปกติเพราะขาดตัวรับชนิด FcγRIIb จึงทำให้ขาดสัญญาณยับยั้ง ส่งผลให้เซลล์แมคโครฟาจมีการติดเชื้อภายในเซลล์จำนวนมาก และพาเชื้อไปยังส่วนต่าง ๆ ของร่างกายโดยกระบวนการ Trojan horse อีกทั้งการที่เซลล์นี้หลั่งสารน้ำ cytokine ดังกล่าวมากขึ้น จึงทำให้เกิดความรุนแรงของโรค cryptococcosis ในหนู FcγRIIb<sup>-/-</sup> มากกว่าในหนูปกติ ดังนั้นการสูญเสียการทำงานของ FcγRIIb จึงเป็นปัจจัยเสี่ยงหนึ่งต่อการเกิดโรค cryptococcosis

สาขาวิชา จุลชีววิทยาทางการแพทย์

ปีการศึกษา 2561

ลายมือชื่อนิสิต .....

ลายมือชื่อ อ.ที่ปรึกษาหลัก .....

ลายมือชื่อ อ.ที่ปรึกษาร่วม .....

ลายมือชื่อ อ.ที่ปรึกษาร่วม .....

# # 5687864220 : MAJOR MEDICAL MICROBIOLOGY

KEYWORD: Fc gamma receptor IIb, *Cryptococcus neoformans*, Macrophage

Saowapha

Surawut

:

THE SEVERITY OF *CRYPTOCOCCUS NEOFORMANS* INFECTION IN FC GAMMA RECEPTOR IIB DEFICIENT MICE.

Advisor: Assoc. Prof. Ariya Chindamporn, Ph.D. Co-advisor: Assoc. Prof. Tanapat Palaga, Ph.D., Asst. Prof. Asada

Leelahavanichkul, M.D., Ph. D.

*Cryptococcus neoformans*, an encapsulated yeast commonly infecting the central nervous system, refers to as cryptococcal meningitis or cryptococcosis is commonly found in Thailand. *C. neoformans* is able to replicate, survive inside host macrophages, evade from the cells and use macrophages as a vehicle to disseminate to the target organs, a mechanism known as Trojan horse. Therefore, the containment of *C. neoformans* in phagocytic cell is important for host protective immunity. Cryptococcosis is common in immunocompromised host such as in patients with low CD4+ T helper cells in HIV-infection and patients taking immunosuppressive drugs. However, the incidence of cryptococcosis in healthy individual (HIV-uninfected) is increasing. Interestingly, it was reported that dysfunctional FcγRIIb polymorphisms are associated with cryptococcosis susceptibility. FcγRIIb is the only inhibitory receptor among the family of FcγRs. FcγRIIb activation leads to suppress of phagocytic activity and reduces cytokine production. Because macrophage is important immune cells against cryptococcosis, we hypothesized that dysfunctional FcγRIIb may influence cryptococcosis susceptibility through the alteration of macrophages functions. We investigated cryptococcosis in the FcγRIIb<sup>-/-</sup> mouse. Mortality after intravenous *C. neoformans*-induced cryptococcosis FcγRIIb<sup>-/-</sup> mice was higher than in age-matched wild-types. Severe cryptococcosis in the FcγRIIb<sup>-/-</sup> mice was demonstrated by high fungal burdens in the internal organs with histological cryptococcoma-like lesions and high levels of TNF-α and IL-6, but not IL-10. Interestingly, FcγRIIb<sup>-/-</sup> macrophages demonstrated more prominent phagocytosis but did not differ in killing activity *in vitro* or the production of TNF-α, IL-6 and IL-10 levels, compared to wild-type cells. Indeed, *in vivo* macrophage depletion with liposomal clodronate attenuated the fungal burdens in FcγRIIb<sup>-/-</sup> mice, but not wild-type mice. Upon transferring to wild-type mice, FcγRIIb<sup>-/-</sup> macrophages with phagocytosed *Cryptococcus* resulted in higher fungal burdens than FcγRIIb<sup>+/+</sup> macrophages with phagocytosed *Cryptococcus*. Moreover, the T cell subpopulation analysis and IFN-γ intracellular staining suggested that cryptococcosis severity in FcγRIIb<sup>-/-</sup> mice did not cause by T helper cell defect. These results support, at least in part, a model whereby, in FcγRIIb<sup>-/-</sup> mice, enhanced *C. neoformans* transmigration occurs through infected macrophages. In summary, prominent phagocytosis, with limited effective killing activity, and high pro-inflammatory cytokine production by FcγRIIb<sup>-/-</sup> macrophages were correlated with more severe cryptococcosis in FcγRIIb<sup>-/-</sup> mice. In clinical translation, we propose FcγRIIb loss-of-function- polymorphisms as a new risk factor for cryptococcosis.

Field of Study: Medical Microbiology

Student's Signature .....

Academic Year: 2018

Advisor's Signature .....

Co-advisor's Signature .....

Co-advisor's Signature .....

## ACKNOWLEDGEMENTS

I would like to express my deepest gratitude and appreciation to my advisor, Associate Professor Ariya Chindamporn, Ph.D. for her support and encouragement throughout the period of this study.

I would like to extend my gratitude to my co-advisors, Assistant Professor Asada Leelahavanichkul, MD. Ph.D., for his advice, kind suggestion, guidance, support, and encouragement; Associate Professor Tanapat Palaga, Ph.D. for his excellent advice, indispensable help, kind suggestion and support throughout this study.

I am very grateful to the members of my thesis committee of their helpful advice, constructive criticism and correction for the completeness for this thesis.

I would like to thank the Mycology Unit, Center of Excellence in Immunology and Immune-Mediated Diseases and the 90th Anniversary of Chulalongkorn University, Rachadapisek Sompote Fund.

I wish to thank the staffs of Department of Microbiology, Faculty of Medicine, Chulalongkorn University, for their friendship, help in the laboratory and support during my study.

Finally, I am deeply indebted to my family for their love, help, encouragement, understanding, and support during this study.

จุฬาลงกรณ์มหาวิทยาลัย  
CHULALONGKORN UNIVERSITY

Saowapha Surawut

## TABLE OF CONTENTS

	Page
.....	iii
ABSTRACT (THAI).....	iii
.....	iv
ABSTRACT (ENGLISH).....	iv
ACKNOWLEDGEMENTS.....	v
TABLE OF CONTENTS.....	vi
LIST OF TABLES.....	viii
LIST OF FIGURES.....	ix
CHAPTER I INTRODUCTION.....	1
CHAPTER II OBJECTIVES.....	5
CHAPTER III LITERATURE REVIEW.....	7
1. Cryptococcosis.....	7
2. Immunity to cryptococcosis.....	11
3. Evidences of intracellular proliferation of <i>C. neoformans</i> .....	14
4. The intracellular life cycle of <i>C. neoformans</i> .....	15
5. Importance of intracellular life-cycle of <i>C. neoformans</i> toward disease virulence .....	19
6. Genetic susceptibility to cryptococcosis.....	23
7. Fc gamma Receptor.....	24
8. Fc $\gamma$ RIIb and microbial infection.....	28
9. Systemic Lupus Erythematosus (SLE) and infection.....	30

CHAPTER IV MATERIALS AND METHODS .....	34
CHAPTER V RESULTS.....	43
CHAPTER VI DISCUSSION .....	90
CHAPTER VII CONCLUSION.....	96
REFERENCES .....	98
APPENDIX.....	121
APPENDIX A MATERIALS AND EQUIPMENT .....	121
APPENDIX B MOUSE GENOTYPING .....	125
APPENDIX C ANTI-DOUBLE STRAND DNA PRODUCTION IN MICE .....	128
APPENDIX D THE HISTOLOGY STAINING.....	130
APPENDIX E BONE MARROW DERIVED MACROPHAGE.....	132
APPENDIX F SPLENOCYTES ISOLATION .....	135
APPENDIX G CULTURE MEDIA .....	136
APPENDIX H CELL VIABILITY BY MTT ASSAY.....	137
VITA.....	138



## LIST OF TABLES

	Page
Table 1. Role of immune components in mouse model of cryptococcosis.....	13
Table 2. Fc $\gamma$ RIIb $-/-$ mice with microbial infection model.....	30



## LIST OF FIGURES

	Page
Figure 1. Cryptococcus neoformans with capsule surrounding by india ink preparation under microscope (400x) .....	8
Figure 2. The relationships and nomenclature of pathogenic Cryptococcus species (42).....	8
Figure 3 .Cryptococcal pathogenesis (42).....	10
Figure 4. The recognition of Cryptococcus neoformans by immune cells. FcR, Fc receptor; MR, mannose receptor; TLR, toll-like receptor (116).....	16
Figure 5. The virulence of clinical isolates of C. neoformans was assessed by flow cytometry following interaction with macrophages (153).....	20
Figure 6. Interactions of C. neoformans with phagocyte and cryptococcal dissemination cross the blood–brain barrier (158).....	22
Figure 7. The family of Fc gamma receptor (165).....	26
Figure 8. Schematic representation of an activating and inhibitory Fc gamma receptor (167).....	27
Figure 9.Characteristics of Fc $\gamma$ R11b <sup>-/-</sup> mice at 8- and 24-weeks-old as demonstrated by serum creatinine (Scr) (A), proteinuria by urine protein creatinine index (UPCI) (B) and anti-dsDNA (C), (n=4/group). The data are shown as the mean $\pm$ SE. * p<0.05, ** p<0.01.....	44
Figure 10. Percent survival in 8-wk-old Fc $\gamma$ R11b <sup>-/-</sup> and wild-type mice after challenged with C. neoformans (n=7/group).....	45
Figure 11. Organ fungal burdens from 8-wk-old Fc $\gamma$ R11b <sup>+/+</sup> and Fc $\gamma$ R11b <sup>-/-</sup> mice after challenged with C. neoformans at moribund stage (n=3-6/group). The data are shown as the mean $\pm$ SE. * p<0.05.....	46

- Figure 12. Representative histology with H&E (hematoxylin and eosin staining) at 100x magnification from 8-week-old mice in the moribund stage after *C. neoformans* administration. Fc $\gamma$ R11b+/+ mice (left column); Fc $\gamma$ R11b-/- mice (right column)..... 47
- Figure 13. Histology scoring of 8 week-old mice after challenged with *C. neoformans* at moribund stage. The data are shown as the mean  $\pm$  SE. \* p<0.05, \*\* p<0.01..... 48
- Figure 14. Organ injury and inflammatory cytokines at the moribund stage in 8-week-old as demonstrated by serum creatinine (Scr) (A), alanine transaminase (ALT) (B), TNF- $\alpha$  (C), IL-6 (D) and IL-10 (E) levels. The data are shown as the mean  $\pm$  SE. \* p<0.05, \*\* p<0.01..... 50
- Figure 15. Fungal burdens in the internal organs of 8-week-old mice at 2 weeks post-*C. neoformans* administration. The data are shown as the mean  $\pm$  SE (n = 4-5/group). \* p<0.05..... 51
- Figure 16. Organ histology with Grocott's silver staining (GMS) at 200x magnification from 8 week-old mice at 2 weeks post-*C. neoformans* infection, demonstrating cryptococcoma-like lesions in the brain and kidney of Fc $\gamma$ R11b+/+ mice (left column), and in several internal organs (brain, kidneys, liver, lung and spleen) of Fc $\gamma$ R11b-/- mice (right column). ..... 52
- Figure 17. Histology scoring of 8 week-old mice at 2 weeks post-*C. neoformans* infection. The data are shown as the mean  $\pm$  SE (n = 4-5/group). \* p<0.05, \*\* p<0.01. .... 53
- Figure 18. Serum cytokines measured include TNF- $\alpha$  (A), IL-6 (B) and IL-10 (C). The data are shown as the mean  $\pm$  SE (n = 4-5/group). \* p<0.05. .... 54
- Figure 19. Representative results from flow cytometry with anti-F4/80 and anti-CD11b antibodies in Fc $\gamma$ R11b+/+ (A) and Fc $\gamma$ R11b-/- (B) macrophages. .... 56
- Figure 20. Representative figure of macrophage with Diff-Quick staining after engulf of *C. neoformans* by phagocytosis mechanism ..... 57
- Figure 21. Percentage of macrophages (M $\Phi$ ) demonstrating phagocytosis (A) and the average number of phagocytosed fungi per M $\Phi$  (total number of phagocytosed

fungi/ total M $\Phi$ ) after incubation with <i>C. neoformans</i> at ratios of fungi:M $\Phi$ of 5:1 and 10:1 (B). * $p < 0.05$ , ** $p < 0.01$ (experiments were performed in triplicate).....	58
Figure 22. The total killing ability (extruded and intracellular yeast) (A) and intracellular proliferation (concerning only intracellular yeast; see methods) (B) of M $\Phi$ determined by the number of <i>C. neoformans</i> colonies after incubation with M $\Phi$ from wild-type and Fc $\gamma$ R11b $^{-/-}$ mice are shown. ....	59
Figure 23. Cytokine levels (TNF- $\alpha$ , IL-6 and IL-10) in the supernatant media from macrophages of Fc $\gamma$ R11b $^{+/+}$ or Fc $\gamma$ R11b $^{-/-}$ mice after activation with heat-killed (A-C) or live <i>C. neoformans</i> (D-F) are shown. * $p < 0.05$ , ** $p < 0.01$ (experiments were performed in triplicate). ....	61
Figure 24 .Timeline of a model for cryptococcosis in liposomal clodronate-induced macrophage depletion in 8-week-old Fc $\gamma$ R11b $^{+/+}$ and Fc $\gamma$ R11b $^{-/-}$ mice. ....	63
Figure 25. Representative immunohistochemistry analysis of macrophages stained with anti-F4/80 from Fc $\gamma$ R11b $^{+/+}$ and Fc $\gamma$ R11b $^{-/-}$ with and without clodronate administration is shown. Only spleens and kidneys were selected as representative organs and red-brown is anti-F4/80 antibodies binding with macrophage. ....	64
Figure 26. Fungal burdens of cryptococcosis in liposomal clodronate-induced macrophage depletion in 8-week-old Fc $\gamma$ R11b $^{+/+}$ and Fc $\gamma$ R11b $^{-/-}$ mice in brain (A), kidney (B), liver (C), lung (D) and spleen (E) are shown (n = 4-5/group). Data are shown as the mean $\pm$ SE. * $p < 0.05$ , ** $p < 0.01$ . ....	66
Figure 27. Organ fungal burdens of Fc $\gamma$ R11b $^{+/+}$ mice at 24 h after infusion of <i>Cryptococcus</i> -containing macrophages (infected macrophages) from Fc $\gamma$ R11b $^{+/+}$ and Fc $\gamma$ R11b $^{-/-}$ mice are shown. (n = 4-5/group). Data are shown as the mean $\pm$ SE. * $p < 0.05$ , ** $p < 0.01$ . ....	67
Figure 28. Percent survival in 24-wk-old Fc $\gamma$ R11b $^{-/-}$ and wild-type mice after challenged with <i>C. neoformans</i> (n = 9-10/group). * $p < 0.05$ . ....	68
Figure 29. Organ fungal burdens from 24-wk-old Fc $\gamma$ R11b $^{+/+}$ and Fc $\gamma$ R11b $^{-/-}$ mice after challenged with <i>C. neoformans</i> at moribund stage (n = 4-5/group). * $p < 0.05$ . ....	68

Figure 30. Representative histology with H&E (hematoxylin and eosin staining) at 100x magnification from 24-week-old mice in the moribund stage after <i>C. neoformans</i> administration. Fc $\gamma$ R11b+/+ mice (left column); Fc $\gamma$ R11b-/- mice (right column).....	69
Figure 31. Histology scoring of 24-week-old mice after challenged with <i>C. neoformans</i> at moribund stage. The data are shown as the mean $\pm$ SE (n = 4-5/group). * p<0.05, ** p<0.01. ....	70
Figure 32. Organ injury and inflammatory cytokines at the moribund stage in 24-week-old as demonstrated by serum creatinine (Scr) (A), alanine transaminase (ALT) (B), TNF- $\alpha$ (C), IL-6 (D) and IL-10 (E) levels. The data are shown as the mean $\pm$ SE (n=4-5/group). * p<0.05. ....	72
Figure 33. Fungal burdens in the internal organs of 24-week-old mice at 2 weeks post- <i>C. neoformans</i> administration. The data are shown as the mean $\pm$ SE (n = 4-5/group). * p<0.05. ....	72
Figure 34. Organ histology with Grocott's silver staining (GMS) at 200x magnification from 24 week-old mice at 2 weeks post- <i>C. neoformans</i> infection, demonstrating cryptococcoma-like lesions in the brain and kidney of Fc $\gamma$ R11b+/+ mice (left column), and in several internal organs (brain, kidneys, liver, lung and spleen) of Fc $\gamma$ R11b-/- mice (right column). ....	73
Figure 35. Histology scoring of 24 week-old mice at 2 weeks post- <i>C. neoformans</i> infection. The data are shown as the mean $\pm$ SE (n = 4-5/group). * p<0.05, ** p<0.01. ....	74
Figure 36. Serum cytokines measured include TNF- $\alpha$ (A), IL-6 (B) and IL-10 (C). The data are shown as the mean $\pm$ SE (n = 4-5/group). * p<0.05. ....	75
Figure 37. The representative result of total number of Th cell (CD3+CD4+CD8-) from spleen of wild-type (Fc $\gamma$ R11b+/+) and Fc $\gamma$ R11b-/- mice by flow cytometry (n=4/group) .....	76

Figure 38. The representative result of naive Th cell (CD44-CD62L+), central memory Th cell (Tcm, CD44+CD62L+), effector Th cell (Tem, CD44+CD62L-) from spleen of wild-type (Fc $\gamma$ R11b+/+) and Fc $\gamma$ R11b-/- mice by flow cytometry (n=4/group). .....	77
Figure 39. The representative result of activated Th cell (CD4+CD69+) from spleen of wild-type (Fc $\gamma$ R11b+/+) and Fc $\gamma$ R11b-/- mice by flow cytometry (n=4/group). .....	77
Figure 40. The spleen analysis for total of Th cell (CD3+CD4+CD8-), naive Th cell (CD44-CD62L+), central memory Th cell (Tcm, CD44+CD62L+), effector Th cell (Tem, CD44+CD62L-) and activated Th cell (CD4+CD69+) from wild-type (Fc $\gamma$ R11b+/+) and Fc $\gamma$ R11b-/- mice by flow cytometry (n=4/group). Data are shown as the mean $\pm$ SE. * p<0.05, ** p<0.01.....	78
Figure 41. The representative result of an intracellular IFN- $\gamma$ of Th cell (CD3+CD4+IFN $\gamma$ +) from spleen of wild-type (Fc $\gamma$ R11b+/+) and Fc $\gamma$ R11b-/- mice by flow cytometry (n=4/group). .....	79
Figure 42. The spleen analysis for an intracellular IFN- $\gamma$ of Th cell (CD3+CD4+IFN $\gamma$ +) from wild-type (Fc $\gamma$ R11b+/+) and Fc $\gamma$ R11b-/- mice by flow cytometry (n=4/group). Data are shown as the mean $\pm$ SE. * p<0.05. ....	79
Figure 43. The severity of cryptococcosis in pristane, Fc $\gamma$ R11b-/- and wild-type mice as determined by the mortality rate (A), fungal burdens in the internal organs (B), area of the fungal infection in the internal organs from Grocott's silver staining (GMS) (C) and serum cytokines (IL-6, TNF- $\alpha$ and IL-10; D-F) were demonstrated. (n= 8-10/group in A and 5-6/ group in B-F); *, p<0.05 vs. wild-type; #, p<0.001 vs. wild-type; $\Phi$ , p<0.05; $\Phi\Phi$ , p<0.01 .....	81
Figure 44. Representative organ histology with Grocott's silver staining (GMS) at 200x magnification from 6-month-old mice at 2 weeks post-C. neoformans infection, demonstrating tumor-like lesions in brain of the wild-type mice (left column), and in several internal organs (brain, kidneys, liver, lung and spleen) of pristane (middle column) and Fc $\gamma$ R11b-/- mice (right column).....	82

- Figure 45. The phagocytosis as determined by fluorescent-conjugated fungi (A) and live-fungi (B) with the killing activity (B) of macrophage in the response against *C. neoformans* were demonstrated (experiments were performed in triplicate)..... 84
- Figure 46. The analysis of spleen from wild-type, pristane and Fc $\gamma$ R11b $^{-/-}$  mice by flow cytometry demonstrated total Th cell (CD3 $^{+}$ CD4 $^{+}$ CD8 $^{-}$ ) (A), naïve Th cell (CD44 $^{-}$ CD62L $^{+}$ ) (B), central memory Th cell (CD44 $^{+}$ CD62L $^{+}$ ) (C), effector Th cell (CD44 $^{+}$ CD62L $^{-}$ ) (D), activated Th cell (CD4 $^{+}$ CD69 $^{+}$ ) (E) and Th cell with inducible T cell co-stimulator (CD4 $^{+}$ ICOS $^{+}$ ) (F) (n=4-6/group). In addition, the intra-cellular IFN- $\gamma$  of Th cell was also demonstrated (G) (n=4-6/group). IFN, interferon ..... 86
- Figure 47. The analysis of serum cytokines, in panels, from wild-type, pristane and Fc $\gamma$ R11b $^{-/-}$  mice by a Luminex-based multiplex method was demonstrated (n=5-7/group). IL, interleukin; MCP-1, monocyte chemoattractant protein-1; GM-CSF, granulocyte-macrophage colony stimulating factor; IFN, interferon..... 88
- Figure 48. The analysis of spleen from wild-type, pristane and Fc $\gamma$ R11b $^{-/-}$  mice after 2 week of the administration by phosphate buffer saline control (uninfected) or *C. neoformans* (CN-infected) with flow cytometry demonstrated activated Th cell (CD4 $^{+}$ CD69 $^{+}$ ) (A), Th cell with inducible T cell co-stimulator (CD4 $^{+}$ ICOS $^{+}$ ) (B) and Th cell with intra-cellular IFN- $\gamma$  (n=5-7/group). IFN, interferon; \*, p<0.05 vs. wild-type; #, p<0.001 vs. wild-type;  $\Phi$ , p<0.05;  $\Phi\Phi$ , p<0.01;  $\delta$ , p<0.05. .... 89

## CHAPTER I

### INTRODUCTION

Cryptococcosis caused by *Cryptococcus neoformans* or *Cryptococcus gattii*. This disease is an opportunistic fungal infection, especially in HIV-infected patients due to CD4 T cell deficiency with more than 950,000 cases and 625,000 deaths per year (1, 2). A major form of this disease is cryptococcal meningitis and usually caused by *C. neoformans*. The natural reservoirs of the genus *Cryptococcus* are in feces dropping of pigeon and in some big tree which could be found throughout Thailand. Normally, the pathogenesis of the disease is initiated by spore inhalation from the environment. Subsequently, yeast could reside in the lung in the granuloma form without clinical symptoms as known as the latent stage or could progress into infectious stage with disseminated-form or target-organ (brain) infection in immunocompromised or immunocompetent hosts, respectively (3).

Polysaccharide capsule is the major virulence factor of *C. neoformans* (4) and the main capsule component is glucuronoxylomannan (GXM) that inhibits macrophage phagocytosis and enhances *C. neoformans* virulence (5). Additionally, *C. neoformans* is able to replicate inside host macrophages and evades from the cells to several target organs as known as “intracellular parasitism” (6). As such, *C. neoformans* could invade blood brain barrier by this property. Interestingly, in lung, *C. neoformans* interacts with alveolar macrophages and reside/multiply within the macrophages (7). Depletion of alveolar macrophages in mice improve survival and delays cryptococcal dissemination, suggesting that alveolar macrophage promote fungal growth and dissemination (8). Recent evidence by Trojan horse mouse model with *C. neoformans* suggested that this pathogen can invade to the brain by monocytes/macrophage act as the carrier (9). Therefore, monocytes/macrophages play an important role in *C. neoformans* pathogenesis.

Interestingly, the incidence of cryptococcosis is increasing in non-HIV patients and *C. gattii* is most frequently described as an etiologic agent of cryptococcosis in patients with HIV seronegative (10, 11), however, *C. neoformans* var. *grubii* also caused



cryptococcosis in patients with HIV seronegative without underlying disease (12, 13). Therefore, the factors that associated with infection susceptibility in such patients are under investigation.

Host genetic background maybe associated with disease susceptibility because gene polymorphisms can affect the host in response to infection. However, small amount of evidences has been reported for this hypothesis (14). The increase susceptibility to cryptococcosis in patients with Fc gamma receptor (Fc $\gamma$ R) polymorphisms have previously been reported (14-17). Fc $\gamma$ R1a 131H/R polymorphism results in amino acid change from histidine (H) to arginine (R) at 131 position and high Fc $\gamma$ R1a 131H expression in macrophages demonstrated the higher phagocytosis activity without the effective killing activity (18, 19). Nevertheless, there was no association between the risk of cryptococcosis and Fc $\gamma$ R1a 131H/R polymorphism in either HIV-infected or non-HIV infected populations (15, 17). In Fc $\gamma$ R1a 158F/V polymorphism results in amino acid substitution of phenylalanine (F) to valine (V) at position 158. Both non HIV-infected (16) and HIV-infected individuals (15) with Fc $\gamma$ R1a 158V polymorphism shows the higher risk of cryptococcosis with more effective phagocytosis and lead to fungal dissemination (14, 15). Recently, in the Chinese population, an association between Fc $\gamma$ R1b polymorphism and cryptococcal meningitis was demonstrated (17). Therefore, Fc $\gamma$ R1b polymorphism maybe result in their functional deficiency lead to easy to infection and disease progression.

Fc $\gamma$ R1b is a receptor for Fc portion of immunoglobulin G and is the only inhibitory receptor among other Fc $\gamma$ Rs. The suppression of phagocytosis and inflammatory cytokine production are demonstrated after Fc $\gamma$ R1b activation. This receptor presents on B cell, macrophages, neutrophils and mast cells, but not on T or NK cells (20). There are some evidences that described the association between Fc $\gamma$ R1b and infection by bacteria, parasite and virus (21-30). Claworthy et al. hypothesized that people with the Fc $\gamma$ R1b polymorphisms are less susceptible to malaria which supported by *Plasmodium* spp. infection in Fc $\gamma$ R1b<sup>-/-</sup> mice is less severe than wildtype due to the enhanced phagocytosis of *Plasmodium falciparum* (21). Fc $\gamma$ R1b<sup>-/-</sup> show enhanced *Mycobacterium tuberculosis* clearance, attenuate disease severity and increase T helper1 cell response in comparison with wildtype (23). In the study of

*Staphylococcus aureus* infection model, FcγRIIb<sup>-/-</sup> mice were enhance protection against a primary infection with *S. aureus* by increase survival rate, IL-10 level and increase phagocytosis in granulocyte and monocytes as compared to control mice (22). In contrast to previous model, FcγRIIb<sup>-/-</sup> mice preconditioning with pneumococcal vaccine before challenging with *Streptococcus pneumoniae*, an encapsulated gram positive bacteria, resulting in the prominent cytokine production and the more severe sepsis compare with wildtype (25). These evidences suggested that the susceptibility and severity of infection in FcγRIIb deficiency as described in FcγRIIb<sup>-/-</sup> mouse model reveal different results depends on the specific organisms. Meanwhile, the FcγRIIb polymorphisms or deficiency showed less susceptible to some infection, the case series in Chinese patients found that FcγRIIb polymorphisms are more susceptible to cryptococcosis (17).

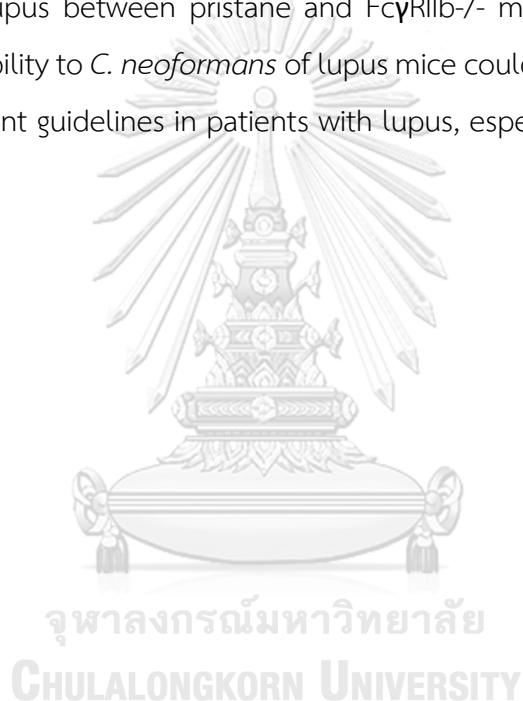
In addition, because FcγRIIb<sup>-/-</sup> mice are established as a lupus mouse model that prone to spontaneous systemic lupus erythematosus (SLE) or lupus (31). However, systemic lupus erythematosus (SLE) is the critical autoimmune diseases with multiple-organ involvement induced by genetics and environmental factors (32, 33). Despite the prominent immune activation against self-antigens in lupus, the defect of immune response against several organisms is reported, even before the era of immunosuppressive therapy (34). While the mechanisms of immunosuppressive therapy induced the susceptibility to infection in patients with SLE have been reported (35), the physiology responsible for spontaneous immunosuppression in lupus is still unclear. As such, insufficient complement component and an immune exhaustion have been mentioned as proposed mechanisms (34, 36).

Interestingly, cryptococcosis is a common systemic fungal infection found in patients with lupus in endemic areas (17) and the defect of inhibitory signaling in FcγRIIb<sup>-/-</sup> mice enhances immune activation, protects from several organisms but induces autoimmune responses (21, 23). However, FcγRIIb dysfunction is not the only mechanism responsible for lupus. Thus, susceptibility against cryptococcosis in another cause of lupus (environmental factor) is interesting.

Indeed, pristane-induced lupus model represents SLE from environmental activation with normal genetic background which is different from genetic-defect

induced lupus of FcγRIIb-/- mice. A single peritoneal injection of pristane (2, 6, 10, 14-tetramethylpentadecane), a hydrocarbon substance derived from shark liver oil, causes chronic peritoneal inflammation and induces lupus characteristics (37).

Therefore, we hypothesized that FcγRIIb associated with cryptococcosis susceptibility by alteration of FcγRIIb-/- macrophages function. We then compared the disease severity against *C. neoformans* in FcγRIIb-/- mice without symptomatic of lupus and wildtype counterpart to determine role of FcγRIIb function and cryptococcal pathogenesis. Subsequently, we also investigated disease severity in mice with symptomatic of lupus between pristane and FcγRIIb-/- mouse models. Information regarding susceptibility to *C. neoformans* of lupus mice could be helpful for developing clinical management guidelines in patients with lupus, especially in endemic areas.



## CHAPTER II

### OBJECTIVES

#### Objectives of this study

1. To determine the severity of *C. neoformans* infection in FcγRIIb<sup>-/-</sup> and wildtype mice without symptomatic of lupus.
2. To characterize the FcγRIIb<sup>-/-</sup> macrophage function in responding to *C. neoformans*.
3. To investigate the severity of *C. neoformans* infection in FcγRIIb<sup>-/-</sup> and pristane mice with symptomatic of lupus.

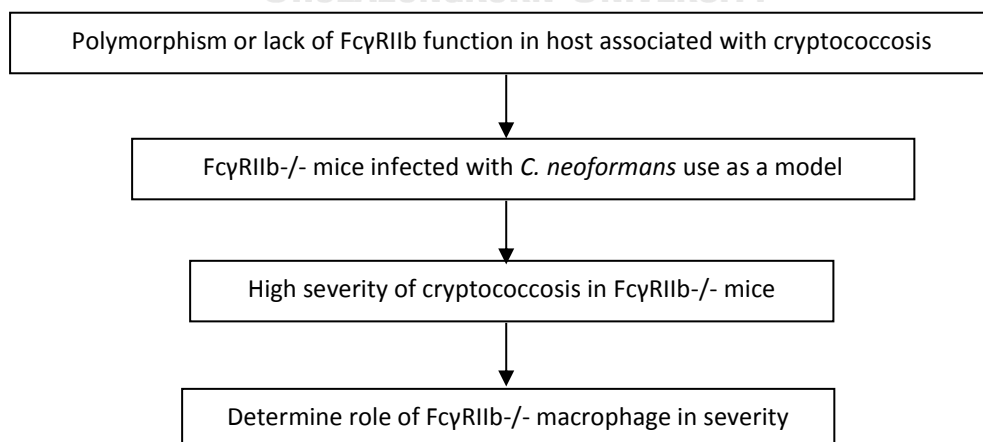
#### Research questions

1. Does cryptococcosis in FcγRIIb<sup>-/-</sup> mice show the higher severity in comparison with wildtype?
2. Does cryptococcosis severity in FcγRIIb<sup>-/-</sup> mice associated with macrophage function?

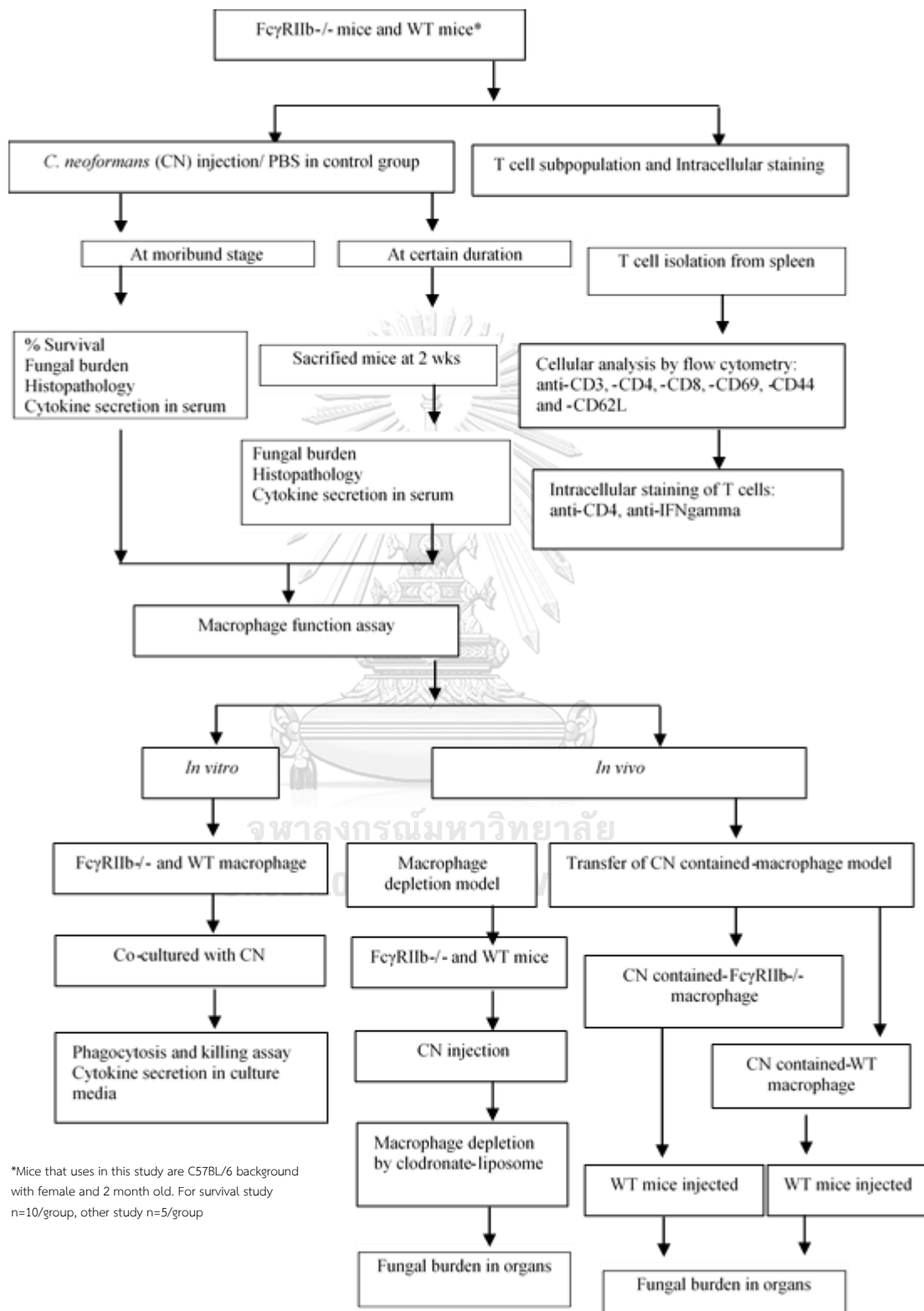
#### Hypothesis

Severe cryptococcosis in FcγRIIb<sup>-/-</sup> mice associated with the alteration of macrophage function.

#### Conceptual framework



## Methodology Workflow



## CHAPTER III

### LITERATURE REVIEW

#### 1. Cryptococcosis

##### 1.1 Etiologic agent

Cryptococcosis caused by encapsulated budding yeast belonging to the fungal genus *Cryptococcus* (Figure 1). *Cryptococcus neoformans* and *Cryptococcus gattii* are frequently found to be a causative agent in human disease (38). These pathogens are classified in variety depend on capsule antigen and each variety consist of different serotype. *C. neoformans* var. *grubii* (serotype A), *C. neoformans* var. *neoformans* (serotype D), a hybrid type of *C. neoformans* (serotype AD,) and *C. gattii* consist of serotype B and C. In addition, the PCR-restriction fragment length polymorphism of *URA5* gene divided *C. neoformans* and *C. gattii* into eight molecular types, VNI to VNIV and VGI to VGIV, respectively (Figure 2). Cryptococcosis is an opportunistic fungal infection; especially in HIV-infected patient. In immunocompromised host, *C. neoformans* var. *grubii* is a major cause of this disease (39, 40). However, *C. gattii* is the most frequently described as an etiologic agent of cryptococcosis in HIV-uninfected patients (10, 11). In addition, *C. neoformans* var. *grubii* also caused cryptococcosis in HIV-uninfected patient without underlying disease in Vietnam (12, 13). Moreover, cryptococcosis in HIV-uninfected patient of China found that the most of causative agents were *C. neoformans* (from 84 patients) with only 1 *C. gattii* (41).



Figure 1. *Cryptococcus neoformans* with capsule surrounding by india ink preparation under microscope (400x)

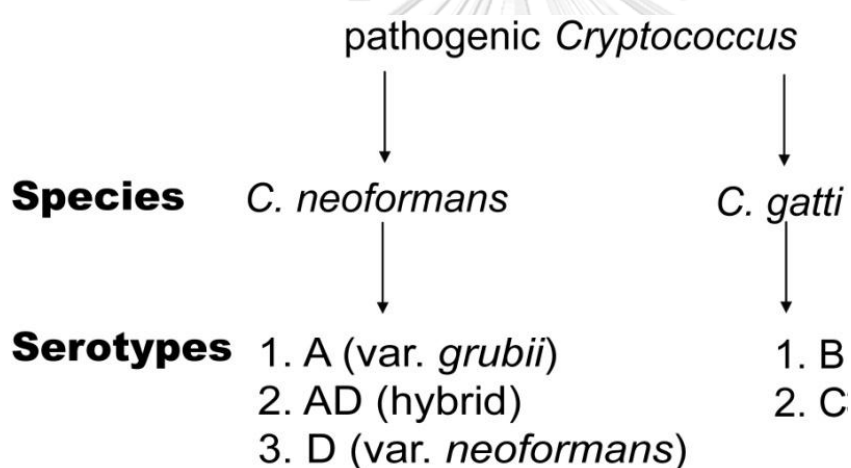


Figure 2. The relationships and nomenclature of pathogenic *Cryptococcus* species (42).

### 1.2 Prevalence and Epidemiology

Before HIV/AIDS epidemic (1980s), cryptococcosis was found in less than 200 cases world-wide (43). In 2009, there was patients with cryptococcosis more than 950,000 cases with 625,000 deaths per year (2) and a major form of this disease is cryptococcal meningitis.

The high incident of cryptococcosis in HIV-infected patient with low CD4 T cells suggested that T cells are major component in host defense against *Cryptococcus neoformans*. However, not only CD4 T cells deficiency but also the importance of

other factors has been reported such as immunosuppressive drug (44), TNF- $\alpha$  inhibitor (adalimumab) (45), pregnancy (46), liver disease (47), genetic causes (48, 49) and anti-GM-CSF autoantibody is also associated with cryptococcal meningitis in healthy individual (50). The studies of cryptococcosis in HIV-uninfected people have been previously reported (10). In China, cryptococcal meningitis in HIV-uninfected patient more cases than in HIV-infected (41). In HIV-uninfected patients, not only cryptococcal meningitis was a major form of clinical manifestation but also found in disseminated cryptococcosis(51). Moreover, cryptococcal meningitis in HIV-uninfected patients revealed high mortality than in HIV-infection (52).

### **1.3 Pathogenesis**

The natural reservoir of the genus *Cryptococcus* is pigeon feces and Eukalyptus tree which could be found throughout Thailand. Cryptococcal infection could be demonstrated locally as Cryptococcal meningitis or presented in a disseminated form as refer to generalized cryptococcosis. Normally, the pathogenesis of the disease is initiated by spore or desiccated yeast cells inhalation from the environment. In most, yeast could reside in the lung in the granuloma form without clinical symptoms as known as the latent stage. However, in some hosts with underlying immune impairment, the latent stage could progresses into disease stage with disseminated-form or target-organ (brain) infection in immunocompromise or immunocompetent hosts, respectively (Figure 3) (3).



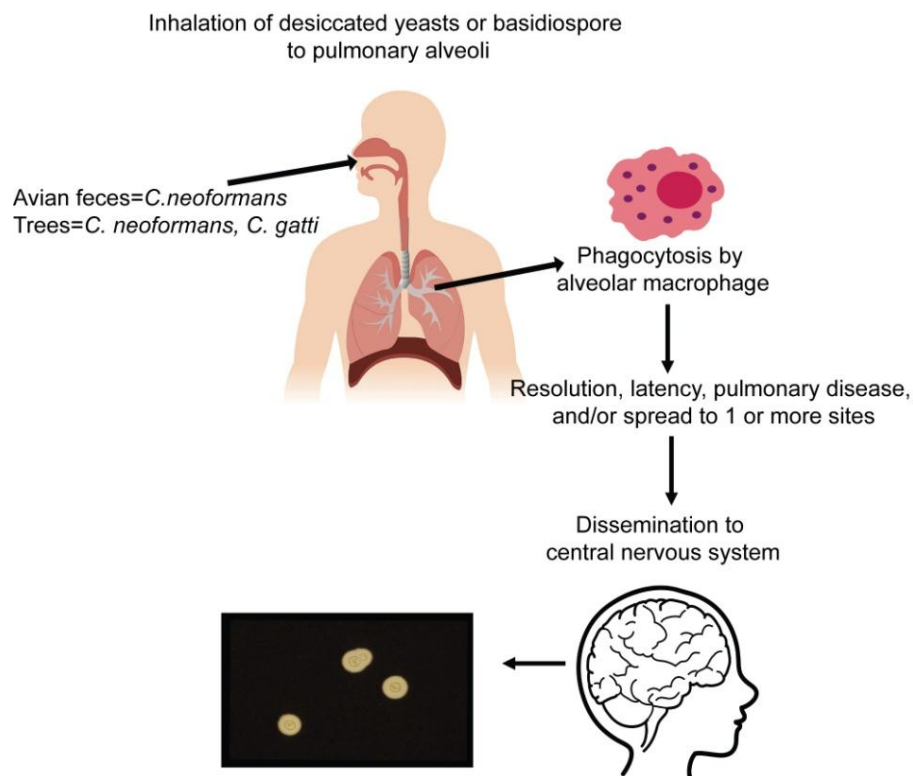


Figure 3 .Cryptococcal pathogenesis (42).

#### 1.4 Virulence factor

The virulence factor of *Cryptococcus neoformans* include growth at 37 °C, melanin pigment production, enzymes secretion (phospholipase B and urease) and polysaccharide capsule have been previous described. Among these factors, the polysaccharide capsule is the major virulence factor for *C. neoformans* infection. There are many evidences suggesting that capsule is important in normal hosts defense because the capsule consists of glucuronoxylomannan (GXM) which have many effects in host immune responses (such as phagocytosis inhibition). In addition, fungal containment in phagocyte is another critical factor for cryptococcal control of host defense mechanisms. Therefore, abnormal function of macrophages or phagocytes against GXM enhances the virulence of *C. neoformans* and their pathogenesis. Moreover, this yeast pathogen could be replicated and survived inside phagocytic cell (6, 53). Subsequently, it can live and disseminate both inside and outside of phagocyte, so this characteristic uses to explain how to *C. neoformans* can enter to bloodstream and central nervous system (CNS).

## 2. Immunity to cryptococcosis

Several fungal species disseminated worldwide but only some species can cause diseases in human (54). Only some fungi can survive at human body temperatures (55) including *Cryptococcus neoformans*, most fungi could not infect in immunocompetent host. Hence, cryptococcosis increases after HIV endemic and immunosuppressive drug use. The normal immunity is enough to protect to cryptococcosis but some of healthy individual are infected with this pathogen and developed this disease. Therefore, the risk factors of cryptococcosis in immunocompetent is interesting. The serological test found that 80 percentages of children in urban environments were infected with *C. neoformans* without clinical manifestations (56, 57). The initiation process of infection is the inhalation of spores (or desiccated yeast) from environment into lungs (58). Subsequently, yeast cells interact with alveolar macrophage or dendritic cell results in immune activation, fungal clearance or restriction of infection within a granuloma that composed of mononuclear phagocytes, histiocytes, and multinucleated giant cells surrounding the yeast cells (59).

The mouse model for cryptococcosis studies provide several evidences associated with immunity to cryptococcosis as shown in table 1. The protective immunity to control *C. neoformans* requires a balance of both T helper (Th) 1 and Th2 responses (60-62). The study by depletion of cytokines suggested that Th1 response is essential to control cryptococcal infection. Actually, different mouse strains reveal different susceptibility that correlate with balance of Th1/Th2 (63) and the presence of C5 complement activation (64). Depletion of interferon gamma (IFN- $\gamma$ ) and interleukin 12 (IL-12) (Th1 cytokines) enhances mouse mortality rate (65, 66), whereas loss of Th2 cytokines increases mouse survival (67).

Moreover, the unbalance of Th1/Th2 cytokine affect both granuloma composition and fungal burdens (68). The predominant Th1 response improves mouse survival but too much Th1 response cannot prevent brain dissemination (69-72). As such, Th2 component is also essential for the effective immune response. The loss of tumor necrosis factor  $\alpha$  (TNF- $\alpha$ ), major cytokine of Th1, does not affect mouse survival, but TNF- $\alpha$  administration attenuates the disease severity (73). In addition, Th17 also

plays an important role for mucosal immunity against fungi (74). But Th17 depletion does not affect the disease outcome or the efficiency of vaccination (75).

Macrophages play an important role for controlling of cryptococcal infection. In mice, alveolar macrophage depletion increases survival rate and reduces cryptococcal dissemination, suggesting that alveolar macrophages promote fungal dissemination (8). But the depletion in rat shows an opposite result (76), suggesting the different interaction between *C. neoformans* and differences host. Both classical and alternative macrophage activation are found in cryptococcosis mouse model (69). And the granulomatous reaction may be associated with cryptococcosis host defense (77). In mice, either excessive eosinophils or neutrophils is correlated with non- efficiency to control cryptococcal infection (78, 79).

The active or passive antibody activation can trigger significant cryptococcal protection (80). However, humoral immunity against cryptococcosis might be not sufficient (80) despite the effective *C. neoformans* immunization (81-83). The immunization with capsular manno-proteins increase mouse survival (81). The constructive activation of IFN- $\gamma$  (a strong Th1-type cytokine) from modified *C. neoformans* strain (75, 84-86) is resulting in the complete protection (85). Currently, there is a consensus agreement that host immunity against cryptococcosis depends on an appropriate collaboration of Th1 cells with macrophages.

*C. neoformans* have an advantage property to evade the internalization by macrophage. The evasion mechanisms are either capsule dependent or capsule independent. The capsule-dependent evasion mechanism is phagocytosis inhibition by capsule (87). The capsule-free mutant strain result in phagocytosis resistance (88) suggesting the important role in diminishing epitope recognition (87). In addition, binding of capsular polysaccharide to toll-like receptors 2, 4 and CD14 resulting in TNF- $\alpha$  inhibition (89). The Fas ligand expression on macrophages was induced by the fungi leads to cell apoptosis (90). In parallel, several capsule-independent mechanisms have been mentioned. Secreted anti-phagocytic protein 1 (App1) bind to complement receptor2 and 3 (CR2 and CR3) inhibits the complement-mediated opsonization (91). Due to these evasion mechanisms, both non-phagocytosed and phagocytosed *C. neoformans* can be survived in host.

Table 1. Role of immune components in mouse model of cryptococcosis

Immune component	Infection route	Result compared with wild-type when immune component removed	References
TLR2	i.p.	Decreased survival	(92)
TLR4	i.p.	No or limited effect	(92, 93)
TLR9	i.n.	Decreased survival	(94)
C3	i.v.	Decreased survival	(95)
C5	i.v.	Decreased survival	(64)
CD36	i.v.	Decreased survival	(96)
Dectin-1	i.v.	No effect	(97)
Mannose receptor	i.n.	Decreased survival	(98)
B cell	i.v.	No effect	(99)
Macrophage	i.v.	Decreased survival	(100)
Macrophage/dendritic	i.t., i.v.	Decreased survival	(83)
Neutrophils	i.t.	Increased survival	(78)
Eosinophils	i.t., i.n.	Increased survival	(77, 79)
CD4+ T cells	i.t.	Decreased survival	(62, 101)
CD8+ T cells	i.v.	Decreased survival	(62, 102)
IFN- $\gamma$	i.v., i.t.	Decreased survival	(65, 102)
TNF- $\alpha$	i.t.	No effect	(73)
IL-12	i.v.	Decreased survival	(67)
IL-18	i.n., i.t.	Decreased survival	(94, 103)
IL-4	i.v.	Increased survival	(67)
IL-13	i.n.	Increased survival	(104)
IL-17	i.n.	Important for early response	(75)
IL-6	i.v.	Earlier death	(105)
IL-10	i.v.	Decreased survival	(105)

i.n.: intranasal; i.p.: intraperitoneal; i.t.: intratrachea; i.v.: intravenous

### 3. Evidences of intracellular proliferation of *C. neoformans*

Cryptococcomas (yeast cell inside the granulomas) are found in autopsies with histopathological examination (59, 106-108) and in mouse model (109). Cryptococcal granulomas show the less inflammatory response than the granulomas of tuberculosis (caused by *Mycobacterium tuberculosis*), suggesting that a dormant stage and controllable of cryptococci., *C. neoformans* found in cytoplasm of giant cells or macrophages in granulomas, while they are found both inside and outside of the cell in the absence of granulomas (108). CD4 T cells are demonstrated in the lesion of immunocompetent host and in animal models [rats (109), mice (110, 111), and rabbits (112)]. In mouse model, *C. neoformans* is rapidly ingested by phagocytes and found intracellular and extracellular yeast cell during the first 24 h (111). At day 7, the intracellular yeast was found with formation of granulomas. At day 28, most yeast cells were found within multinucleated giant cells. In this model, the budding index of intracellular was higher than extracellular, lead to hypothesize that *C. neoformans* prefer intracellular growth. Therefore, both early infection and long-term persistence, this yeast cell involved with macrophages, these indicated the importance of intracellular life-cycle of *C. neoformans* within macrophage (111).

In animal model, fungal survival within macrophages allows the fungus to persist in tissue. In *C. neoformans* infection model, rats are more resistant than mice, but both rat and mice have provided contrast results. Rat is resistant to cryptococcosis with a more effective macrophage killing activity via increased production of lysozyme and reactive oxygen species (ROS) (76, 109). In rat, *C. neoformans* resistance is associated with a strong Th1 response with sufficient Th2 component (68). To control the infection, rat develop granulomas containing eosinophils however rats with an excessive Th1 response develop more inflammatory granulomas with central necrosis and caseation. Prominent extracellular yeast presented in early phase of the infection and increased intracellular yeast with reduced fungal burden is found after granuloma formation (113). Moreover, the evidence that macrophage depletion prevents *C. neoformans* dissemination into mouse brain has been described (8, 9).

Therefore, macrophages are essential for cryptococcosis especially for brain dissemination. As such, *C. neoformans* prefer growth within murine macrophages

because they can be survived within acidic environments of phagosome. A mutate *C. neoformans* that survived only intracellular environment still shows the virulent in natural killer and T cell depleted mice, indicating that yeast virulence occurs from the intracellular compartment (8). In addition, depletion of alveolar macrophages delayed mouse death, supporting the idea that the macrophages are a niche for intracellular survival of *C. neoformans* (8).

#### 4. The intracellular life cycle of *C. neoformans*

##### 4.1 Fungal entry and recognition

The  $\alpha$ -glucans,  $\beta$ -glucans, and chitin are fungal cell wall composition and are recognized by pattern recognition receptors (PRR) that found on the immune cells. However, fungal capsules polysaccharide has an antiphagocytic property to prevent phagocytosis. Without opsonin, there is no effective phagocytosis of this fungus. Because acapsular *C. neoformans* strain is easily ingested via complement receptors and/or  $\beta$ -glucan receptors (114). Therefore, capsule hides out most of the fungal PRR ligands resulting in decreased phagocytosis activity of immune cells (115, 116) (Figure 4). Actually, antibody and complement as opsonin are essential for the effective phagocytosis, *in vitro* (117).

*C. neoformans* are rapidly ingested due to the opsonin *in vivo*. Mice with complement-deficiency are highly susceptible to cryptococcal infection (64, 95). On the other hand, *C. neoformans* spores are no capsule, so their surfaces expose more  $\beta$ -glucans than the yeasts cell surfaces. Therefore, if spores act as infectious particles, Dectin-1 and other  $\beta$ -glucan PRR may be easily activated (8) and resulting in rapid ingestion. The PRRs of *C. neoformans* include; Dectin-1, Toll-like receptor 2 (TLR2), Nod like receptors and several scavenger receptors that could recognize  $\beta$ -glucans of fungal cell wall. Additionally, CD36 and scavenger receptor F1 (SCARF1) are responsible for immune cell binding of *C. neoformans* in the mouse lung (96).

In summary, mannose receptor, complement receptors, CD36, SCARF1, TLR2, and TLR9 are all crucial receptors for *C. neoformans* recognition in lung, and the cross-talk between multiple PRRs is necessary for maximal immune response. However, non-

immune cells might important for *C. neoformans* recognition as IL-8 secretion by epithelial cells has been demonstrated (118).

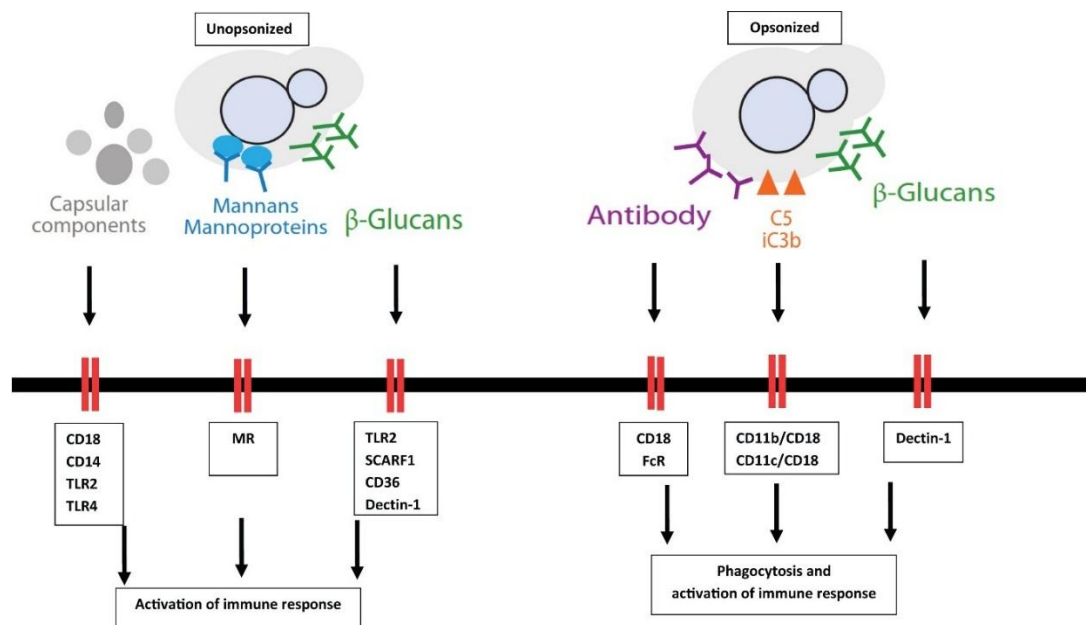


Figure 4. The recognition of *Cryptococcus neoformans* by immune cells. FcR, Fc receptor; MR, mannose receptor; TLR, toll-like receptor (116).

## 4.2 Phagocytosis of *C. neoformans*

Despite anti-phagocytosis properties, the yeast cells are found intra-cellularly of phagocyte after a few hours of infection (111) suggesting the counter effect of this property. Two counter mechanisms are previously explained; i) complement or antibody opsonization (opsonin-dependent phagocytosis) and ii) direct phagocytic receptors against capsules (opsonin-independent phagocytosis).

### 4.2.1 Opsonin-dependent phagocytosis

Both antibody and complement are opsonin for induce phagocytosis of *C. neoformans*. Antibody-mediated phagocytosis involves in binding of Fc portion of antibody to Fc receptor of phagocyte. Several factors affect with the efficiency of antibody-mediated phagocytosis such as the binding patterns and antibody isotypes (119-121). For the complement-mediated phagocytosis, cryptococcal capsule can

activate complement via alternative pathway, results in C3b deposit on capsule (122, 123), that induces phagocytosis via complement receptors (CR) such as CR3 (117, 124). However, some strains of *C. neoformans* cannot be phagocytosed through complement (125). Many evidences suggest that the effective of phagocytosis via complement system depends on the size of capsule (126).

#### **4.2.2 Opsonin-independent phagocytosis (direct interaction of capsule with phagocyte receptor)**

The capsule prevents the interaction between receptors of phagocyte and fungal epitope resulting in phagocytic activity evasion. However, some studies report the interaction of capsule by some receptors. In the IgM mediated phagocytosis, this isotype bind to capsule of *C. neoformans*, rearranges polysaccharide structure and expressed the capsule epitope that is recognizable by complement receptor and CD18 (117). Another study found that Fab fragments not only opsonize encapsulated yeast cell but also inducing the binding of CR3 and capsule (127). In addition, FcγRIIb binds with capsule trigger the inhibitory signals results in unresponsiveness of immunity (90, 128). GXM on capsule binds to toll-like receptors (TLR2, TLR4) and CD14 induces macrophage activation (129). Finally, dendritic cells directly recognize capsule via mannose receptor that could induce *C. neoformans* uptake (128).

#### **4.3 Survival of *C. neoformans* in macrophage**

Phagocytosis mechanism internalized organisms into phagosome and phagosome-lysosome fusion (phagolysosome formation) induces the acidic pH with hydrolytic enzymes to kill pathogens (130).

The intracellular pathogen survives or adapt to the phagolysosome stress-environment. *Cryptococcus neoformans* replicated faster intracellular macrophages than the outside cell (131) despite the acidic pH (132). Surprisingly, increased phagolysosome pH results in reducing of intracellular replication. Therefore, *C. neoformans* prefer growing at intracellular acidic environment. Inositol phosphoryl ceramide synthase-1 mutant of *Cryptococcus neoformans* (acidic pH susceptible strain) reduces the intracellular proliferation property (133). The alteration of the fungal burdens, inside and outside of the host cell, is also demonstrated. Most of the yeasts



are found inside macrophage at 8 h of incubation (8 h) but found mostly outside the cell at 16–24 h (111).

Several mechanisms that allow the pathogen survive inside the host cell, such as inhibiting fusion of phagosome and lysosome. Large phagolysosomes with *C. neoformans* results in phagolysosomes leakage (134, 135) with pore formation observed by electron microscope at phagosome membrane (7). Additionally, intracellular *C. neoformans* reduces nitric oxide production of phagocytic cell (136) that is an important killing mechanisms.

Thus, capsule is the major virulence factor of *C. neoformans* to avoid killing and interfering normal macrophage functions. Several evidences reported that capsule reduces the host immunity in several levels (126) and is required for survival within host cell. As such, the mutant strain without capsule cannot proliferate inside macrophages (111). In addition, laccase enzyme is another factor for avoiding killing activity. The enzyme catalyzes melanin formation on fungal cell wall (137) and melanin (and other anti-oxidant enzymes) protects against reactive nitrogen and oxygen species (138-140). *C. neoformans* mutant strain that lack of laccase shows the less virulence (141).

In summary, *C. neoformans* has several mechanisms include capsule, melanin and anti-oxidant enzymes for resistance against the stress environment resulting in the advantage on survival and replication within macrophage.

#### **4.4 *C. neoformans* and macrophage interaction after phagocytosis**

*C. neoformans* survives and replicates inside the macrophages as previous described. This leads to the several interactions between yeast and macrophage.

##### **4.4.1 Macrophage fusion and division**

While macrophage proliferates with different conditions (142-144), *C. neoformans* acts as a facultative intracellular pathogen and survives intra-cellularly. Unsurprisingly, the division of infected macrophage results in the increase pathogen dissemination and enhances the disease severity (145). Moreover, after macrophages division, *C. neoformans* can accumulates to perform in a larger group of fungi (145).

#### 4.4.2 Expulsion from macrophage (vomocytosis or nonlytic exocytosis)

*C. neoformans* have ability to exit from macrophages which result in an increasing of fungal burden in tissues of host. The several mechanisms that contribute to fungal escape from the macrophage have previous explained. *C. neoformans* causes macrophage-lysis by multiple divisions inside macrophage (5, 53). Or yeasts are able to exit the macrophages without killing the phagocyte (6, 146, 147). This mechanism called vomocytosis or nonlytic exocytosis or extrusion (148). These mechanisms found in macrophage of mice and human. The experiment by real-time imaging show that nonlytic exocytosis depends on viability of yeast (6). Moreover, the opsonization of yeast with monoclonal antibody were more often removed than by complement (6). The phagosome extrusion was not associated with actin rearrangements (6, 146). A recent study show that nonlytic exocytosis is observed using flow cytometry techniques (149), and found in both *in vitro* and *in vivo*.

#### 4.4.3 Lateral transfer by macrophage

The yeast transfer between macrophage and other cells have been described only in live cryptococci (150, 151). Conversely to the extrusion, yeast transfer among macrophages (called lateral transfer) depends on actin rearrangement (151). This event may occur during latent stage and allow the yeast to hide from the protective immune response and from antifungal agents (151).

### 5. Importance of intracellular life-cycle of *C. neoformans* toward disease virulence

Several evidences suggested that *C. neoformans* can avoid macrophages killing. This property is important to the development of cryptococcosis. The studies in several hosts demonstrate that cryptococcosis susceptibility correspondences with intracellular yeast proliferation. Mice are more susceptible to the infection than rats (113). Rat macrophage shows the more antifungal activity than mouse macrophage (76). In addition, different mouse strains have the different cryptococcal susceptibility due to the diverse phagocytosis activity in each strain (63). The susceptibility against *Cryptococcus gattii* also depends on intracellular proliferation that vary in different mouse strains (11).

More importantly, the association of intracellular proliferation and clinical outcome of cryptococcosis is previous described (152). The clinical outcomes such as yeast clearance from cerebral spinal fluid (CSF) is strongly correlated with *in vitro* phagocytic indexes (152). The cryptococcal isolates with high intracellular proliferation results in significantly increased mortality. In contrast, infected patients with the isolates of low intracellular proliferation property shows the lower clinical severity (153) (Figure 5).

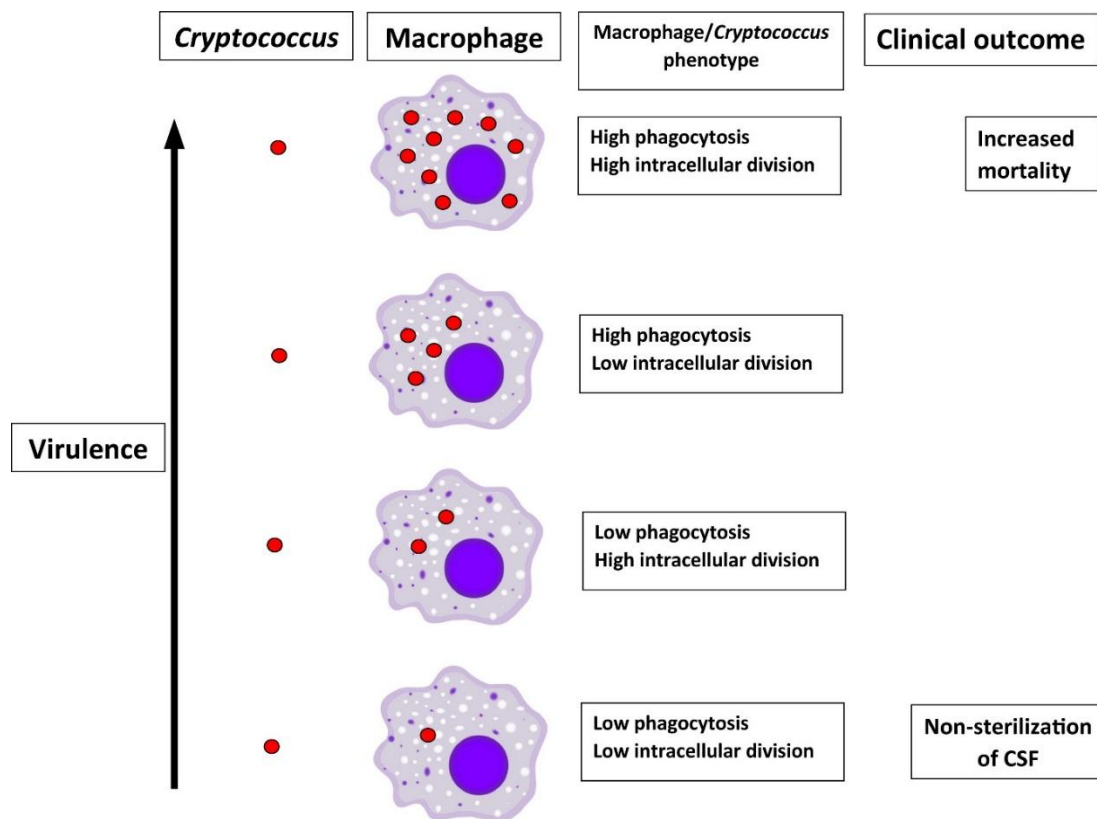


Figure 5. The virulence of clinical isolates of *C. neoformans* was assessed by flow cytometry following interaction with macrophages (153).

### **5.1 Cryptococcal replication and dissemination**

The survival of intracellular and extracellular *C. neoformans* associates with cryptococcosis disease progression. The yeast strains that can replicate inside the host cell associate with the worsen cryptococcosis (8). In mice, the macrophage depletion by clodronate injection results in decrease fungal burdens in lung, but the depletion in rats increases fungal burdens and correlates with the resistance macrophage killing activity. In parallel, clodronate-treated mice decrease fungal burdens in brain (8, 9). These evidences indicated that *C. neoformans* survives and replicates within macrophage and disseminate to other organs by macrophage.

*C. neoformans* can cross blood brain barrier (BBB), an important step of cryptococcal meningitis development, through several mechanisms. The first mechanism associates with individual yeast cell or free yeast cross the biological barriers. The intra-vital microscopy shows that this fungus have ability to pass endothelial cell as refer to “transcytosis” (154). These yeast cells are internalized by endothelial cells and pass through the cell cytoplasm into brain (155).

Another mechanism is crossing BBB by staying inside macrophage as called “Trojan Horse” dissemination model (130, 156). The Trojan Horse theory explained that live yeast cells travel to other organs inside macrophage, avoiding from the immune system (157) (Figure 6). Likewise, mice injected with infected macrophages that contained intracellular *C. neoformans in vitro* results in the higher level of fungal burdens (9, 158).

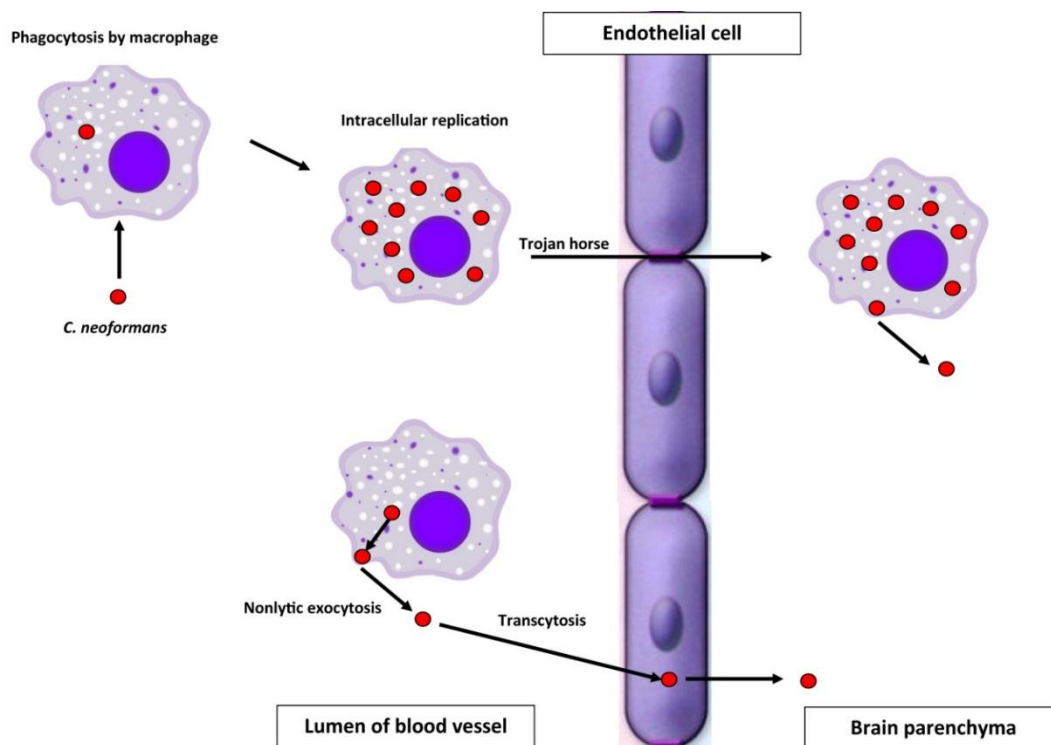


Figure 6. Interactions of *C. neoformans* with phagocyte and cryptococcal dissemination cross the blood–brain barrier (158).

## 5.2 Cryptococcal latency and reactivation

The persistence and development of latent state with asymptomatic manifestation are the important characteristics of *C. neoformans*. The latent state transit to disease state is an important event to development of cryptococcosis in immunosuppression. Factors contribute to the latent state are still unknown. A recent study indicates that this fungus develops the giant cells that resists to stress environment and stay in the host for long time periods (159, 160). Additionally, the ability to survive intracellularly of *C. neoformans* protects the fungi from immune system and antimicrobial agents so that they are dormant in the host. Rats are resistant to cryptococcal infection so they are suitable for the observation of persistent and latent state (76). In early phase of the infection in rat, fungal burdens in lungs increase. At the late phase, the burdens decrease but stay positive for months, without any disease manifestation. In chronic infection in rat, most of yeast cells are found intracellular (epithelium and macrophage) in the latent stage (109). Moreover,

corticosteroid administration results in cryptococcal reactivation in rats (109) that resulting in the increased extracellular fungal burdens (109). In human, latent infection and reactivation can be demonstrated by the detection of cryptococcal antibodies in childhood with the periodical re-activation together with the latent state (56).

## **6. Genetic susceptibility to cryptococcosis**

Although some HIV-infected patients develop cryptococcal disease due to CD4 T cell deficiency, healthy individual can also develop this disease. Therefore, other risk factors might be associated with cryptococcosis. The postulation that host genetic background maybe impacts disease susceptibility because polymorphisms can affect the expression of several genes in host in response to infection. However, small amount of evidences have been reported for this hypothesis (14).

### **6.1 Mannose binding lectin (MBL) polymorphisms**

MBL is a circulating C-type lectin that recognizes glycans on surfaces of microbial pathogen to induce opsonization and complement activation via lectin pathway. The complement activation results in the induction of inflammatory response. MBL is encoded by *mb12* gene with 6 single nucleotide polymorphisms (SNPs) which resulting in MBL deficiency. Indeed, MBL deficiency associates with an increase cryptococcosis susceptibility in HIV-uninfected individuals (161).

### **6.2 Fc gamma receptor polymorphisms**

Fc gamma receptor (Fc $\gamma$ R) is found on surface of the immune cells such as macrophages, neutrophils and B cells. The function of Fc $\gamma$ R is binding to immunoglobulin G (IgG) and triggering the immune response or inflammatory response (162). The association of Fc $\gamma$ R polymorphisms and autoimmune diseases or susceptibility to infections (163, 164), such as cryptococcal infection, have been reported (15-17).

Fc $\gamma$ RIIa 131H/R polymorphism results in amino acid change from histidine (H) to arginine (R) at amino acid of position131. Fc $\gamma$ RIIa 131H-allele shows more effective IgG-binding property than 131R-allele. Thus, macrophages with high Fc $\gamma$ RIIa 131H

expression show higher phagocytosis capability (18, 19). The correlation of FcγRIIIa 131R in HIV-uninfected and organ transplanted patients with cryptococcosis have been reported (16). It is postulated that the ineffective phagocytosis of immune complex resulting in a higher susceptibility to cryptococcal infection in FcγRIIIa 131R donors (16). Nevertheless, there is no association between the risk of cryptococcosis and FcγRIIIa 131H/R polymorphism in either HIV-infected or non-HIV infected populations (15, 17).

FcγRIIIa 158F/V polymorphism results in amino acid change from phenylalanine (F) to valine (V) at position 158. Both non HIV-infected (16) and HIV-infected individuals (15) with FcγRIIIa 158V polymorphism shows the higher risk of cryptococcosis because of the higher phagocytosis activity (15). These results suggest that 158V polymorphism induces *C. neoformans*-IgG complexes binding, improves phagocytosis (Trojan horse mechanism) and enhances yeast dissemination (14, 15). Surprisingly, there is an association between FcγRIIIa 158F/V polymorphism and cryptococcosis in Caucasian (17) but not in Chinese (15, 16).

It is interesting to note that FcγRIIb is the only inhibitory receptor among other FcγRs. The suppression of phagocytosis and inflammatory cytokine production are demonstrated after FcγRIIb activation. FcγRIIb presents on most of the immune cells including macrophages, mast cells, neutrophils and B cell but not on T cell and NK cells. FcγRIIb 232T/T is a risk factor for developing SLE and is resistant to malarial infection (20). In the Chinese study, an association between FcγRIIb 232I/I and cryptococcal meningitis is demonstrated (17).

## 7. Fc gamma Receptor

Due to the negative and positive regulation of Fc gamma receptors, the coordination of these receptors determines the direction of immune cell. With positive signals domination, the cell process is directed into the pro-inflammatory responses. With negative signal predomination, the cell process run toward the anti-inflammatory response. The balance between different families of Fc gamma receptor provides a well-balanced of immune response (165). In some patients with systemic lupus erythematosus (SLE) (an autoimmune disease with autoantibody production), there might be the abnormal expression of FcγRIIb (the inhibitory receptor) resulting in hyper-

immune response and auto-immune activation. Low expression and dysfunction of Fc $\gamma$ RIIb contributes to the pathogenesis of SLE in some patients and might associated with the susceptibility of some infections (20).

Therefore, Fc $\gamma$ Rs are associated with the regulation of immune response both innate and adaptive immunity that makes these receptors as the interesting targets for the development of new therapeutic procedure.

### **7.1 The family of Fc gamma receptors**

In general, the Fc $\gamma$ Rs consist of two classes depend on cell signaling pathway. Firstly, the activating receptors characterized by the presence of an immunoreceptor tyrosine-based activation motif (ITAM) sequence. Secondly, the inhibitory receptor characterized by the presence of an immunoreceptor tyrosine-based inhibitory motif (ITIM) sequence (165, 166). These two classes of receptors are coordinate of their function and are usually co-expressed on cell surface. Because activation and inhibitory receptors bind IgG with comparable affinity and specificity (17, 20), the engagement of both signaling pathways regulate a multitude of innate and adaptive immune responses.

However, classification of Fc $\gamma$ Rs by structure of these receptor in mice consists of Fc $\gamma$ RI, Fc $\gamma$ RIIb, Fc $\gamma$ RIII and Fc $\gamma$ RIV (165). And in human contains Fc $\gamma$ RI, Fc $\gamma$ RIIa, Fc $\gamma$ RIIb, Fc $\gamma$ RIIc, Fc $\gamma$ RIIIa and Fc $\gamma$ RIIIb (Figure 7).



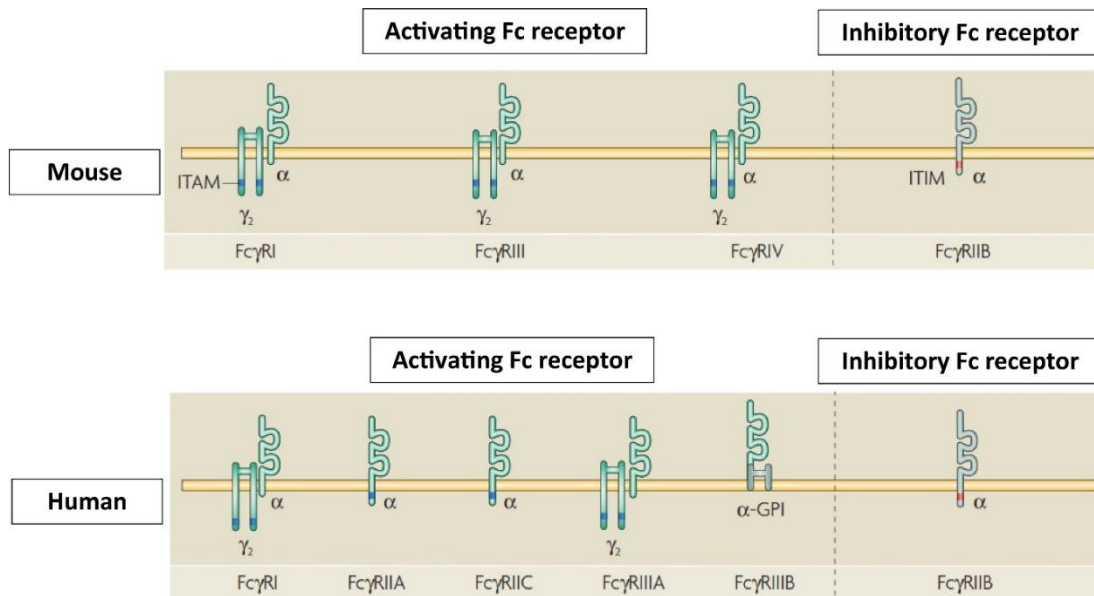


Figure 7. The family of Fc gamma receptor (165).

Based on the genomic location and similarity of these sequences in the extracellular portion, mouse FcγRIV and FcγRIII is the orthologue and closely related to human FcγRIIIA and FcγRIIA, respectively. Because of the difference between mouse and human, there is some concerns for the translation of the data from animal studies into human conditions (166).

Additionally, the IgG subclasses consist of IgG1–IgG4 (in human) and IgG1, IgG2a, IgG2b and IgG3 (in mice) that bind with various affinity and specificity to different FcγR receptors. Actually, the IgG subclasses in different species show some variations among organism. In humans and mice, the most pro-inflammatory IgG subclasses are IgG1, IgG3 and IgG2a, IgG2b, respectively and mice IgG2a, IgG2b show more activity than mouse IgG1 and IgG3 in several murine models (165). FcγRIa is the only high-affinity receptor in both mice and humans. This receptor binds IgG2a in mice or IgG1 and IgG3 in humans with an affinity of  $10^8$ - $10^9$  M<sup>-1</sup>. However, other receptors have a 100–1000 fold lower affinity in the low to medium micromolar range and show a broader IgG subclass specificity.

Accordingly, FcγRs are found on surface of the immune cell. In mice, monocyte and macrophages found both activating and inhibitory FcγRs, neutrophils found mainly

the inhibitory Fc $\gamma$ RIIb and the some activating Fc $\gamma$ RIII and Fc $\gamma$ RIV, dendritic cell found Fc $\gamma$ RI, Fc $\gamma$ RIIb and Fc $\gamma$ RIII on the cell surface. There are two cell types that do not co-express activating and inhibitory receptors: NK cells only express only the activating receptor (Fc $\gamma$ RIII) whereas B cells only express the inhibitory receptor (Fc $\gamma$ RIIb). The function of Fc $\gamma$ RIIb on B cells is an important regulator of activating signals that are triggered by B cell receptor (BCR).

However, Fc $\gamma$ RIIb is conserved in mice and humans and is the only inhibitory receptor among Fc gamma receptor family. This receptor transmits inhibitory signals via an ITIM that contained in cytoplasmic region. All other activating receptors, except human GPI-anchored Fc $\gamma$ RIIIb, activate the signal through ITAM in their cytoplasmic regions (167). Therefore, the study of Fc $\gamma$ R function in murine model is valuable to translate the role of Fc $\gamma$ R activity, especially the Fc $\gamma$ RIIb which is similar between human and mouse.

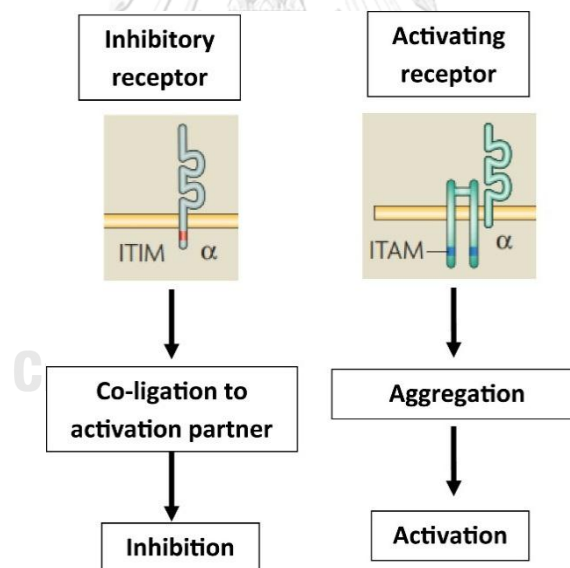


Figure 8. Schematic representation of an activating and inhibitory Fc gamma receptor (167).

## 7.2 The functions of Fc $\gamma$ RIIb

The main function of Fc $\gamma$ RIIb is to inhibit activating signals by engagement of Fc $\gamma$ RIIb with either activating Fc $\gamma$ R or with the BCR by immune complexes. The

inhibitory functions of FcγRIIb are well studied in B cells and other immune cells (41). Engagement of the BCR with FcγRIIb inhibits BCR signaling and downstream signaling response. The first step in FcγRIIb signaling is phosphorylation of ITIM by Lyn protein in the cytoplasmic domain of FcγRIIb. This process results in the SH-domain-containing inositol phosphatases (SHIP) recruitment. SHIP plays a major role to hydrolyze phosphatidylinositol-3,4,5-triphosphate (PI(3,4,5)P3) into phosphatidylinositol-3,4-bisphosphate (PI(3,4)P2) that leads to the blocking membrane translocation of PH domain containing molecules Btk and PLCγ reducing BCR-mediated calcium mobilization and protein kinase C activation (167).

In macrophages, co-ligation of FcγRIIb with other FcγRs results in the reduction of FcγR mediated phagocytosis and cytokine release such as tumor necrosis factor (TNF)-α and interleukin-6 (IL-6). In other immune cells, FcγRIIb co-ligation with IgE receptor inhibits various characteristics of mast cell and basophil function such as reduction of degranulation and histamine releasing. In mouse neutrophils, an engagement of FcγRIIb results in the inhibition of phagocytosis, production of superoxide and reduction of neutrophil adhesion, rolling and migration (20). In murine model, mice that knockout *fcγriib* gene (FcγRIIb<sup>-/-</sup>) result in spontaneous autoimmune disease with autoantibody production (31) and shows the different responses toward various pathogens (21-30).

## 8. FcγRIIb and microbial infection

An association of FcγRIIb and microbial infection including bacteria, parasite and virus infection have previously described (21-30) (Table 2). Claworthy *et al.* hypothesized that people with the FcγRIIb polymorphisms are less susceptible to malaria. This is supported by the less severe *Plasmodium* spp. infection in FcγRIIb<sup>-/-</sup> mice in comparison with the wild-type due to the enhanced phagocytosis of *Plasmodium* spp. (21). FcγRIIb<sup>-/-</sup> mice show enhanced *Mycobacterium tuberculosis* phagocytosis, attenuate disease severity and increase T helper1 cell response in comparison with wildtype (23). In the study of *Staphylococcus aureus* infection model, FcγRIIb<sup>-/-</sup> mice enhance protection against a primary infection with *S. aureus* by

increase survival rate, IL-10 level and increase phagocytosis in granulocyte and monocytes as compared to control mice (22).

The *in vitro* study of *Streptococcus pneumoniae*, a gram positive bacterium with capsule, reveals that macrophages from FcγRIIb<sup>-/-</sup> mice infected with opsonized *S. pneumoniae* result in increasing of phagocytosis and inflammatory cytokines. Subsequently, infected FcγRIIb-deficient mice showed increase survival from streptococcal peritonitis (25). In contrast to previous model, FcγRIIb<sup>-/-</sup> mice preconditioning with pneumococcal vaccine before challenging with *S. pneumoniae*, resulting in the prominent cytokine production and the more severe sepsis compare with wildtype mice. A murine model with FcγRIIb overexpression on macrophages (but not B cells) demonstrates the high susceptibility toward pneumococcal peritonitis and pneumonia (25, 168).

In contrast, FcγRIIb does not essential for the phagocytosis of *Salmonella typhimurium* (26) and *Francisella tularensis*, an intracellular gram negative bacterium, with *in vitro* experiments and the immunization with *Plasmodium berghei* vaccine before inducing infection does not worsen the natural course of the disease (27). Moreover, the preconditioning with inactivated *F. tularensis* before introducing infection attenuates disease severity in FcγRIIb<sup>-/-</sup> mice (24).

Additionally, there are a few studies in viral infection associated with FcγRIIb. In FcγRIIb<sup>-/-</sup> mice infected with human papilloma virus-like particles showed that dendritic cell reduced uptake of particles and reduce antiviral antibody and T cell response (28). The cross-linking of FcγRIIb with dengue viral immune complex inhibits the immune complex-uptake (29). Porcine reproductive and respiratory syndrome virus (PRRSV) bind with FcγRIIb in pulmonary alveolar macrophage resulting in the up-regulation of mRNA level of IFN- $\alpha$ , TNF- $\alpha$  but not IL-10 (30).

Therefore, the infection susceptibility of host with FcγRIIb deficiency depends on the specific organisms. Meanwhile, the FcγRIIb polymorphisms or deficiency showed less susceptible to some infections, the case series in Chinese patients found that FcγRIIb dysfunction-polymorphisms are more susceptible to cryptococcosis (17).

Table 2. *FcγRIIb* *-/-* mice with microbial infection model.

Model	Microbe	Results	References
<i>FcγRIIb</i> <i>-/-</i> mice	<i>Plasmodium falciparum</i>	less severe than wildtype due to the enhanced phagocytosis	(21)
<i>FcγRIIb</i> <i>-/-</i> mice	<i>Mycobacterium tuberculosis</i>	enhanced <i>Mycobacterium tuberculosis</i> phagocytosis, attenuate disease severity in comparison with wild-type	(23)
<i>FcγRIIb</i> <i>-/-</i> mice	<i>Staphylococcus aureus</i>	enhance protection against a primary infection with <i>S. aureus</i> by increase survival rate, IL-10 level and increase phagocytosis in granulocyte and monocytes as compared to control mice	(22)
<i>FcγRIIb</i> <i>-/-</i> mice	<i>Streptococcus pneumonia</i>	the prominent cytokine production and the more severe sepsis compare with wildtype	(25)

## 9. Systemic Lupus Erythematosus (SLE) and infection

Systemic Lupus Erythematosus (SLE) is the autoimmune disease with predominant auto-antibody due to the defect of self-tolerance processes. The circulating immune complex deposition in several organs cause multiple organ injury(32). SLE is one of the important health care problems in Asia region due to the possibility of the patients with severe disease and chronic condition lead to economic burden of the region. The current diagnosis of SLE followed American College of Rheumatology (ACR) 1997 including, anti-nuclear antibody (ANA) positive more than 1:160 plus at least 4 of clinical symptoms in different organs (32). The cause of SLE is

unknown but involved in multi-factorial including genetic and environmental factors. Despite several advance in therapeutic strategies, infection is still a major cause of morbidity and mortality among SLE patients (169-172). The understanding of the immune response to the severe infection in SLE patients will lead to the proper treatment strategies.

Infections are the leading causes of mortality and morbidity in patients with SLE (173-178). It is estimated that at least 50% of SLE patients suffer from severe infectious episodes during the course of the disease (179). Moreover, leading cause of death in SLE patients was infectious complications which accounted for 20–55% of all causes in worldwide literatures (169, 180, 181) and approximately 51.7% in Thailand (182). Patients with SLE are susceptible to not only common but also opportunistic or uncommon microorganisms. Several immunological aberrations of SLE responsible to the higher susceptibility to infections such as phagocytosis defect (174, 183) cellular mediated immune response alteration (184), reduced effective immunoglobulin production (185), low complement levels and ineffective elimination of microorganisms by reticuloendothelial systems and spleen (186, 187). Furthermore, steroids and immunosuppressive therapy for SLE treatment give rise to increased risk of infections as well. Bacteria, virus, protozoa and fungi are considered the main cause of infection in SLE (188-191). Interestingly, there has been a debate regarding to the susceptibility of infection in SLE is responsible from the immunosuppressive drugs used for the treatment or due to the genetic defect itself (20, 21, 192-195).

Nevertheless, the data of SLE patients without treatment are very limited due to the limitation regarding to the ethic for the available proper therapy. Then the animal studies should be able to fulfill this gap of knowledge. Moreover, a better understanding of the spectrum of pathogenic agents involved in infections in SLE patients is crucial for the optimal management of these patients.

The prevalence and incidence of SLE in Asian-pacific is high compare with other world regions (196). Several genetic abnormality in SLE have been published, however, only few of the single gene defects are associated with SLE, such as complement deficiency (C1, C2, C4) and Fc $\gamma$ RIIIb deficiency (33). The defect of Fc $\gamma$ RIIIb, inhibitory signal, leads to adaptive immune response hyper-responsiveness and

autoimmune disease. Accidentally, the prevalence of Fc $\gamma$ RIIb polymorphism is also common in Asia especially in Thai, Chinese and Japanese (193, 194, 197, 198).

Moreover, Fc $\gamma$ RIIb polymorphisms are associated with SLE in Thai (195, 197). The study of Fc $\gamma$ RIIb might be appropriate for Thai SLE characters. The reason for the high prevalence of Fc $\gamma$ RIIb polymorphisms in Asian is explained, at least in part, by the natural selection of malaria in the region (21).

Hu *et al.* (2012) reported the associations between cryptococcal meningitis and SLE patients with FCGR2B 232I/T polymorphism, suggested the importance role of Fc $\gamma$ RIIb in SLE. They concluded that Fc $\gamma$ RIIb genetic polymorphism contribute to the susceptibility of cryptococcal meningitis (17). Recently, Chen, *et al.*, (2007) was a retrospective review of 18 SLE patients with invasive fungal disease compared to *Mycobacterium* and other bacterial infections. They showed that half of the patients with invasive fungal infection caused by *Cryptococcus* spp., mostly found in lungs and central nervous system or with a disseminated disease. Patients with invasive fungal disease were younger with shorter disease duration and higher doses of immunosuppressive drugs (199). Yang, *et al.* (2007) also found that etiology of CNS infection in SLE is *C. neoformans* about 31.6% in Shanghai, China (200).

The Fc gamma Receptor IIb deficient mice (Fc $\gamma$ RIIb<sup>-/-</sup>) is one of the established SLE model (31). Together, the study in SLE mouse model is more proper than the human studies due to several limitations and confounding factors in patients. The mechanistic studies of infection in Fc gamma Receptor IIb deficient (Fc $\gamma$ RIIb<sup>-/-</sup>) SLE mouse model will increase the understanding of the pathophysiology of infection in SLE.

In addition, regarding pristane induced lupus model, pristane (2,6,10,14-tetramethylpentadecane) is a hydrocarbon naturally found in shark liver oil that could induce profound inflammation after intraperitoneal injection (201). Injection of pristane leads to increase serum auto-antibodies (anti-histone, anti-dsDNA, etc.) at 4-6 months after injection (37). The proposed pathophysiology of pristane induced lupus is through the strong immune responses intraperitoneally as multiple oil droplets with lymphoid like-tissue demonstrated in pristane mice. It is postulated that

the vigorously activation of type 1 IFN due to TLR-7 activation is the most important mechanism.

Therefore, we aim to use the FcγRIIb<sup>-/-</sup> and pristane induced SLE mouse model to compared cryptococcosis severity between these mice. This knowledge will allow us to understand the susceptibility of fungal infection in SLE patients and hopefully lead to the more proper management in such patients.





## CHAPTER IV

### MATERIALS AND METHODS

#### 1. *Cryptococcus neoformans* and animal preparation

*Cryptococcus neoformans* was isolated from a patient sample (Mycology Unit, King Chulalongkorn Memorial Hospital), identified by morphology, together with urease production and melanin synthesis (L-3, 4-dihydroxyphenylalanine or DOPA test) and stored in Sabouraud Dextrose Broth (SDB) with glycerol and glass bead at -80°C. Before conducting all of the experiments, *C. neoformans* was subcultured on SDB at 37°C for 24h and number of yeast cell was counted by hemocytometer. The FcγRIIb<sup>-/-</sup> mice were available for our research unit due to the connection with the National institute of health (NIH), Maryland, USA. Female C57BL/6 wild type mice, age-matched to FcγRIIb<sup>-/-</sup> mice, were purchased from the National Laboratory Animal Center, Nakornpathom, Thailand. FcγRIIb<sup>-/-</sup> mice genotyping was confirmed by Polymerase Chain Reaction (PCR) as previous publication and in appendix B (202). The animal protocols, in accordance with the US National Institutes of Health (NIH) animal care and use protocols, were approved by Faculty of Medicine, Chulalongkorn University followed the NIH criteria. Because FcγRIIb<sup>-/-</sup> mice are prone to spontaneous autoimmune disease or systemic lupus erythematosus (SLE) or lupus when the age upto 3 month (31), therefore, FcγRIIb<sup>-/-</sup> mice were observed for clinical manifestation of lupus by anti-dsDNA antibodies in several age range (appendix B). In this study, we investigated cryptococcosis susceptibility in FcγRIIb<sup>-/-</sup> mice either asymptomatic or symptomatic of lupus and in pristane-induce lupus mice.

#### 2. *Cryptococcus neoformans* injection model

To determine the severity of cryptococcosis in the absence of FcγRIIb receptor without effect of symptomatic by Lupus, Female 8-week-old of FcγRIIb<sup>-/-</sup> and C57BL/6 wildtype mice were used. Mice were injected, via tail vein, with  $1 \times 10^5$  yeast cells diluted in 200 μl of PBS. Survival analyses were evaluated by recorded observation every 24h after *C. neoformans* injection then mice were sacrificed at 90 days later or

reaching the moribund stage, determined by the inability to walk after the touch stimulation. In parallel, to evaluate the severity of infection at the certain duration after fungal administration, mice were sacrificed at 2 weeks after fungal administration. At 2 days before fungal administration, blood was collected through tail-vein nicking for the baseline serum with simultaneous spot urine collection. At the time of euthanasia, blood was collected through cardiac puncture under isoflurane anesthesia and internal organs (brain, lung, kidney, liver and spleen) were fixed with 10% formalin for histology or processed for fungal burdens experiments (details later). However, the study in either Fc $\gamma$ R11b<sup>-/-</sup> symptomatic lupus mice (24-week-old) or pristane mice and age-matched wild-type control were also injected with *C. neoformans* and experiment was performed as previous described above.

### 3. Histology study

For histology, the tissue samples were fixed in 10% formalin and embedded in paraffin; 4- $\mu$ m sections were stained with haematoxylin and eosin colour (H&E) and Grocott's silver stain (GMS) for *C. neoformans* identification (appendix D). Quantitative measurement of the fungal infection area was performed by 2 blinded observers. Fields (10 selected randomly) were examined at 200x magnification, with the following criteria: 0, no fungi; 1, area of fungal infection <25%; 2, infected area involving 25–50% of the field; and 3, infected area  $\geq$  50% of the field.

### 4. Fungal burden investigation

For measuring the internal organs fungal burdens between infected Fc $\gamma$ R11b<sup>-/-</sup> and wild-type mice, the organs were weighed and homogenized then the homogenized organs were plated in a serial volume onto Sabouraud Dextrose Agar (SDA) at 37°C and counted for fungal colonies at 48 h later.

### 5. Blood, urine chemistry and cytokine analysis

To determine SLE manifestation in mice, kidney injury was determined by serum creatinine (Scr) (QuantiChrom Creatinine Assay, DICT-500, BioAssay, Hayward, CA, USA), and liver injury was assessed via alanine transaminase levels (ALT) (EnzyChrom

ALT assay, EALT-100, BioAssay). Serum total protein and urine protein were measured by Bradford protein assay (Thermo Scientific, USA). Urine protein creatinine index (UPCI), a representative of 24 h urine protein, was determined by the following equation; UPCI = spot urine protein/spot urine creatinine. Cytokine measurement (TNF- $\alpha$ , IL-6 and IL-10) in serum and supernatant media were measured using ELISA assays (eBioscience, San Diego, CA, USA).

#### **6. Anti-dsDNA antibody detection.**

Calf DNA (Invitrogen, Carlsbad, CA, USA) coated on 96-well plates was used for measuring anti-dsDNA antibodies, following a previously published protocol (203). In brief, the plates were coated with calf DNA at 100  $\mu\text{g}/\text{well}$  and incubated overnight at 4 °C. The plates were dried, filled with 100  $\mu\text{l}/\text{well}$  of blocking solution, incubated at room temperature for 1.5 h and washed. Subsequently, mouse serum samples at 100  $\mu\text{l}/\text{well}$  were added and incubated for 1 h. Then, the plate was washed, incubated with peroxidase-conjugated goat anti-mouse antibodies (BioLegend, USA) at 100  $\mu\text{l}/\text{well}$  at room temperature for 1 h, washed and developed with ABTS peroxidase substrate solution (TMB Substrate Set; BioLegend) for 10 min in the dark. Finally, the stop solution (2 N  $\text{H}_2\text{SO}_4$ ) was added, and the plate was read with a microplate photometer at a wavelength of 450 nm.

#### **7. Generation of bone marrow derived macrophages**

Bone marrows (BM) derived macrophages method follows the established protocol (204) (appendix E). In short, mice were sacrificed, and femoral bone marrows were isolated. In brief, cells were washed from BM cavity and incubated for 7 days in DMEM media (high glucose DMEM supplement with 10% fetal bovine serum, 1% penicillin/streptomycin, 1% HEPES, 1% sodium pyruvate, 5% horse serum and 20% L929-conditional media) in a humidified 5%  $\text{CO}_2$  incubator at 37 °C. Subsequently, cells were harvested at the end of the culture period using cold PBS and confirmed macrophage phenotype with anti-F4/80 and anti-CD11b antibodies (BioLegend, CA, USA) by flow cytometry. For macrophage activation, BM-derived macrophages were incubated for 17 h with IFN- $\gamma$  (10 ng/ml final concentration; BioLegend, USA). Then,

LPS (100 ng/ml final concentration; Sigma-Aldrich) was added and incubation continued for 24 h. The activated macrophages were investigated by IL-12p70 production with ELISA (eBioscience, USA).

### 8. Peritoneal macrophage isolation

Bone-marrow-derived macrophage of pristane is not different from the wild-type control due to the several *in vitro* processes and cell-stimulators. However, there is less influence of the *in vitro* process in the isolation of peritoneal macrophage. Then peritoneal macrophages were isolated from 6 month-old mice (pristane, FcγRIIb<sup>-/-</sup> and control group) following an established protocol (205). In short, the peritoneal cavity was washed several times with ice-cold PBS after euthanasia. Subsequently, the samples were centrifuged, discarded supernatants and induced red blood cell lysis by lysis buffer solution (NH<sub>4</sub>Cl solution) for 5 min. After that, the cells were separated by centrifugation and incubated with DMEM complete media (HyClone, South Logan, UT, USA) in 5% CO<sub>2</sub> at 37 °C overnight. The non-adherent cells were removed and wash with warm PBS. The adherence cells were collected by washed vigorously with ice cold-PBS. Cell viability was estimated by staining with 0.4% Trypan blue (Gibco, USA). More than 97% of the adherent cells had morphological characteristics of macrophages by Diff-Quick staining and the macrophage phenotype was confirmed by flow cytometry with anti-F4/80 and anti-CD11b antibodies (Biolegend, San Diego, CA, USA).

### 9. Phagocytosis assay

Although FcγRIIb<sup>-/-</sup> macrophages enhance phagocytosis and clearance in some pathogens as previous publication (21-30) but *C. neoformans* could be survive and replicate within macrophages by several immune evasion mechanisms (21-30). Therefore, we hypothesized that FcγRIIb<sup>-/-</sup> macrophages should have more phagocytic activity. The phagocytosis activity assessments were performed according to a previous protocol, with slight modifications (206, 207). Briefly, BM-derived macrophages were added to 96-well plates at 2.5x10<sup>4</sup> cells/well in DMEM complete and incubated overnight. After the incubation, the medium was then removed and 100 μl of complete

DMEM with 20% normal mouse serum, as a source of opsonin, were added with heat-killed *C. neoformans* at 5:1 and 10:1 ratios of fungal cells to macrophages. These were incubated for 2h and 4h. After incubation, the wells were washed with 200  $\mu$ l of PBS at least 3 times to remove un-ingested yeast and then the macrophages were detached with 200  $\mu$ l of cold PBS. Then, the macrophages were transferred to a CytoSpin chamber (Thermo Scientific) and centrifuged at 600 rpm for 5 min to concentrate the cells into a single cell-layer for easier visualization. The macrophages were stained with Diff-Quick stain (Life Science Dynamic Division, Nonthaburi, Thailand). Macrophages containing yeast were counted as showing phagocytosis. At least 100 macrophages per well were counted. In parallel, the ingestion ability of each individual macrophage was determined as the average number of fungal cells in each macrophage (phagocytosis index), calculated as the total number of ingested fungi divided by the total number of macrophages. The phagocytosis activity was determined as the percentage of macrophages with phagocytosed cryptococci and phagocytosis index. All of the experiments were performed in triplicate.

#### **10. *C. neoformans*-FITC phagocytosis assays**

The phagocytosis activity assessments were performed with heat-killed fluorescent conjugated fungi and live fungi according to a previous protocol (208). Briefly, for heat-killed fluorescent conjugated fungi,  $1 \times 10^8$  cells of heat-killed *C. neoformans* were incubated with 500  $\mu$ g/ml fluorescein isothiocyanate (FITC) (Sigma, USA) in PBS for the *C. neoformans*-FITC labeling. Then peritoneal macrophages at  $2.5 \times 10^4$  cells/well were added to 96-well plates in 200  $\mu$ l of DMEM and incubated overnight. After that, macrophages were challenged with *C. neoformans*-FITC at multiplicity of infection (MOI; yeast per macrophage ratio) at 5:1 with 20% normal mouse serum as a source of the opsonin. These were incubated for the various durations (2-24h). Subsequently, all media and extracellular yeast were removed and washout by PBS. Then 0.4% trypan blue at 100  $\mu$ l per well were added for 2 min at room temperature for quenching extracellular *C. neoformans*-FITC. All dyes were removed and read the fluorescence intensity at the excitation and emission wavelength at 492 and 518 nm, respectively.

## 11. Macrophage total killing activity and intracellular proliferation assays

Total cryptococcal cell killing activity was assessed using a previously published method which both extruded and intracellular yeasts were determined (206, 207). Briefly, BM-derived macrophages at  $1 \times 10^5$  cells/well were co-cultured with live *C. neoformans* at a ratio of 1:1 for 2, 4 and 24 h for phagocytosis as mentioned above in the presence of 20% normal mouse serum containing media to promote phagocytosis. After incubation, the culture supernatant was separated, and a lysis medium (distilled water containing 0.01% bovine serum albumin and 0.01% Tween-80) was added to the wells, for 20 min at  $37^\circ\text{C}$ , to rupture the macrophage cell membranes. Then, the supernatant and the lysate were well mixed. Serial dilutions of the mixed lysates were plated on SDA for viable yeast colony forming unit (CFU) counts. Control cultures consisted of incubation medium alone plus *C. neoformans*. Macrophage total killing activity is inversely correlated with the number of yeast colonies. The intracellular and extracellular killing activity of macrophages was evaluated with this method.

Moreover, to determine only the intracellular killing activity, the intracellular proliferation assay was performed with methods that were slightly modified from those previously published (209, 210). Briefly, BM-derived macrophages, at  $2.5 \times 10^4$  cells/well were co-cultured with live *C. neoformans*, at a ratio of 5:1, were added and incubated for 2 h in 20% normal mouse serum containing media. After 2 h, the wells were extensively washed (4-5 times) to remove extracellular fungi. This was set as the 0 h time-point. For some of the culture wells at this time-point, macrophage cells lysis was induced by lysis medium and plated on SDA for the visualization of intracellular fungal viability for “phagocytosis activity at the 0 h time-point” for the further calculation. The remaining culture wells from the 0 h time-point were maintained in DMEM media at  $37^\circ\text{C}$ , and the cells were subsequently lysed at 2, 4 and 24 h, for the determination intracellular fungal viability, as mentioned above. Because the difference in intracellular fungi might be due to the difference in phagocytosis activity at the 0 h time-point, the phagocytosis activity at the 0 h time-point was used for the normalization with the following equation: intracellular proliferation at specific time

points = CFU of fungi at 2, 4 or 24 h after the 0 h time-point / CFU of fungi after phagocytosis at the 0 h time-point. Macrophage intracellular killing activity is inversely correlated with the number of yeast colonies (intracellular proliferation).

## **12. *In vitro* *Cryptococcus neoformans* stimulated macrophage cytokines production**

To compare the cytokine response to *C. neoformans in vitro* by macrophage, heat-killed *C. neoformans*, (immersion in a 60°C water bath for 1 h) or live *C. neoformans*, at a dose of  $5 \times 10^5$  yeast cells/well, were incubated with macrophages ( $1 \times 10^5$  cells/well) in 96-well polystyrene tissue culture plates (211). The culture supernatants were collected at 24, 48, 72 and 96 h after the incubation and stored at -80°C until cytokine determination (TNF-alpha, IL-6, IL-10) by ELISA assays (eBioscience, USA). After the incubation, cell viability was measured by MTS assay (Promega Corporation, WI, USA) according to the manufacturer's instruction (212). In short, 20 µl of MTS was added to the culture plates for 2h at 37°C in 5% CO<sub>2</sub> incubator then read with microplate photometers with a wavelength at 490 nm (appendix I).

## **13. *In vivo* macrophage depletion**

The role of macrophage in fungal dissemination was evaluated in Clodronate-liposome (Encapsula Nanoscience, USA) induced macrophage depletion *in vivo* after onset of infection as previously described (9). Female 8-week-old FcγRIIb<sup>-/-</sup> and wild-type mice were administered *C. neoformans* via the tail vein. Then, 200 µl/mouse liposomal clodronate (Encapsula Nanoscience, Nashville, TN, USA) (5 mg/ml) or control liposomes were injected to induce sustained monocyte depletion. The daily injections began on the third day of fungal administration and continued for 4 consecutive days. At 7 days post-inoculation, the mice were sacrificed and the internal organs were processed for fungal burdens and fixed in 10% formalin to confirm macrophage depletion (by immunohistochemical staining with an F4/80 antibody; Biolegend, San Diego, CA, USA). Macrophages were not detectable in organs after liposomal clodronate treatment in either FcγRIIb<sup>-/-</sup> or wild-type mice.

#### 14. Transfer of *Cryptococcus* contained-macrophages *in vivo*

To see if there is the difference in phagocytosis capacity of Fc $\gamma$ R11b<sup>-/-</sup> versus wildtype macrophages *in vivo*, cryptococci contained- Fc $\gamma$ R11b<sup>-/-</sup> and wild-type macrophages were injected in wild-type mice. Bone marrow derived macrophage (BM) macrophages from Fc $\gamma$ R11b<sup>-/-</sup> and wild-type were allowed to phagocytose yeasts before infusion into wild-type mice as previously described (206, 207). Briefly, BM macrophages cultured in 96-well plate at  $2.5 \times 10^4$  cells/well with 20% mouse serum were incubated with *C. neoformans* at the ratio of yeast per macrophage of 5:1 for 2 h. The un-ingested fungi were washed out with DMEM (3-5 washes). Subsequently, the macrophages were detached with cold-PBS washing (3-5 times), centrifuged at 1,000 rpm for 10 min at 4°C and the cell-pellets were re-suspended with DMEM. The macrophages were counted and stained with trypan blue. Either Fc $\gamma$ R11b<sup>-/-</sup> or wild-type macrophages with internalized *Cryptococcus*, at  $2.5 \times 10^4$  cells/ml, were intravenously administered to wild-type mice through the tail-vein. Mice were sacrificed at 24h to determine fungal burdens.

#### 15. T cells isolation from spleen and flow cytometry analysis

Because of an influence of T-lymphocyte on macrophage functions, we explored spleen lymphocyte of these mice follow the protocol of a previous publication (213). In short, splenocytes were isolated from 6-month-old mice of all experiment groups. Spleens were dispersed through a cell strainer to generate a single-cell suspension and eliminated red blood cells by an osmotic agent (ACK buffer: NH<sub>4</sub>Cl, KHCO<sub>3</sub> and EDTA). T cells were isolated and purified using the CD4<sup>+</sup> T Cell Isolation Kit, (Miltenyi biotec, Auburn, CA, USA). The viability and purity of both cell types were examined by flow cytometer. Then, CD4<sup>+</sup> T cells were stained with anti-CD4, -CD8, -CD69, -CD44, -CD62L and -ICOS (Inducible T cell Costimulator) (Biolegend, San Diego, CA, USA).

To determine the activity of Th cells, the intracellular staining of anti-IFN- $\gamma$  (Biolegend, USA) was performed. The intracellular staining flow-cytometry protocol was



followed (213). In short,  $2 \times 10^5$  cells of CD4<sup>+</sup> T cells were plated in 200  $\mu$ l of complete medium supplemented with 25 ng/ml PMA (Sigma-Aldrich), 1  $\mu$ g/ml ionomycin (Sigma-Aldrich) and 1X GolgiPlug (brefeldin A, Biolegend). As control, the cells were stimulated with GolgiPlug. After 4 h of incubation at 37°C and 5% CO<sub>2</sub>, cells were stained with anti-CD3 and anti-CD4 before following the cytokines intracellular staining for anti-IFN- $\gamma$  (Biolegend, San Diego, CA, USA). The flow cytometry analysis was performed using BD LSR-II and FlowJo software. In addition, to represent the influence of *C. neoformans* infection toward the alteration of immune responses in lupus, spleen of mice in wild-type, pristane and Fc $\gamma$ R11b<sup>-/-</sup> after 2 weeks of *C. neoformans* administration (infected group) or PBS control (uninfected group) were analyzed.

#### 16. Statistical analysis

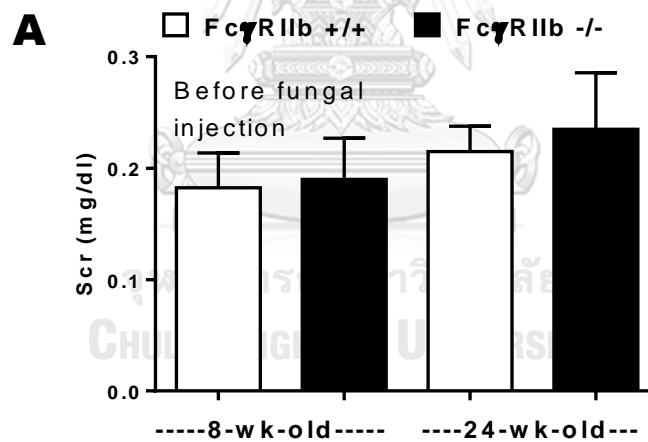
The mean  $\pm$  SE was used for the data presentation and the differences between groups were examined for statistical significance using the unpaired Student t-test or one-way analysis of variance (ANOVA) with Tukey's comparison test for the analysis of experiments with 2 and 3 groups, respectively. Survival analyses were evaluated using the log-rank test. *P* values < 0.05 was considered statistically significant. SPSS 11.5 software (SPSS Inc., Chicago, IL, USA) was used for all statistical analysis.

## CHAPTER V

### RESULTS

#### 1. Determination of lupus manifestation in mice before use.

Because FcγRIIb<sup>-/-</sup> (knock out) mice are prone to spontaneously lupus disease, so that these mice have to determine lupus manifestation before perform experiment by examine serum creatinine (scr), urine protein creatinine index (UPCI) and anti-dsDNA. The FcγRIIb<sup>-/-</sup> mice with age 8-week-old were classified in asymptomatic group. This group show not significant difference by scr, UPCI and anti-dsDNA. In contrast, mice with 24-week-old were classified in symptomatic group because these mice reveal significant higher UPCI and anti-dsDNA than previous group (Figure 9 A, B and C). The FcγRIIb<sup>+/+</sup> (wild-type) mice with sex and age match were used as control group.



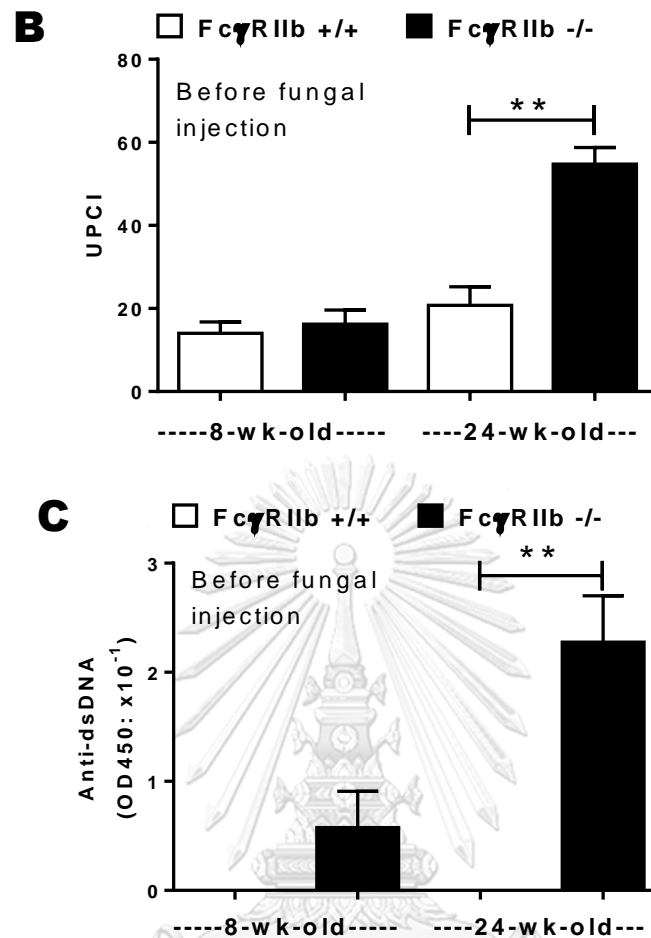


Figure 9. Characteristics of FcγRIIb<sup>-/-</sup> mice at 8- and 24-weeks-old as demonstrated by serum creatinine (Scr) (A), proteinuria by urine protein creatinine index (UPCI) (B) and anti-dsDNA (C), (n=4/group). The data are shown as the mean ± SE. \* p<0.05, \*\* p<0.01.

## 2. Increased severity of cryptococcosis in Fc gamma receptor IIb deficient mice

To determine percent survival in FcγRIIb<sup>-/-</sup> mice that lack FcγRIIb function without symptomatic of lupus compare with control wild-type mice after *C. neoformans* infection. The FcγRIIb<sup>-/-</sup> mice were challenged with *C. neoformans* by tail-vein injection and monitored survival. The FcγRIIb<sup>+/+</sup> (wild-type) mice with *C. neoformans* injection and FcγRIIb<sup>-/-</sup> with PBS injection were used as control group. The result found that FcγRIIb<sup>-/-</sup> mice reveal high susceptible to *C. neoformans* infection with significantly lower percent survival than control group as show in figure

10. All of the FcγRIIb<sup>-/-</sup> mice, but only 57% of the wild-type mice, died or became moribund within 90 days of challenge.

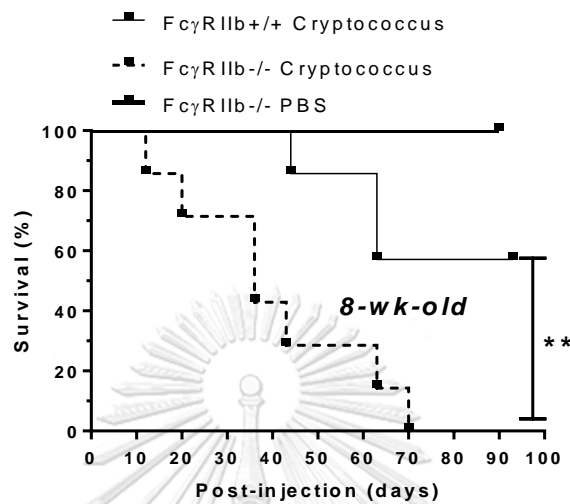


Figure 10. Percent survival in 8-wk-old FcγRIIb<sup>-/-</sup> and wild-type mice after challenged with *C. neoformans* (n=7/group).

To determine fungal burden after *C. neoformans* infection by CFU count per organ at moribund stage. Both of FcγRIIb<sup>+/+</sup> and FcγRIIb<sup>-/-</sup> mice were challenged with *C. neoformans*. At the moribund stage, organs including brain, kidney, liver, lung and spleen were homogenized and spread on Sabouraud Dextrose Agar (SDA) to examine number of yeast cell in each organ (CFU/g organ). The results show that moribund FcγRIIb<sup>-/-</sup> mice demonstrated higher fungal burdens (Figure 11) and cryptococcoma-like-lesions in several internal organs, namely brain, kidney, liver, lung and spleen (Figure 12) with significant histopathological scoring (Figure 13). In contrast, wild-type mice found predominant lesion in the brain, a major organ of infection, at the moribund stage (Figure 11 and 12).

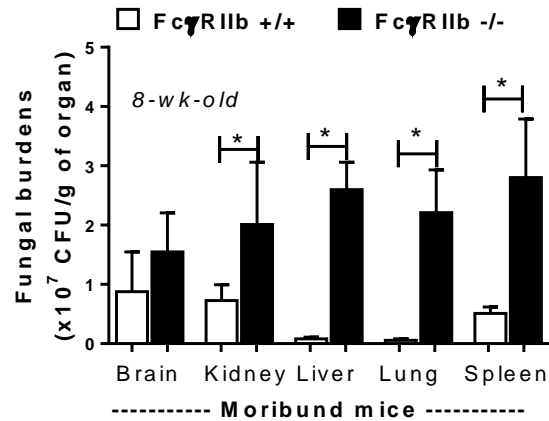


Figure 11. Organ fungal burdens from 8-wk-old Fc $\gamma$ RIIb+/+ and Fc $\gamma$ RIIb-/- mice after challenged with *C. neoformans* at moribund stage (n=3-6/group). The data are shown as the mean  $\pm$  SE. \* p<0.05.

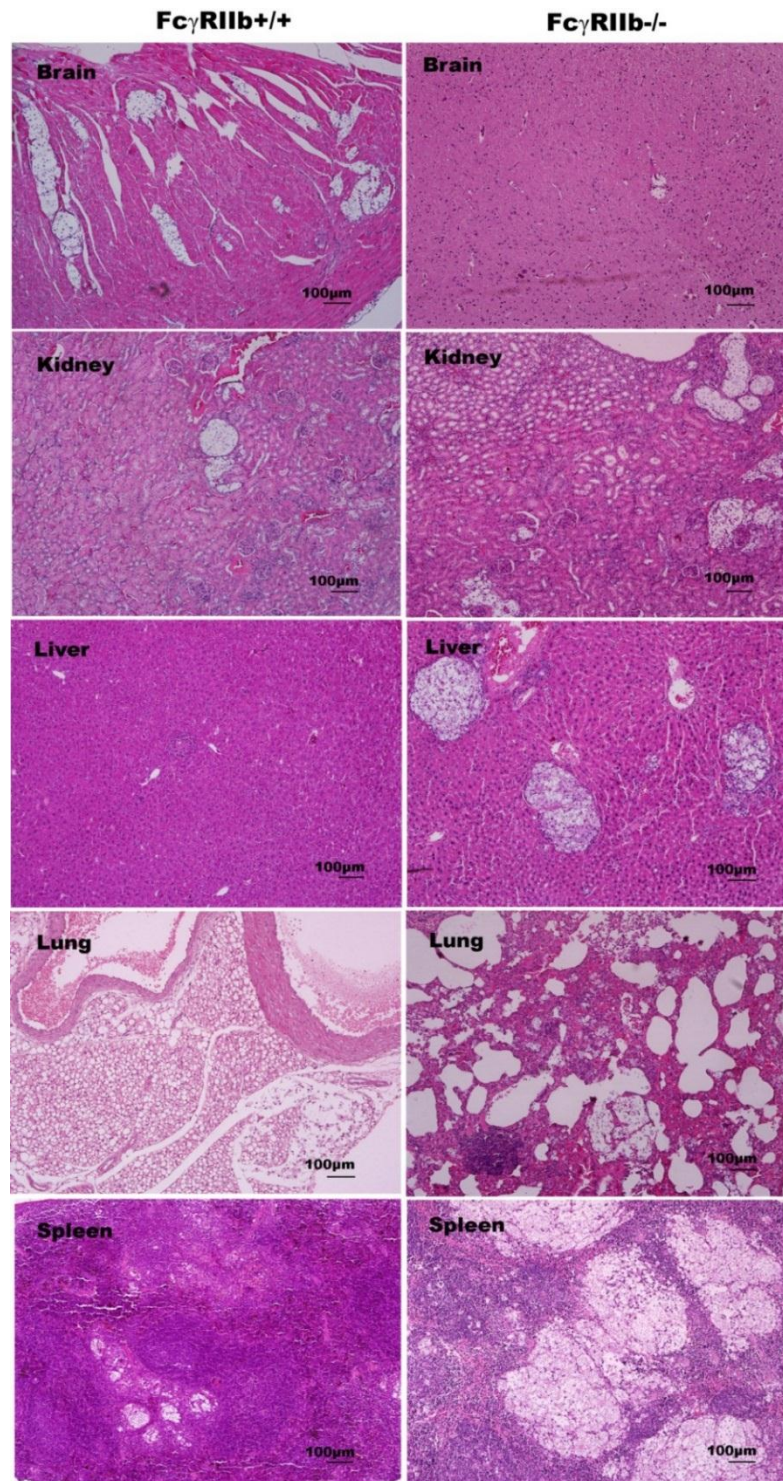


Figure 12. Representative histology with H&E (hematoxylin and eosin staining) at 100x magnification from 8-week-old mice in the moribund stage after *C. neoformans* administration. *FcγRIIb*<sup>+/+</sup> mice (left column); *FcγRIIb*<sup>-/-</sup> mice (right column)

Histopathology analysis in 8-wk-old *FcγRIIb*<sup>+/+</sup> and *FcγRIIb*<sup>-/-</sup> mice after challenged with *C. neoformans* at moribund stage.

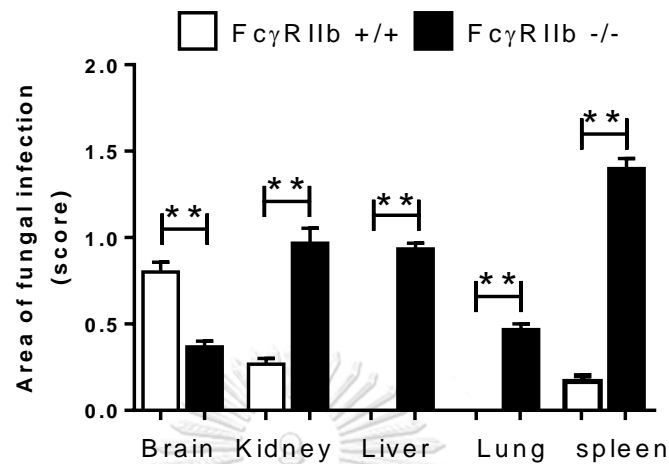
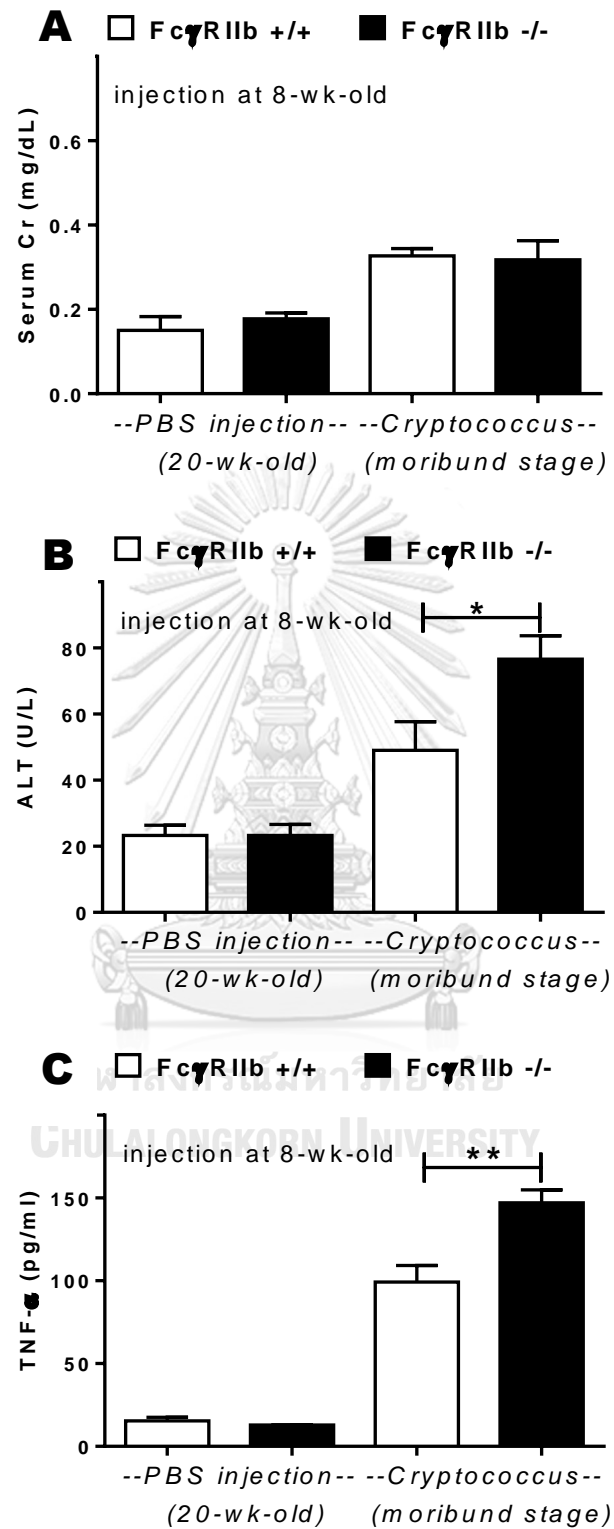


Figure 13. Histology scoring of 8 week-old mice after challenged with *C. neoformans* at moribund stage. The data are shown as the mean  $\pm$  SE. \*  $p < 0.05$ , \*\*  $p < 0.01$ .

At the moribund stage, cryptococcosis was more severe in 8-wk-old *FcγRIIb*<sup>-/-</sup> mice. Serums were collected from wild-type and *FcγRIIb*<sup>-/-</sup> mice after challenged with *C. neoformans* and determine secreted cytokine at moribund stage. The serum from 8-wk-old *FcγRIIb*<sup>-/-</sup> mice were determined scr and ALT to check kidney and liver function, respectively. The levels of Scr, ALT and cytokines (TNF- $\alpha$ , IL-6 and IL-10) in wild-type were  $0.33 \pm 0.02$  mg/dl,  $49 \pm 9$  U/L and  $99 \pm 10$ ,  $89 \pm 14$  and  $389 \pm 142$  pg/ml and in *FcγRIIb*<sup>-/-</sup> young mice were  $0.32 \pm 0.04$  mg/dl,  $77 \pm 7$  U/L, and  $147 \pm 8$ ,  $257 \pm 48$  and  $446 \pm 199$  pg/ml (Figure 14. A-E). The infected *FcγRIIb*<sup>-/-</sup> mice reveal more significant different in ALT detection but not in serum creatinine, when compared with wild-type. Additionally, *FcγRIIb*<sup>-/-</sup> mice are significantly more TNF- $\alpha$  and IL-6 but not IL-10 production in serum than wild-type at moribund stage.





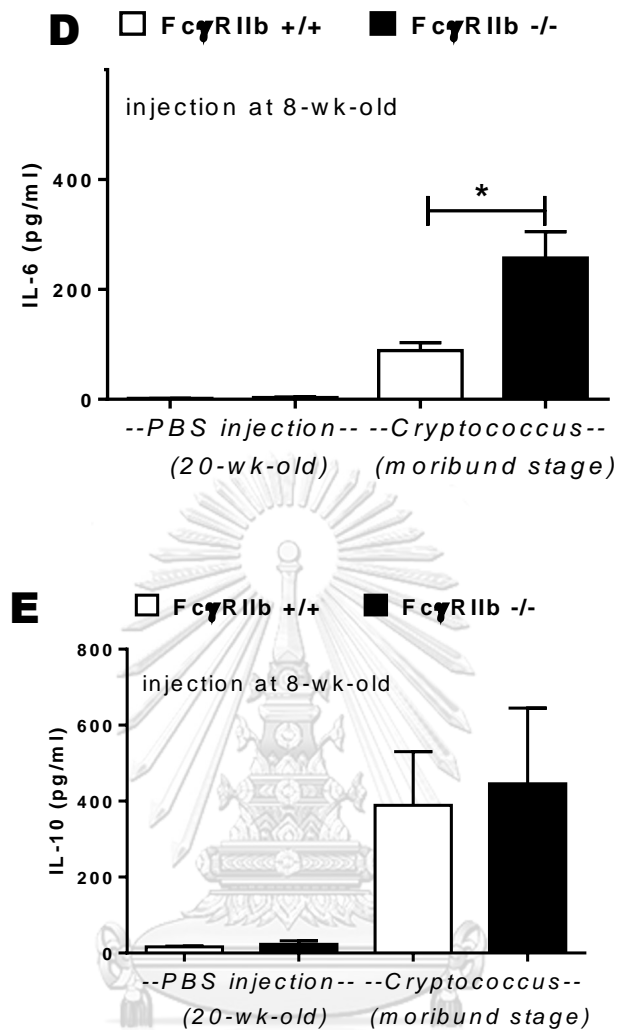


Figure 14. Organ injury and inflammatory cytokines at the moribund stage in 8-week-old as demonstrated by serum creatinine (Scr) (A), alanine transaminase (ALT) (B), TNF- $\alpha$  (C), IL-6 (D) and IL-10 (E) levels. The data are shown as the mean  $\pm$  SE. \*  $p < 0.05$ , \*\*  $p < 0.01$ .

Organ fungal burden and secreted cytokine of 8-wk-old Fc $\gamma$ RIIb-/- mice after injection with *C. neoformans* at early stage was determined. The 8-wk-old Fc $\gamma$ RIIb-/- mice were challenged with *C. neoformans* for 2 weeks and then sacrificed to determine fungal burden. The result found that Fc $\gamma$ RIIb-/- mice reveal higher fungal burdens (Figure 15). Cryptococcoma-like lesions were found in most organs in Fc $\gamma$ RIIb-/- mice with significant histology scoring (Figure 17), but only in the brain and kidney in wild-type mice (Figure 16).

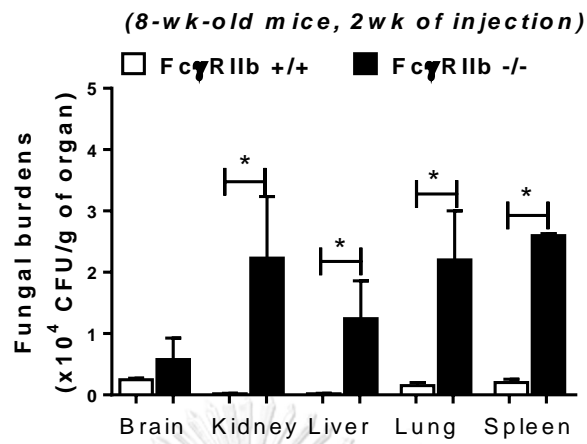


Figure 15. Fungal burdens in the internal organs of 8-week-old mice at 2 weeks post-*C. neoformans* administration. The data are shown as the mean  $\pm$  SE ( $n = 4-5$ /group). \*  $p < 0.05$ .

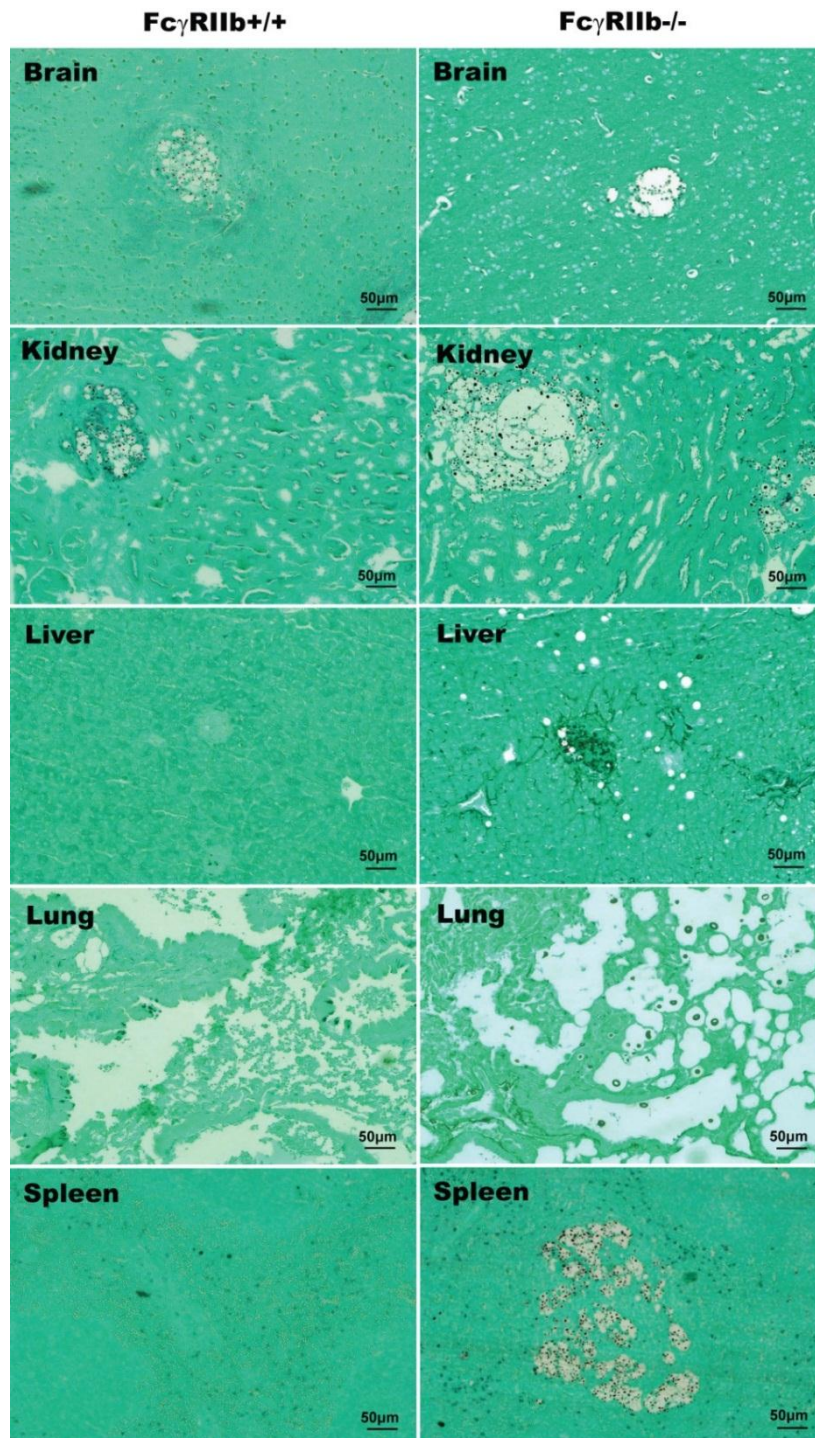


Figure 16. Organ histology with Grocott's silver staining (GMS) at 200x magnification from 8 week-old mice at 2 weeks post-*C. neoformans* infection, demonstrating cryptococcoma-like lesions in the brain and kidney of Fc $\gamma$ RIIb<sup>+/+</sup> mice (left column), and in several internal organs (brain, kidneys, liver, lung and spleen) of Fc $\gamma$ RIIb<sup>-/-</sup> mice (right column).

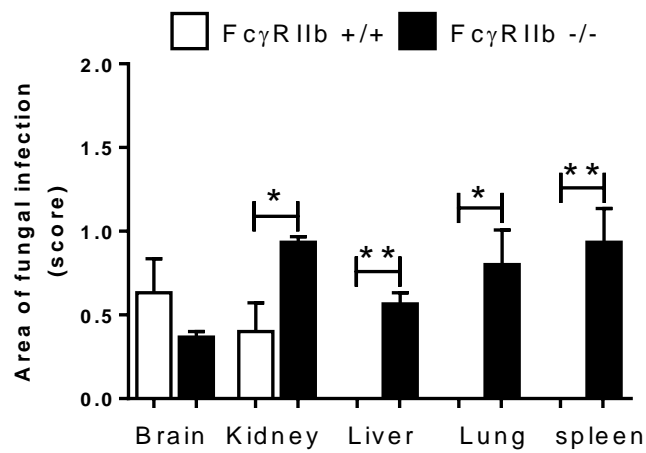
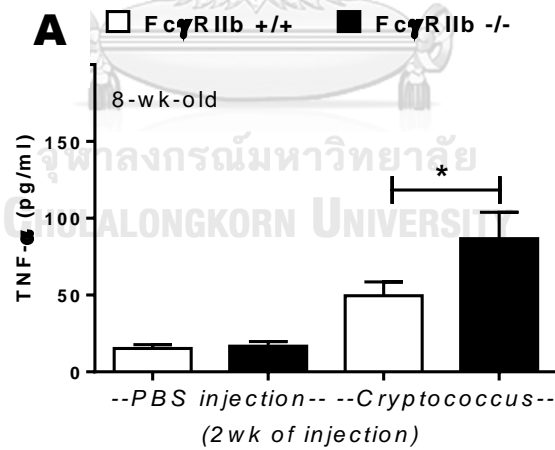


Figure 17. Histology scoring of 8 week-old mice at 2 weeks post-*C. neoformans* infection. The data are shown as the mean  $\pm$  SE (n = 4-5/group). \*  $p < 0.05$ , \*\*  $p < 0.01$ .

To determine secreted cytokine in serum reveal that Fc $\gamma$ RIIb-/- mice are significantly more TNF-alpha and IL-6 production in serum but not IL-10 at early stage of infection (2 weeks) (Figure 18)



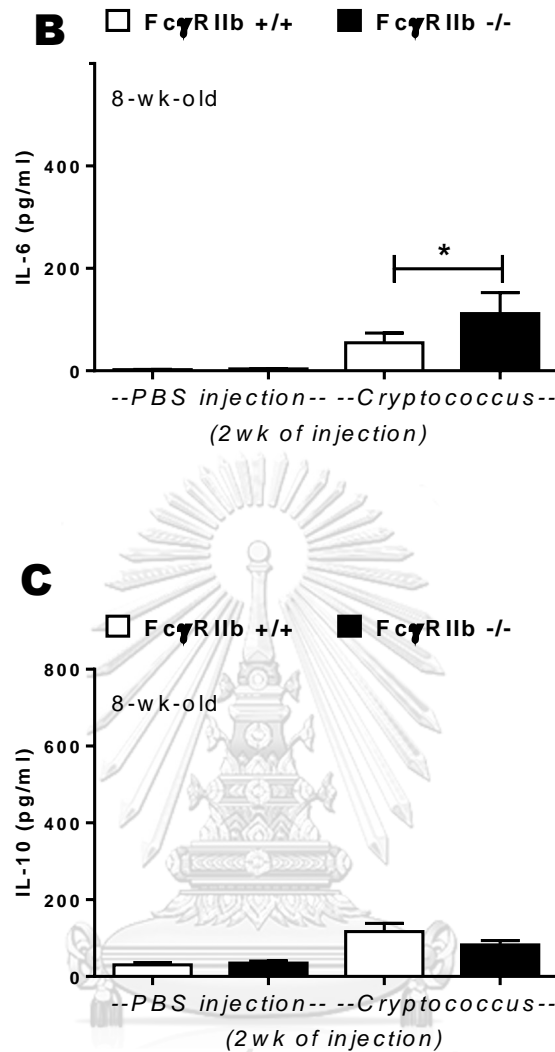


Figure 18. Serum cytokines measured include  $TNF-\alpha$  (A), IL-6 (B) and IL-10 (C). The data are shown as the mean  $\pm$  SE ( $n = 4-5$ /group). \*  $p < 0.05$ .

The FcγRIIb<sup>-/-</sup> mice also show high severity of cryptococcosis than wild-type counterpart. The cryptococcosis, either at 2 weeks or when moribund, was more severe in FcγRIIb<sup>-/-</sup> than wild-type mice, as demonstrated by higher fungal burdens in most internal organs, higher liver enzyme levels, and higher pro-inflammatory cytokine levels but not higher anti-inflammatory cytokine levels. Therefore, high cryptococcosis severity in FcγRIIb<sup>-/-</sup> mice depend on lack of FcγRIIb function and lupus symptomatic independent.

### 3. FcγRIIb<sup>-/-</sup> macrophage responses to *C. neoformans*: prominent phagocytosis and pro-inflammatory cytokine production.

Due to the importance of macrophages in fungal infection response and the presence of FcγRIIb in macrophages, we determine phagocytosis and killing function of macrophage with *C. neoformans in vitro*. Bone marrow derived macrophages from wild-type and FcγRIIb<sup>-/-</sup> mice were generated and confirmed for macrophage phenotype by flow cytometry with anti-F4/80 and anti-CD11b (Figure 19). These macrophages were co-cultured with heat killed *C. neoformans* at 5:1, 10:1 yeast per macrophage ratio in the presence of 20% mouse serum as source of opsonin and incubate for 2h and 4h time points. With the ratio of fungal cells to macrophages of 5:1, the percentages of macrophages with phagocytosed *C. neoformans* in wild-type and FcγRIIb<sup>-/-</sup> after 2h incubation were 47.5±17.5% and 90.1±6.2%, respectively, and after 4h incubation were 42.1±4.2% and 91.5±1.5%, respectively. At the ratio of 10:1, the percentages of phagocytosed macrophages in wild-type and FcγRIIb<sup>-/-</sup> after 2 h incubation were 69.5±0.5% and 90.5±0.5%, respectively, and after 4 h incubation were 67.5±1.5% and 91.5±1.5%, respectively (Figure 21A). Additionally, the average number of fungi in each macrophage was higher in FcγRIIb<sup>-/-</sup> cells, as determined by the phagocytosis index (number of internalized fungi / total macrophages) (Figure 21B). FcγRIIb<sup>-/-</sup> macrophage reveal significant higher percent phagocytosis and more phagocytosis index than wild-type macrophage (Figure 20 and 21).

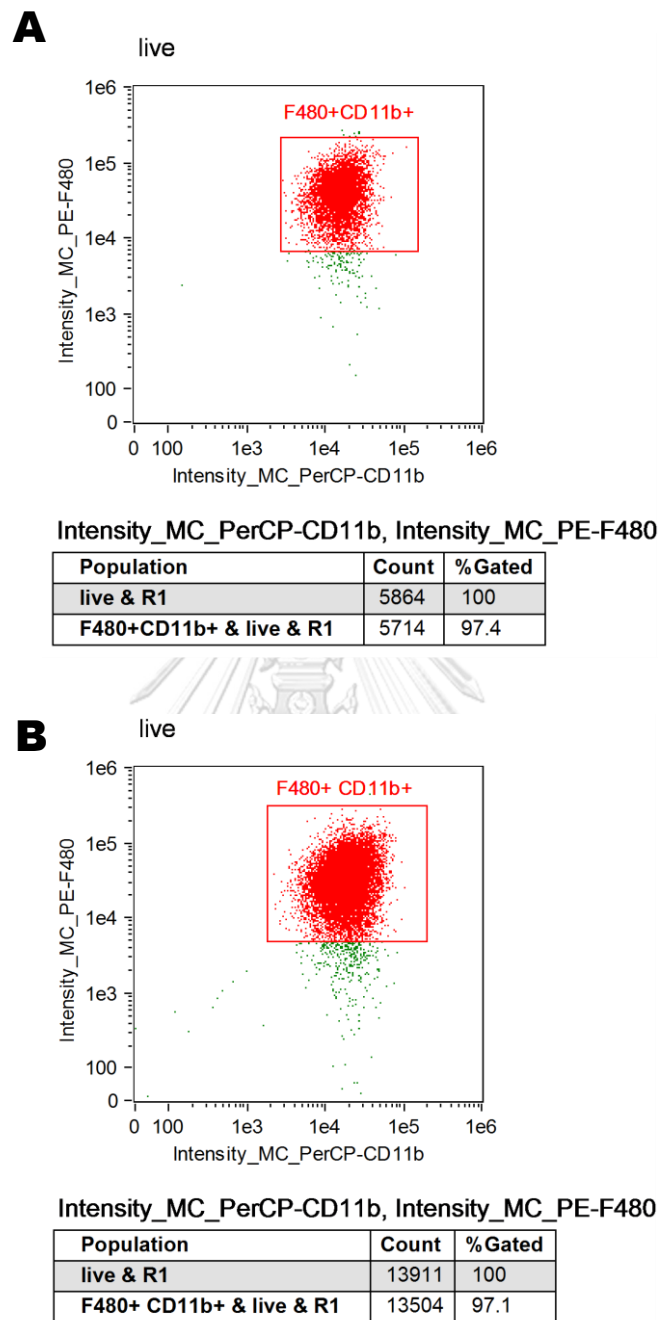


Figure 19. Representative results from flow cytometry with anti-F4/80 and anti-CD11b antibodies in *FcγRIIb*<sup>+/+</sup> (A) and *FcγRIIb*<sup>-/-</sup> (B) macrophages.

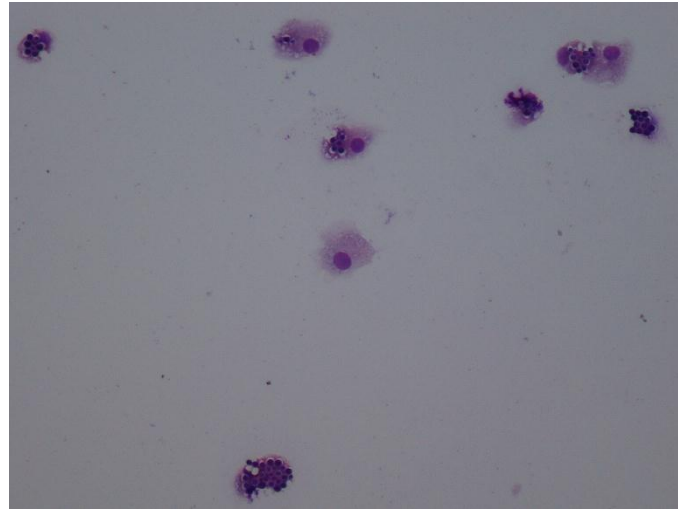
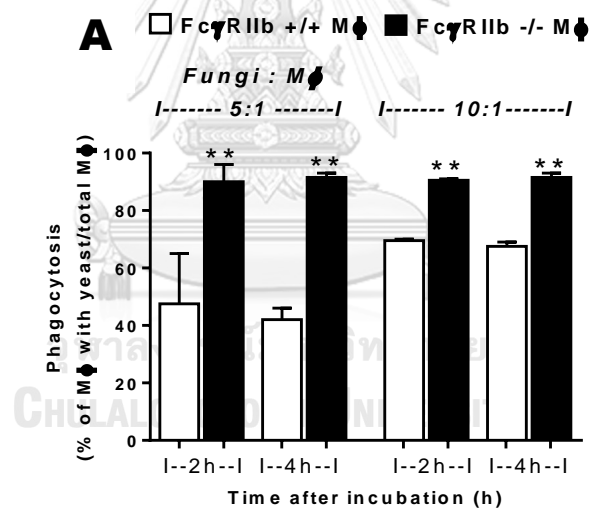


Figure 20. Representative figure of macrophage with Diff-Quick staining after engulf of *C. neoformans* by phagocytosis mechanism





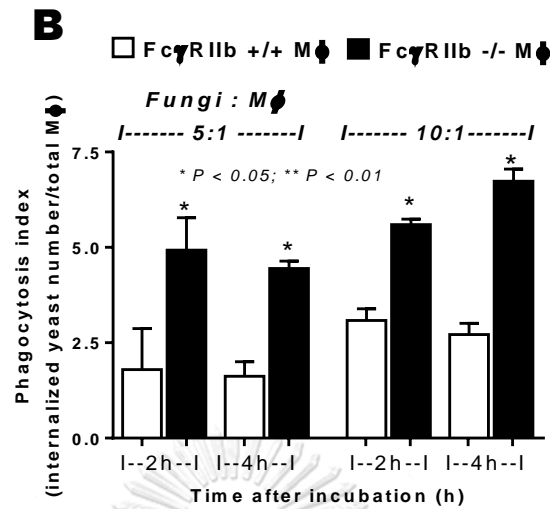


Figure 21. Percentage of macrophages ( $M\Phi$ ) demonstrating phagocytosis (A) and the average number of phagocytosed fungi per  $M\Phi$  (total number of phagocytosed fungi/total  $M\Phi$ ) after incubation with *C. neoformans* at ratios of fungi: $M\Phi$  of 5:1 and 10:1 (B). \*  $p < 0.05$ , \*\*  $p < 0.01$  (experiments were performed in triplicate).

In contrast, the macrophage killing activity, as determined by fungal viability after incubation with macrophages for 2, 4 and 24 h, was not different between wild-type and  $Fc\gamma RIIb^{-/-}$  cells. The numbers of viable fungi in the macrophages with total killing ability (both extruded and intracellular yeasts were determined; see methods), *in vitro*, at 2, 4, and 24 h of fungal incubation with wild-type cells versus  $Fc\gamma RIIb^{-/-}$  macrophages were  $8.2 \pm 0.8$ ,  $4.4 \pm 0.5$  and  $5.5 \pm 0.7$  vs.  $20.6 \pm 2.8$ ,  $15.6 \pm 2.1$  and  $14.9 \pm 2.1$  ( $\times 10^4$ ) CFU/ml, respectively (Figure 22A). No difference in macrophage killing activity was observed using the intracellular proliferation assay. This determined the viability of only intracellular yeasts (see methods). Indeed, the intracellular proliferation amounts at 2, 4, and 24 h of fungi incubated with wild-type cells versus fungi incubated with  $Fc\gamma RIIb^{-/-}$  macrophages were  $1.3 \pm 0.2$ ,  $1.0 \pm 0.2$  and  $12.3 \pm 1.8$  vs.  $1.3 \pm 0.1$ ,  $0.7 \pm 0.2$  and  $8.8 \pm 1.9$  units, respectively (Figure 22B). Although a trend toward greater intracellular-killing by  $Fc\gamma RIIb^{-/-}$  macrophages was observed, it was not statistically significant. The presence of macrophages did not reduce the colony count of fungi in the fungicidal activity assay, implying that cryptococci were viable, intracellularly.

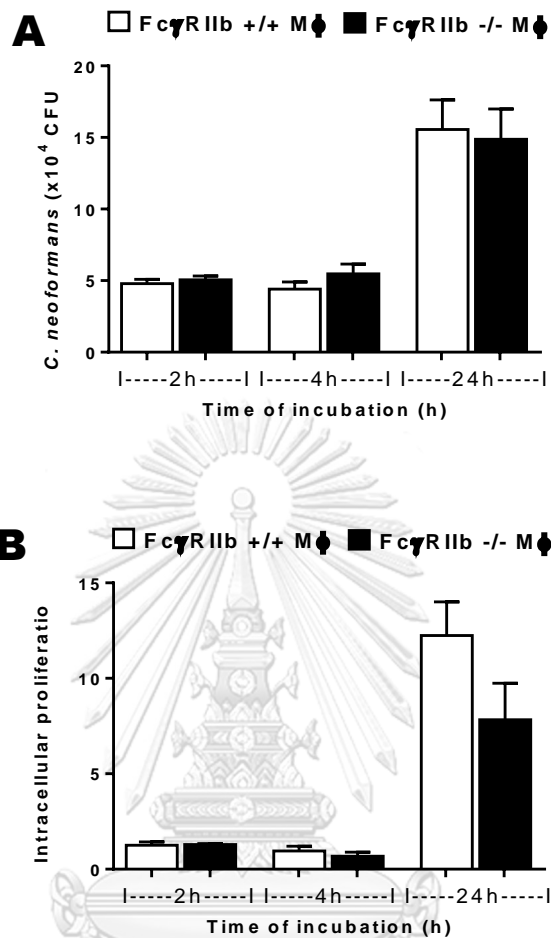
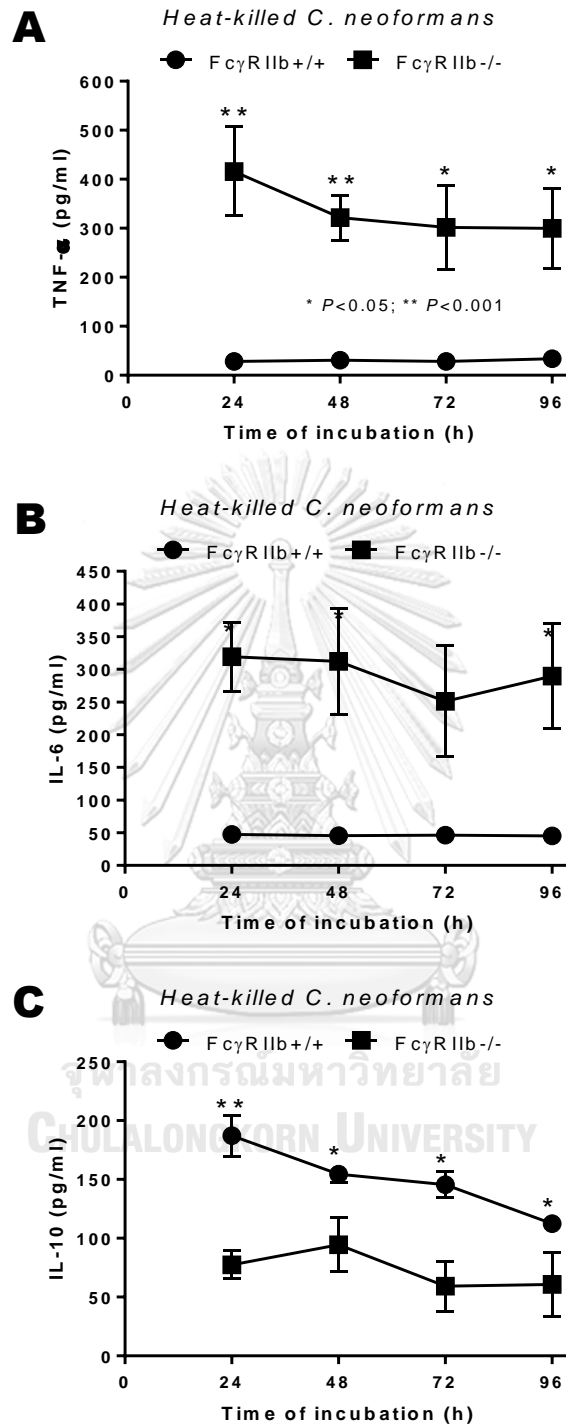


Figure 22. The total killing ability (extruded and intracellular yeast) (A) and intracellular proliferation (concerning only intracellular yeast; see methods) (B) of M $\Phi$  determined by the number of *C. neoformans* colonies after incubation with M $\Phi$  from wild-type and Fc $\gamma$ RIIb<sup>-/-</sup> mice are shown.

To determine function of macrophage with *C. neoformans* by secreted cytokine in vitro. Bone marrow derived macrophages were co-cultured with heat killed (Figure 23A-C) or live *C. neoformans* (Figure 23D-F) at 5:1 (yeast:macrophage) for various time points and then culture supernatant were collected to determine cytokine production by ELISA. The results found that bone marrow derived macrophage from Fc $\gamma$ RIIb<sup>-/-</sup> mice secreted significantly more TNF-alpha and IL-6 than wild type but not IL-10.



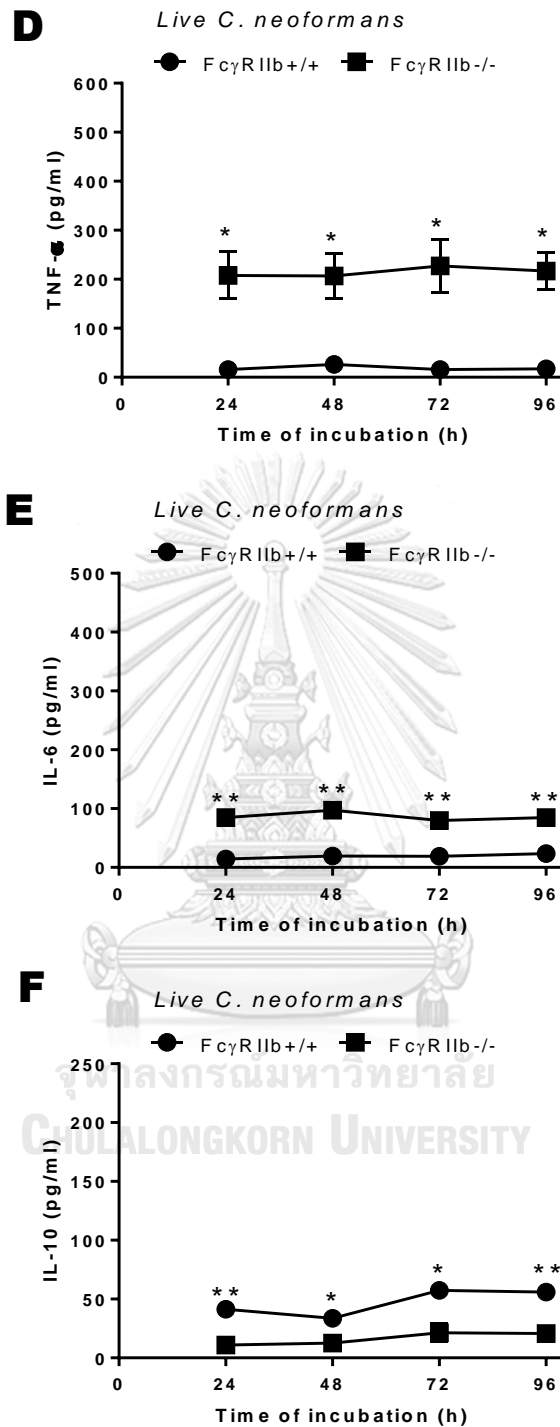


Figure 23. Cytokine levels (TNF- $\alpha$ , IL-6 and IL-10) in the supernatant media from macrophages of Fc $\gamma$ RIIb+/+ or Fc $\gamma$ RIIb-/- mice after activation with heat-killed (A-C) or live *C. neoformans* (D-F) are shown. \*  $p < 0.05$ , \*\*  $p < 0.01$  (experiments were performed in triplicate).

#### 4. FcγRIIb-/- macrophages enhance the dissemination of cryptococci

*C. neoformans* is a facultative intracellular pathogen that demonstrates intracellular viability. Host phagocytes are used for fungal dissemination, and this is referred to as a “Trojan horse” mechanism (214). Observing enhanced phagocytosis capacity but limited killing activity of FcγRIIb-/- macrophages, we hypothesized that FcγRIIb-/- macrophages may be responsible for more severe cryptococcosis *in vivo*. Accordingly, we tested cryptococcosis in FcγRIIb-/- and wild-type mice with liposomal clodronate-induced macrophage depletion (Figure 24) and macrophage depletion were confirmed by immunohistochemistry with anti-F4/80 antibody as show in figure 25. Interestingly, macrophage depletion attenuated the fungal burdens in liver, lung and spleen in FcγRIIb-/-mice, but not in wild-type mice (Figure 26). Fungal burdens at 7 days after fungal administration in the brain, kidney, liver, lung and spleen of FcγRIIb-/- mice with control (PBS) liposomes versus liposomal clodronate were  $2.8 \pm 1.2$ ,  $2.8 \pm 0.9$ ,  $3.7 \pm 1.0$ ,  $4.4 \pm 1.4$  and  $5.5 \pm 0.1$  vs.  $1.9 \pm 1.4$ ,  $1.8 \pm 0.6$ ,  $1.0 \pm 0.2$ ,  $0.9 \pm 0.3$  and  $0.7 \pm 0.2$  ( $\times 10^4$ ) CFU per organ weight (g), respectively (Figure 26). Subsequently, to determine if the high phagocytosis capacity of FcγRIIb-/- macrophages enhanced cryptococcal dissemination, we incubated yeast with wild-type and FcγRIIb-/- macrophages and administered the cells, with the phagocytosed cryptococcal cells, into wild-type mice. Indeed, the fungal burdens both in the brain, a major target organ of cryptococcosis, and in the liver, were higher in mice receiving *Cryptococcus*-containing FcγRIIb-/- cells (Figure 27). The fungal burdens in brain, kidney, liver, lung and spleen at 1 day after the administration of wild-type or FcγRIIb-/- macrophages were  $1.1 \pm 0.2$ ,  $8.3 \pm 2.5$ ,  $15.1 \pm 3.4$ ,  $16.1 \pm 5.3$  and  $20 \pm 7.7$  vs.  $2.9 \pm 0.4$ ,  $31.4 \pm 9.5$ ,  $44.8 \pm 5.2$ ,  $70.7 \pm 31.2$  and  $53.3 \pm 15.7$  ( $\times 10^2$ ) CFU per gram organ weight, respectively (Figure 27).

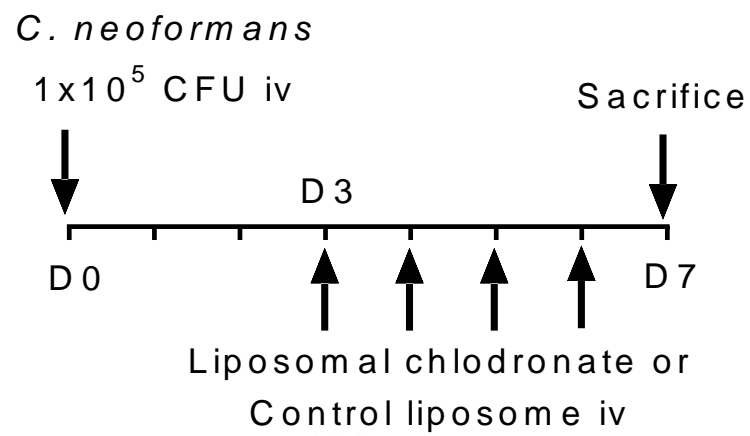


Figure 24 .Timeline of a model for cryptococcosis in liposomal clodronate-induced macrophage depletion in 8-week-old *FcyRIIb*<sup>+/+</sup> and *FcyRIIb*<sup>-/-</sup> mice.

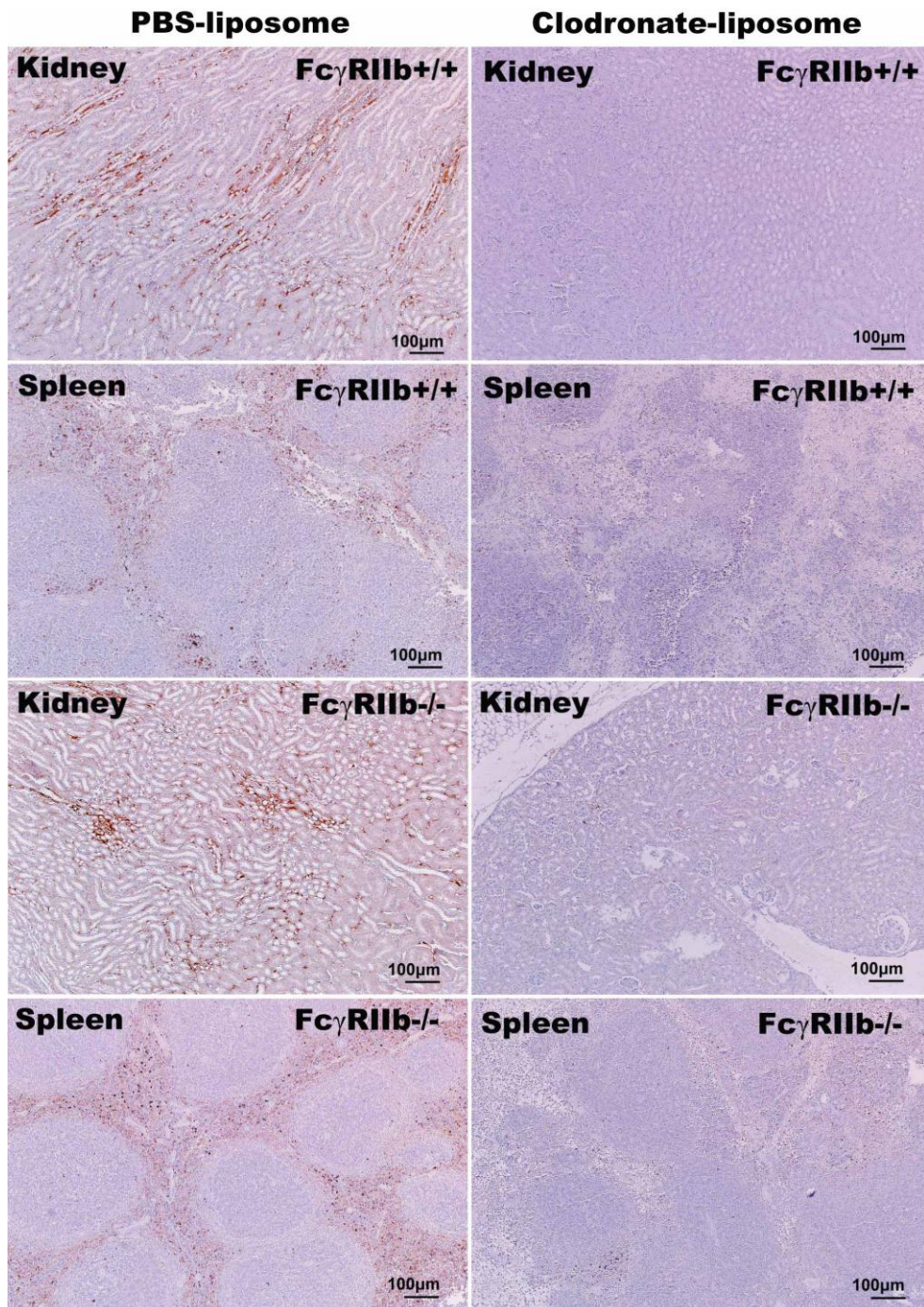
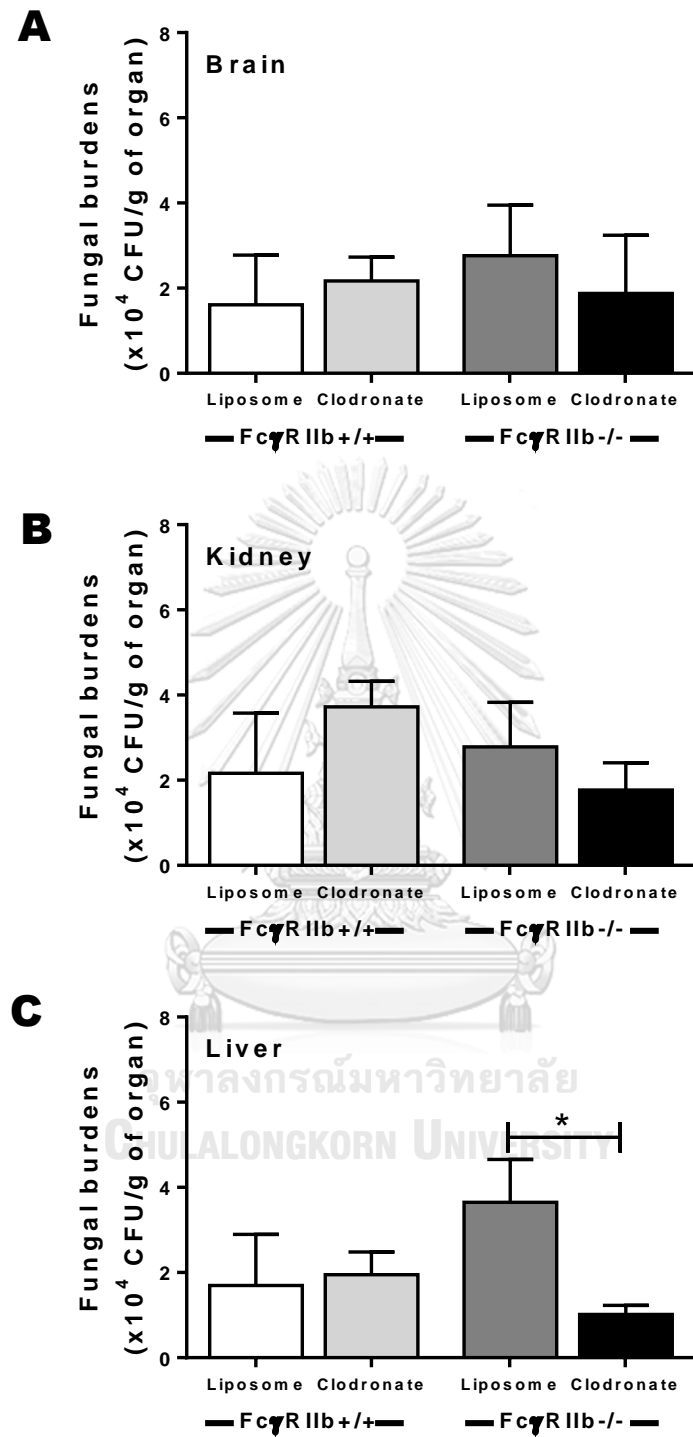


Figure 25. Representative immunohistochemistry analysis of macrophages stained with anti-F4/80 from Fc $\gamma$ RIIb+/+ and Fc $\gamma$ RIIb-/- with and without clodronate administration is shown. Only spleens and kidneys were selected as representative organs and red-brown is anti-F4/80 antibodies binding with macrophage.





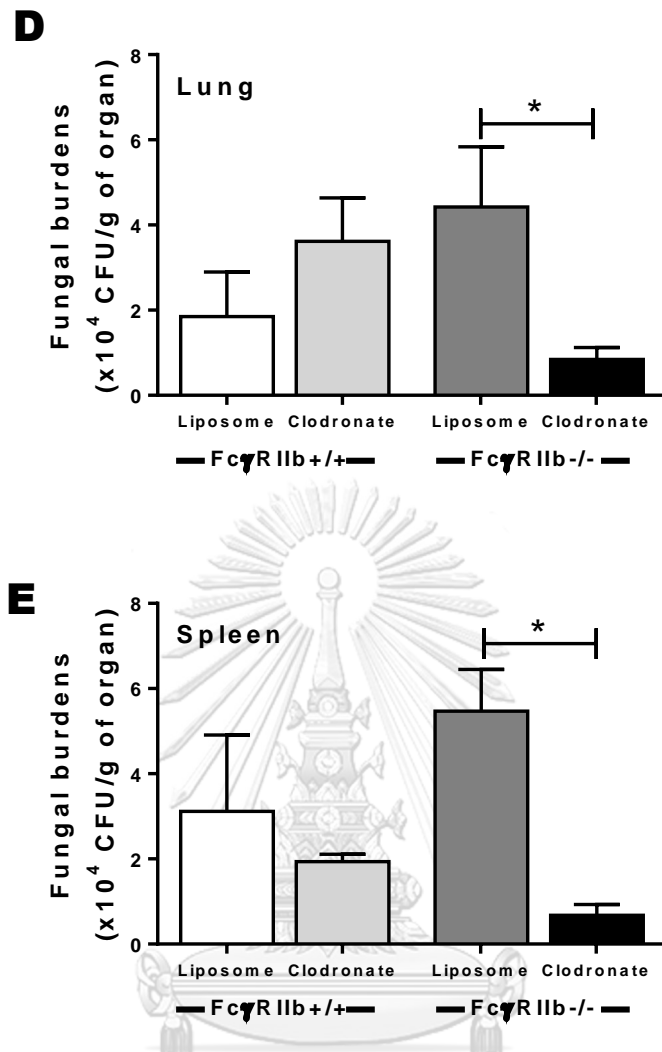


Figure 26. Fungal burdens of cryptococcosis in liposomal clodronate-induced macrophage depletion in 8-week-old Fc $\gamma$ R IIb<sup>+/+</sup> and Fc $\gamma$ R IIb<sup>-/-</sup> mice in brain (A), kidney (B), liver (C), lung (D) and spleen (E) are shown (n = 4-5/group). Data are shown as the mean  $\pm$  SE. \* p<0.05, \*\* p<0.01.

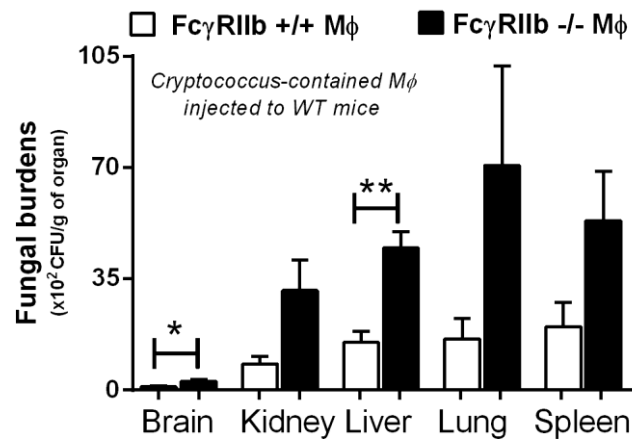


Figure 27. Organ fungal burdens of Fc $\gamma$ RIIb+/+ mice at 24 h after infusion of *Cryptococcus*-containing macrophages (infected macrophages) from Fc $\gamma$ RIIb+/+ and Fc $\gamma$ RIIb-/- mice are shown. (n = 4-5/group). Data are shown as the mean  $\pm$  SE. \* p<0.05, \*\* p<0.01.

##### 5. Cryptococcosis severity in 24-wk-old Fc $\gamma$ RIIb-/- mice (with symptomatic of lupus)

After *C. neoformans* administration, Fc $\gamma$ RIIb-/- mice demonstrated higher mortality than the age-matched wild-type control mice in both the asymptomatic (8-wk-old) and symptomatic lupus groups (24-wk-old). All of the older mice (24-wk-old) with cryptococcosis died or became moribund by 40 and 90 days in the Fc $\gamma$ RIIb-/- and wild-type groups, respectively (Figure 28). Interestingly, at moribund stage, 24-wk-old Fc $\gamma$ RIIb-/- mice also demonstrated higher fungal burdens (Figure 29) and cryptococcoma-like-lesions in several internal organs with significant histology analysis scoring as show in figure 30 and 31 but in wild-type mice the lesions were found in only the brain.

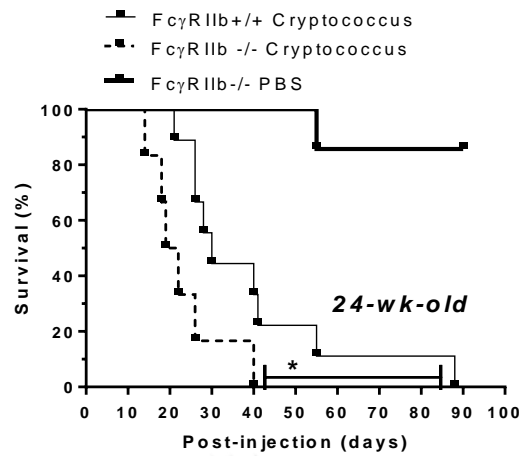


Figure 28. Percent survival in 24-wk-old *FcγRIIb*<sup>-/-</sup> and wild-type mice after challenged with *C. neoformans* ( $n = 9-10/\text{group}$ ). \*  $p < 0.05$ .

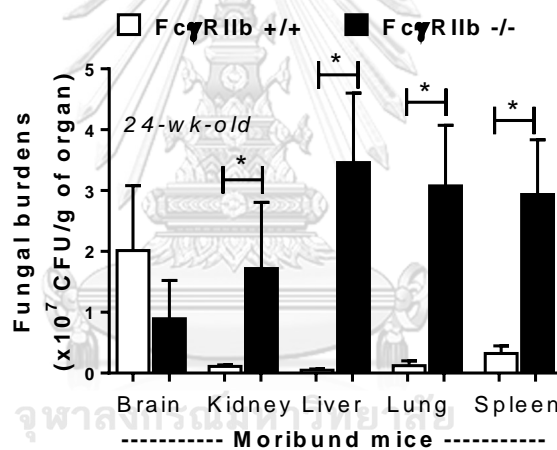


Figure 29. Organ fungal burdens from 24-wk-old *FcγRIIb*<sup>+/+</sup> and *FcγRIIb*<sup>-/-</sup> mice after challenged with *C. neoformans* at moribund stage ( $n = 4-5/\text{group}$ ). \*  $p < 0.05$ .

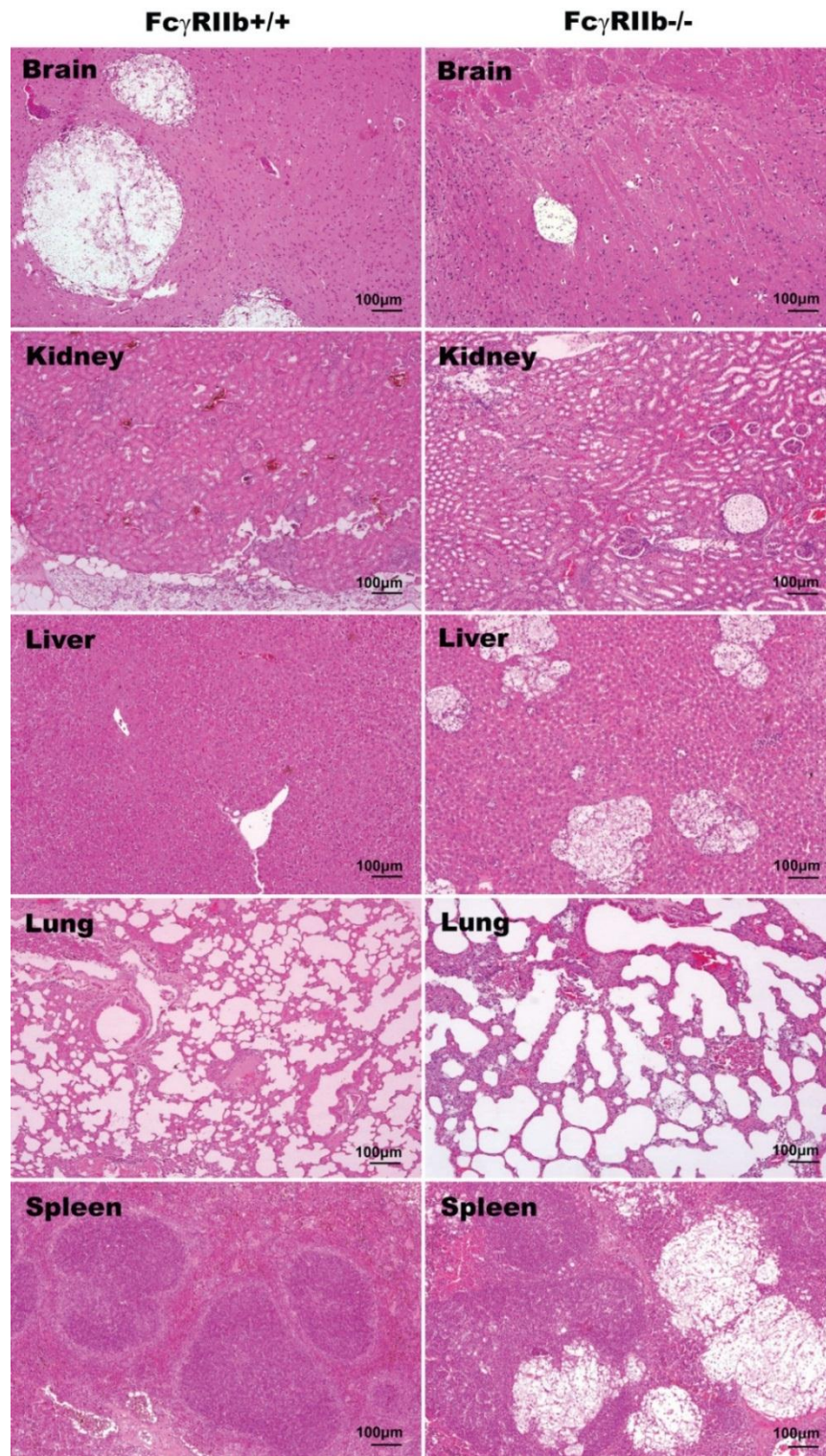


Figure 30. Representative histology with H&E (hematoxylin and eosin staining) at 100x magnification from 24-week-old mice in the moribund stage after *C. neoformans* administration. Fc $\gamma$ RIIb<sup>+/+</sup> mice (left column); Fc $\gamma$ RIIb<sup>-/-</sup> mice (right column)

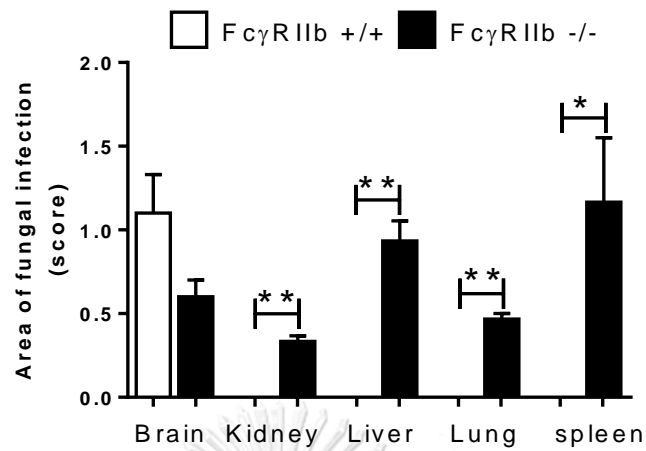
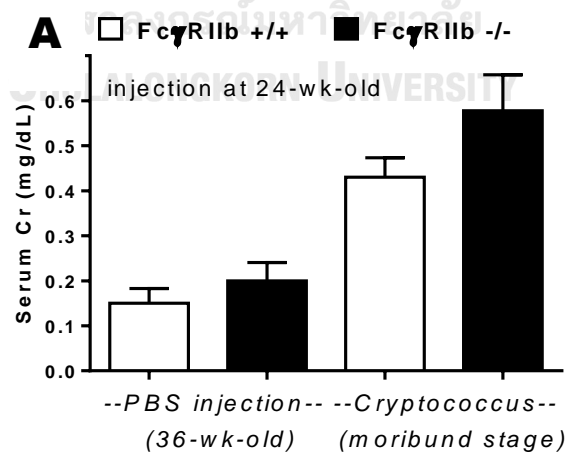
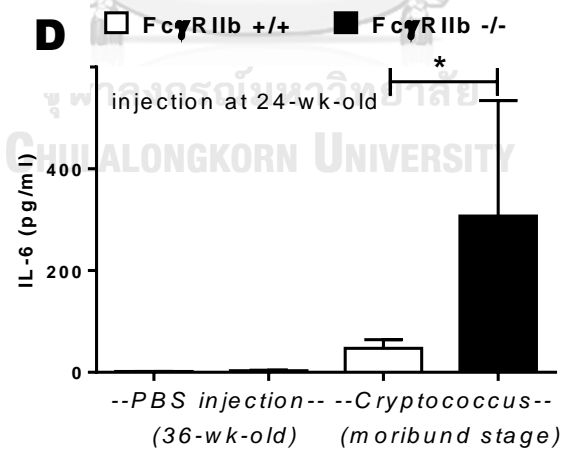
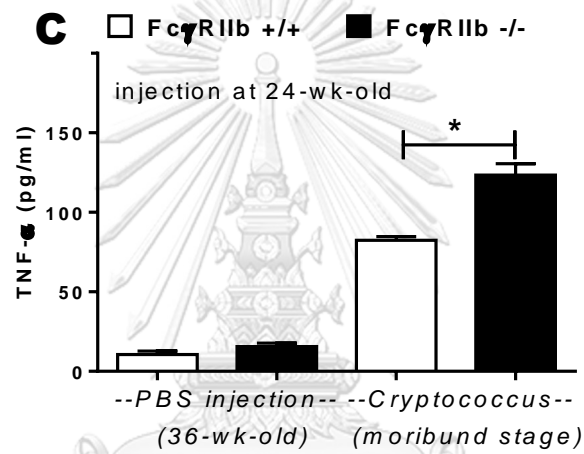
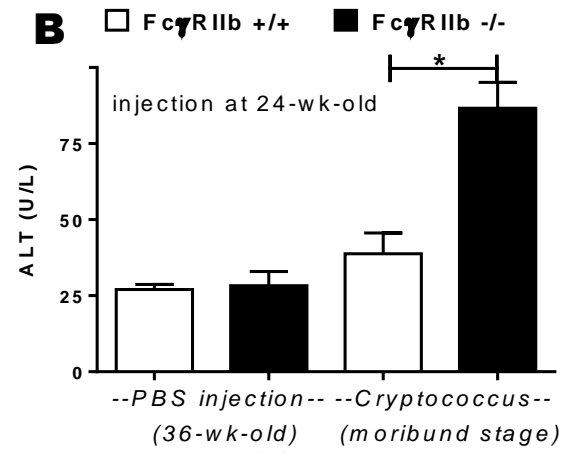


Figure 31. Histology scoring of 24-week-old mice after challenged with *C. neoformans* at moribund stage. The data are shown as the mean  $\pm$  SE ( $n = 4-5$ /group). \*  $p < 0.05$ , \*\*  $p < 0.01$ .

At the moribund stage of 24-wk-old mice, the levels of Scr, ALT and cytokines (TNF- $\alpha$ , IL-6 and IL-10) in wild-type were  $0.43 \pm 0.04$  mg/dl,  $39 \pm 7$  U/L, and  $82 \pm 2$ ,  $47 \pm 16$  and  $327 \pm 50$  pg/ml and in Fc $\gamma$ RIIb-/- old mice were  $0.58 \pm 0.08$  mg/dl,  $87 \pm 9$  U/L and  $123 \pm 7$ ,  $307 \pm 227$  and  $403 \pm 59$  pg/ml (Figure 32. A-E).





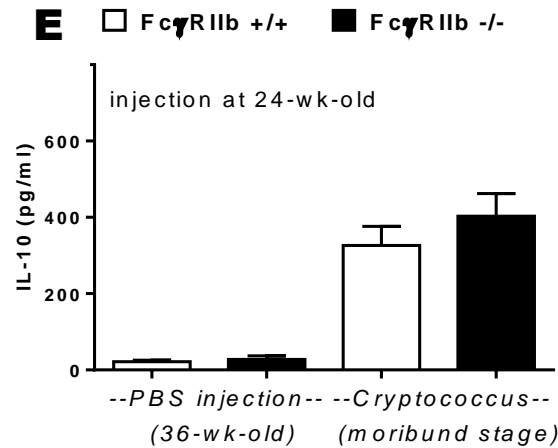


Figure 32. Organ injury and inflammatory cytokines at the moribund stage in 24-week-old as demonstrated by serum creatinine (Scr) (A), alanine transaminase (ALT) (B), TNF- $\alpha$  (C), IL-6 (D) and IL-10 (E) levels. The data are shown as the mean  $\pm$  SE (n=4-5/group). \* p<0.05.

After 2 weeks of cryptococcal infection, the fungal burdens in the internal organs were also higher in 24-wk-old FcγRIIb-/- mice (Figure 33). Cryptococcoma-like lesions were found in most organs in FcγRIIb-/- mice with significant histopathology scoring (Figure 34 and 35), but only in the brain and kidney in wild-type mice.

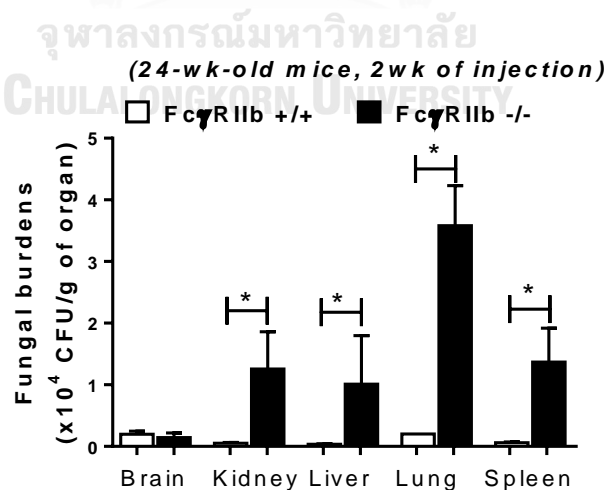


Figure 33. Fungal burdens in the internal organs of 24-week-old mice at 2 weeks post-*C. neoformans* administration. The data are shown as the mean  $\pm$  SE (n = 4-5/group). \* p<0.05.

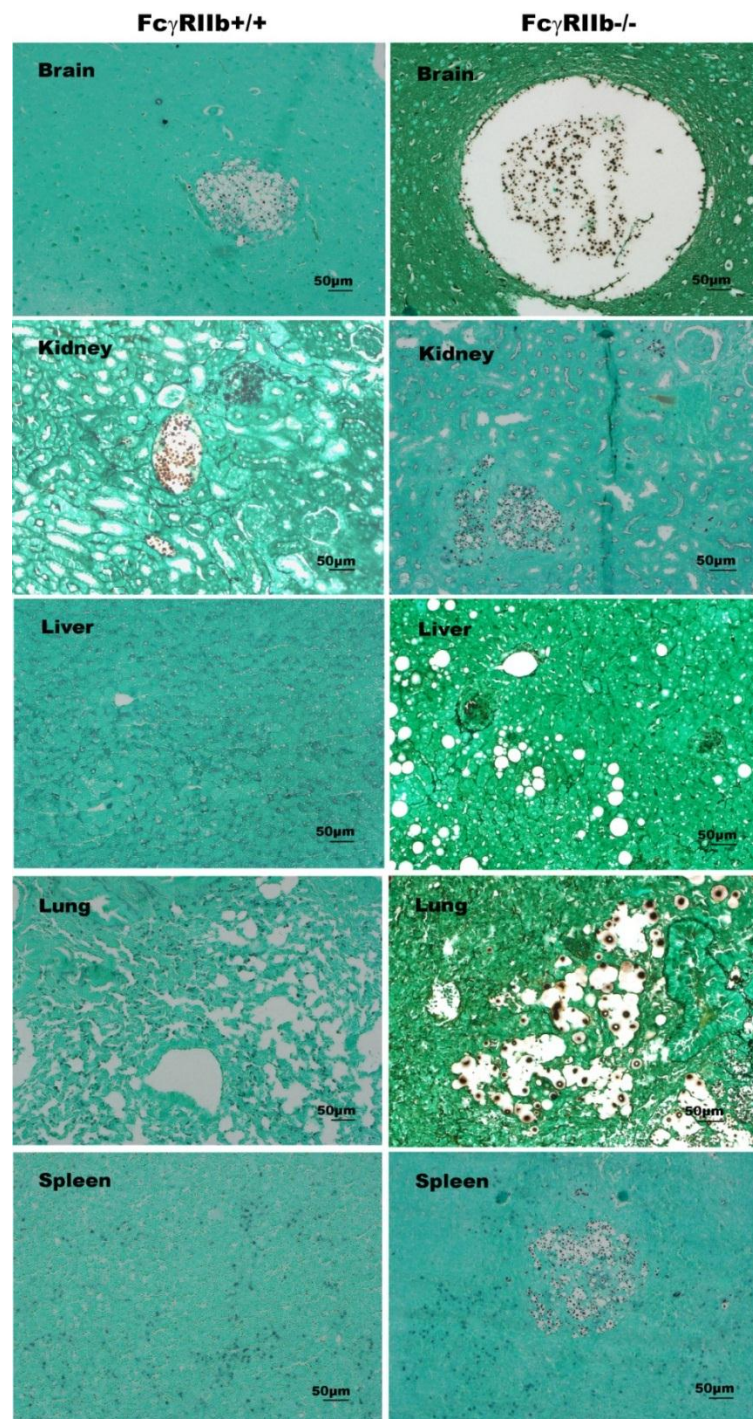


Figure 34. Organ histology with Grocott's silver staining (GMS) at 200x magnification from 24 week-old mice at 2 weeks post-C. neoformans infection, demonstrating cryptococcoma-like lesions in the brain and kidney of Fc $\gamma$ RIIb+/+ mice (left column), and in several internal organs (brain, kidneys, liver, lung and spleen) of Fc $\gamma$ RIIb-/- mice (right column).



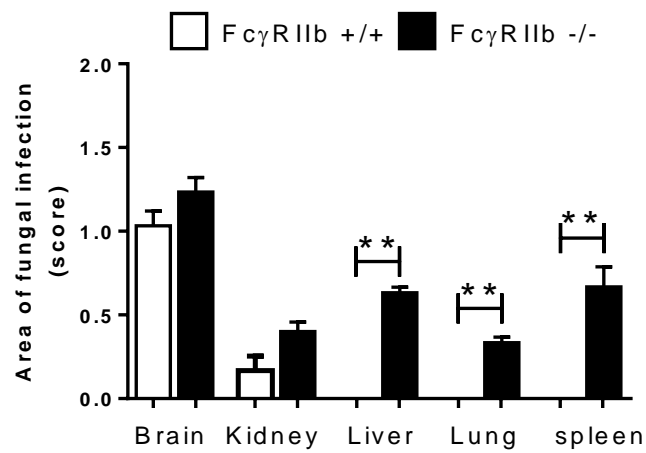
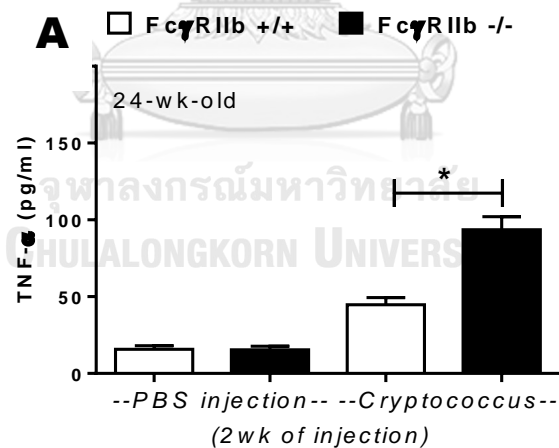


Figure 35. Histology scoring of 24 week-old mice at 2 weeks post-*C. neoformans* infection. The data are shown as the mean  $\pm$  SE (n = 4-5/group). \* p<0.05, \*\* p<0.01.

To determine secreted cytokine in serum found that 24-wk-old Fc $\gamma$ RIIb-/- mice are significantly more TNF-alpha and IL-6 production in serum but not IL-10 at 2 weeks of infection (Figure 36).



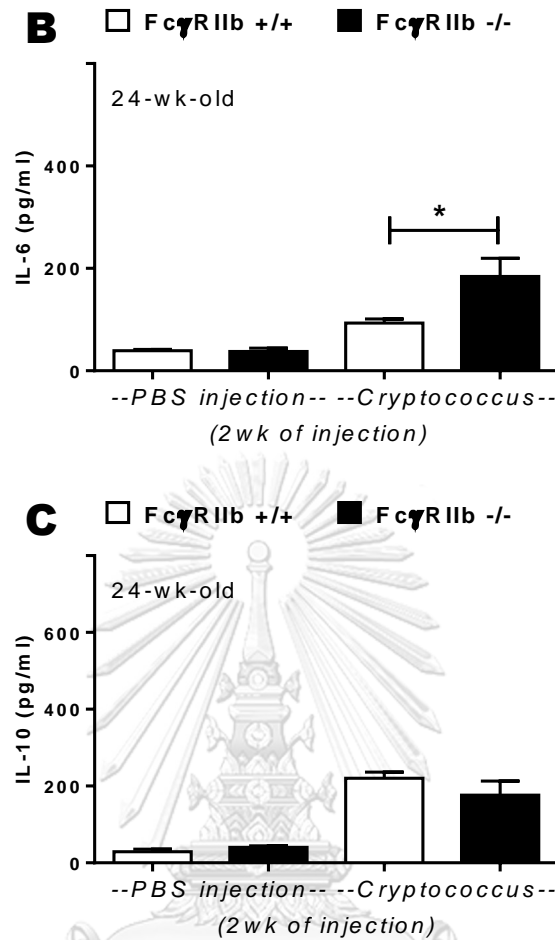


Figure 36. Serum cytokines measured include TNF- $\alpha$  (A), IL-6 (B) and IL-10 (C). The data are shown as the mean  $\pm$  SE ( $n = 4-5$ /group). \*  $p < 0.05$ .

Both asymptomatic and symptomatic of lupus FcγRIIb<sup>-/-</sup> mice also show high severity of cryptococcosis than wild-type counterpart. The cryptococcosis, either at 2 weeks or when moribund, was more severe in FcγRIIb<sup>-/-</sup> than wild-type mice, as demonstrated by higher fungal burdens in most internal organs, higher liver enzyme levels, and higher pro-inflammatory cytokine levels but not higher anti-inflammatory cytokine levels. Therefore, high cryptococcosis severity in FcγRIIb<sup>-/-</sup> mice depend on lack of FcγRIIb function and lupus symptomatic independent.

## 6. T cells analysis from spleen

Because of the *in vivo* association between macrophage and T cell, we analyzed T cells from spleen in  $Fc\gamma RIIb^{-/-}$  and wild-type mice. The total number of Th cell ( $CD3+CD4+CD8^{-}$ ) in spleen was more predominant in  $Fc\gamma RIIb^{-/-}$  mice than the wild-type. (Figure 37 and 40). In contrast, the naïve Th cell ( $CD44-CD62L+$ ) and the central memory Th cell (Tcm,  $CD44+CD62L+$ ) of wild-type were higher than  $Fc\gamma RIIb^{-/-}$  mice (Figure 39 and 40). Moreover, the populations of active Th cell such as effector Th cell (Tem,  $CD44+CD62L^{-}$ ) and the Th cell with intracellular  $IFN-\gamma$  ( $CD3+CD4+IFN\gamma+$ ) (Figure 38, 41, 42), a cytokine of macrophage activation, were predominant in  $Fc\gamma RIIb^{-/-}$  mice except activated Th cell ( $CD4+CD69+$ ) that show not significant difference (Figure 39 and 40).

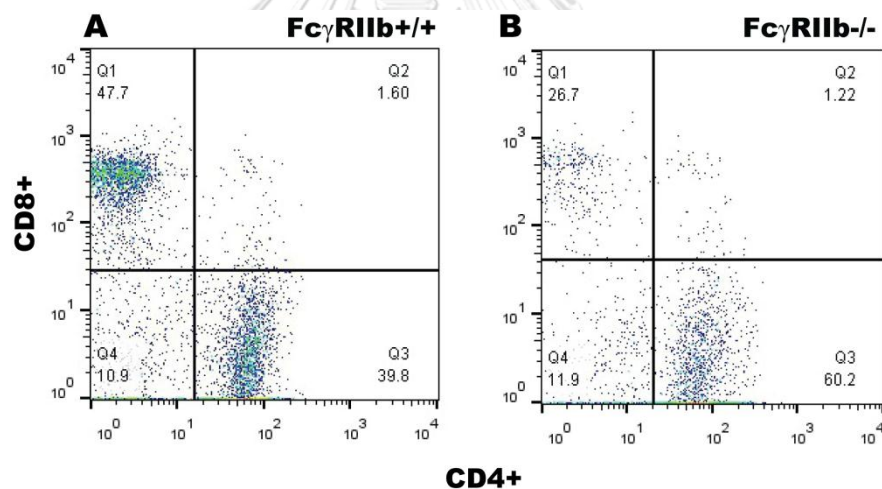


Figure 37. The representative result of total number of Th cell ( $CD3+CD4+CD8^{-}$ ) from spleen of wild-type ( $Fc\gamma RIIb^{+/+}$ ) and  $Fc\gamma RIIb^{-/-}$  mice by flow cytometry ( $n=4/group$ )

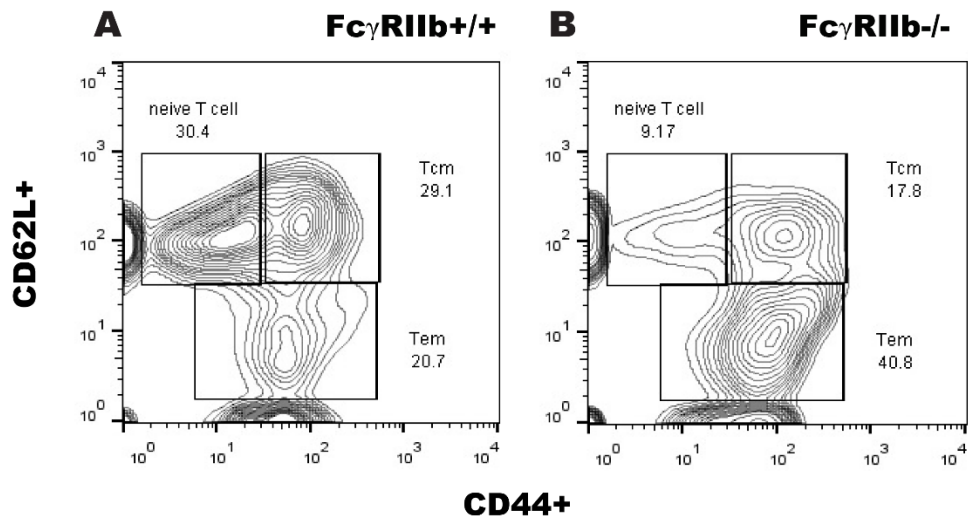


Figure 38. The representative result of naive Th cell (CD44-CD62L+), central memory Th cell (Tcm, CD44+CD62L+), effector Th cell (Tem, CD44+CD62L-) from spleen of wild-type (Fc $\gamma$ RIIb<sup>+/+</sup>) and Fc $\gamma$ RIIb<sup>-/-</sup> mice by flow cytometry (n=4/group).

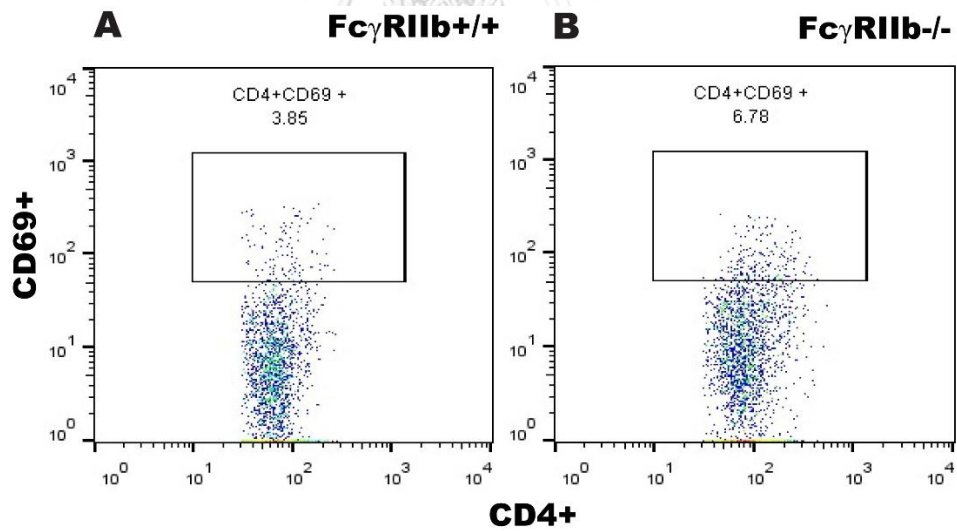


Figure 39. The representative result of activated Th cell (CD4+CD69+) from spleen of wild-type (Fc $\gamma$ RIIb<sup>+/+</sup>) and Fc $\gamma$ RIIb<sup>-/-</sup> mice by flow cytometry (n=4/group).

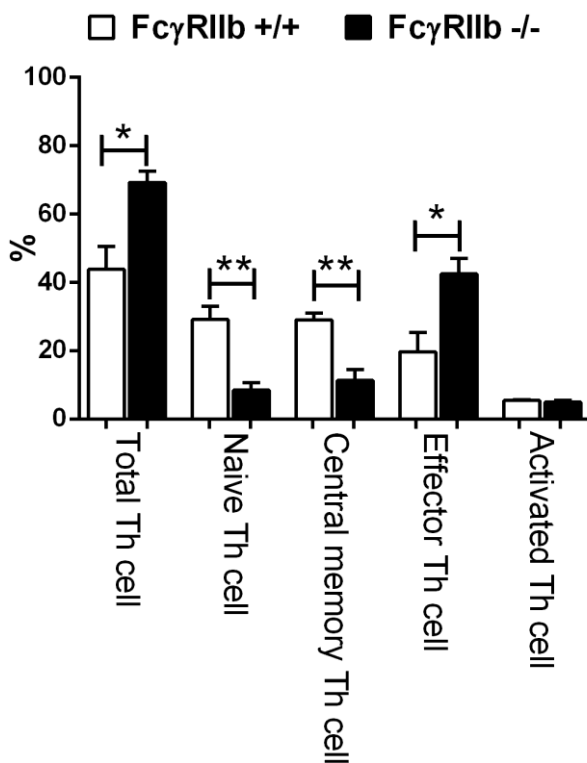


Figure 40. The spleen analysis for total of Th cell (CD3+CD4+CD8-), naive Th cell (CD44-CD62L+), central memory Th cell (Tcm, CD44+CD62L+), effector Th cell (Tem, CD44+CD62L-) and activated Th cell (CD4+CD69+) from wild-type (FcγRIIb+/+) and FcγRIIb-/- mice by flow cytometry (n=4/group). Data are shown as the mean ± SE. \* p<0.05, \*\* p<0.01.

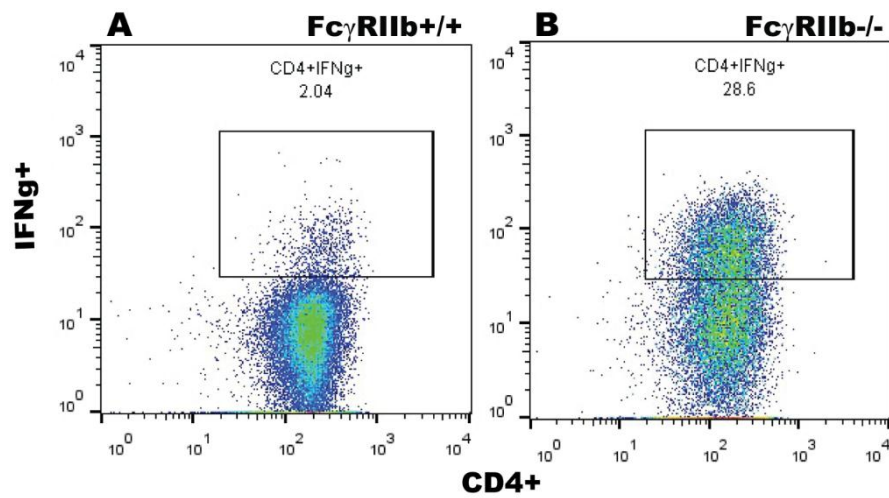


Figure 41. The representative result of an intracellular IFN- $\gamma$  of Th cell (CD3+CD4+IFN $\gamma$ +) from spleen of wild-type (FcyRIIb+/+) and FcyRIIb-/- mice by flow cytometry (n=4/group).

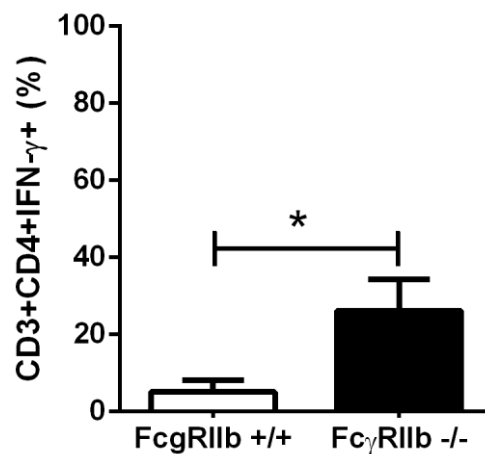


Figure 42. The spleen analysis for an intracellular IFN- $\gamma$  of Th cell (CD3+CD4+IFN $\gamma$ +) from wild-type (FcyRIIb+/+) and FcyRIIb-/- mice by flow cytometry (n=4/group). Data are shown as the mean  $\pm$  SE. \*  $p < 0.05$ .

Therefore, the Th cell analysis from spleen of wild-type and FcyRIIb-/- mice suggested that the high susceptibility of cryptococcosis in FcyRIIb-/- mice depend on the function of FcyRIIb-/- macrophage and independent from Th cell activity related macrophage function.

## 7. Comparison of cryptococcosis severity in lupus FcγRIIb-/- and pristane mice

To test the severity of cryptococcosis in lupus, *C. neoformans* were administered in 6-month-old mice of both lupus models and in age-matched wild-type. In parallel, PBS injection in 6 month-old mice of these 3 groups was used as the control. After 3 months of PBS injection, there was no mortality in either lupus mice or wild-type groups. But, with the fungal administration, all mice in pristane and FcγRIIb-/- mice died within 55 and 47 days, respectively, and the mortality was demonstrated as early as 20 days of the administration (Figure 43A). Cryptococcosis in the wild-type showed 87% mortality rate (7 in 8 mice died) and the mortality started after the 1<sup>st</sup> month of fungal administration (Figure 43A). Fungal burdens in all of the selected internal organs (except for brain) of lupus mice were higher than the wild-types without the difference between pristane and FcγRIIb-/- (Figure 43B). Similarly, the semi-quantitative histopathology analysis of infected area of FcγRIIb-/- was not different from pristane (Figure 43C, 44). In addition, cryptococcal infection in both lupus models induced prominent serum inflammatory cytokines in comparison with the wild-types (Figure 43D-F).

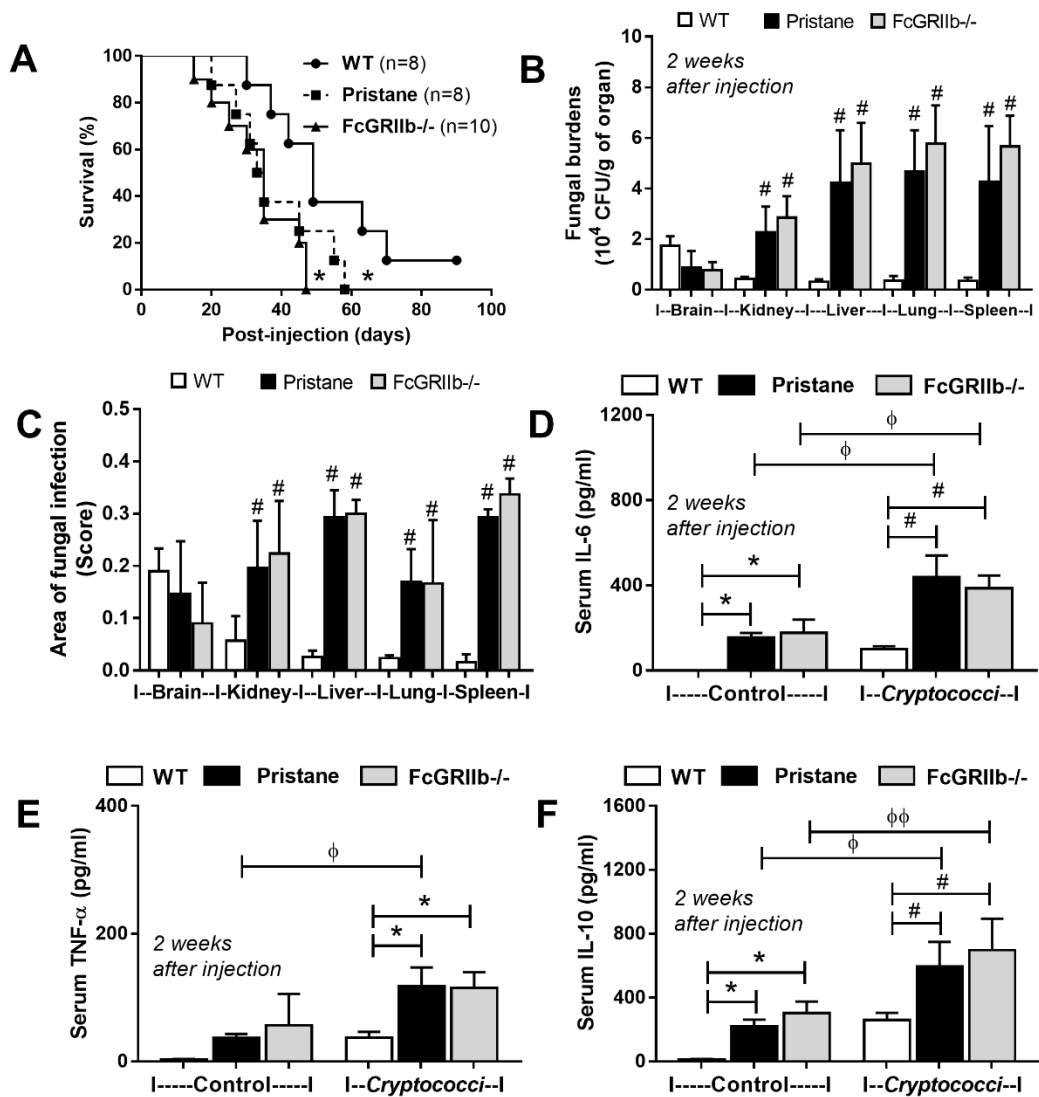


Figure 43. The severity of cryptococcosis in pristane, FcγRIIb<sup>-/-</sup> and wild-type mice as determined by the mortality rate (A), fungal burdens in the internal organs (B), area of the fungal infection in the internal organs from Grocott's silver staining (GMS) (C) and serum cytokines (IL-6, TNF-α and IL-10; D-F) were demonstrated. (n= 8-10/group in A and 5-6/ group in B-F); \*, p<0.05 vs. wild-type; #, p<0.001 vs. wild-type; Φ, p<0.05; ΦΦ, p<0.01



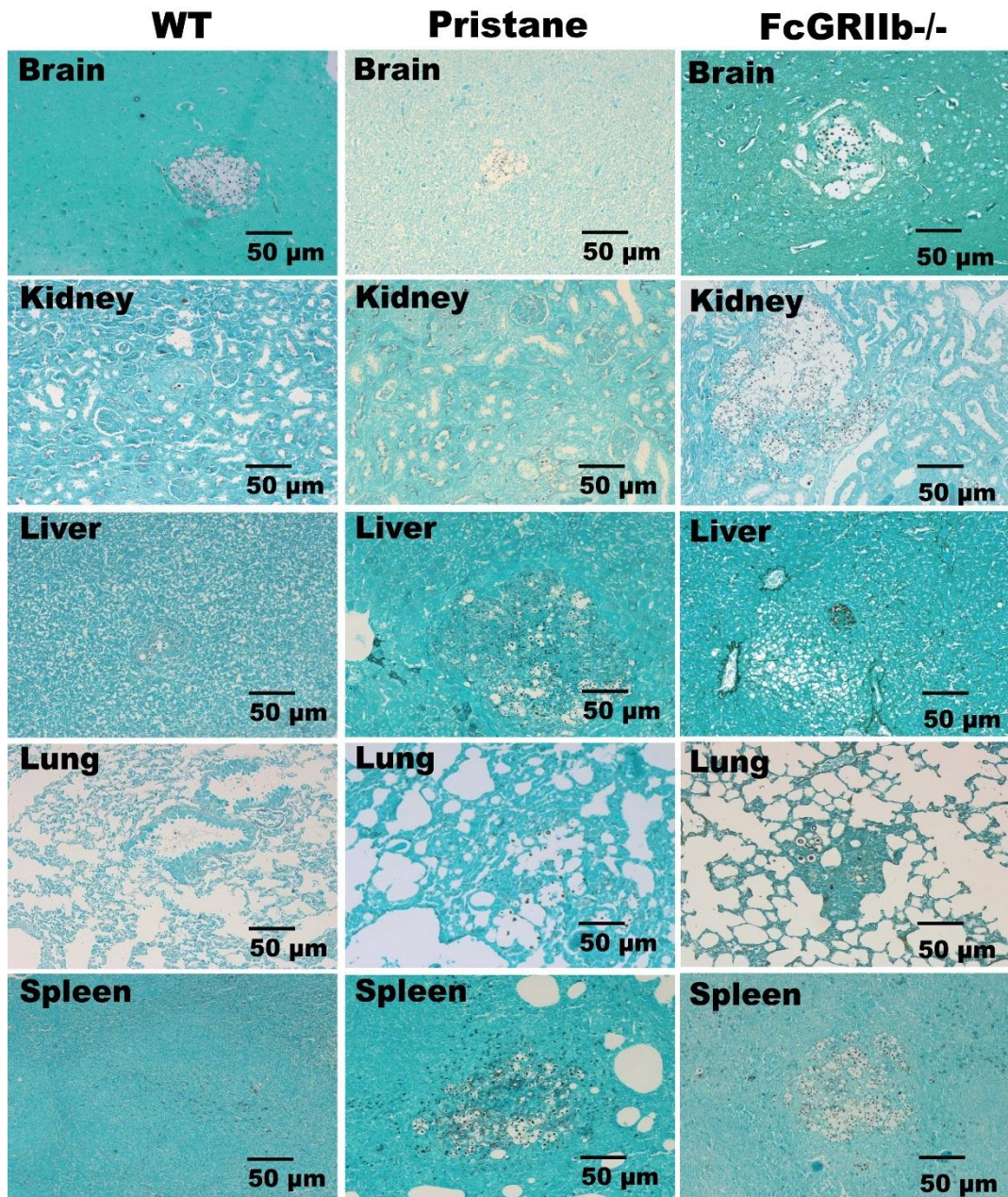


Figure 44. Representative organ histology with Grocott's silver staining (GMS) at 200x magnification from 6-month-old mice at 2 weeks post-*C. neoformans* infection, demonstrating tumor-like lesions in brain of the wild-type mice (left column), and in several internal organs (brain, kidneys, liver, lung and spleen) of pristane (middle column) and *Fc $\gamma$ RIIb<sup>-/-</sup>* mice (right column).

The analysis of macrophage and T helper (Th) cell were performed because of the importance of these cells for the organism control of cryptococcosis (9, 148, 215-217). As such, the macrophage phagocytosis of Fc $\gamma$ R11b<sup>-/-</sup> and pristane was more predominant than wild-types as early as 2h after the incubation by both methods of phagocytosis assays (Figure 45A, B). But, the macrophage killing activity as demonstrated by intracellular proliferation test was not different among these groups (Figure 45C). Hence, it is possible that severe cryptococcosis in both lupus mice is a result of the prominent phagocytosis and limited killing activity of macrophage.



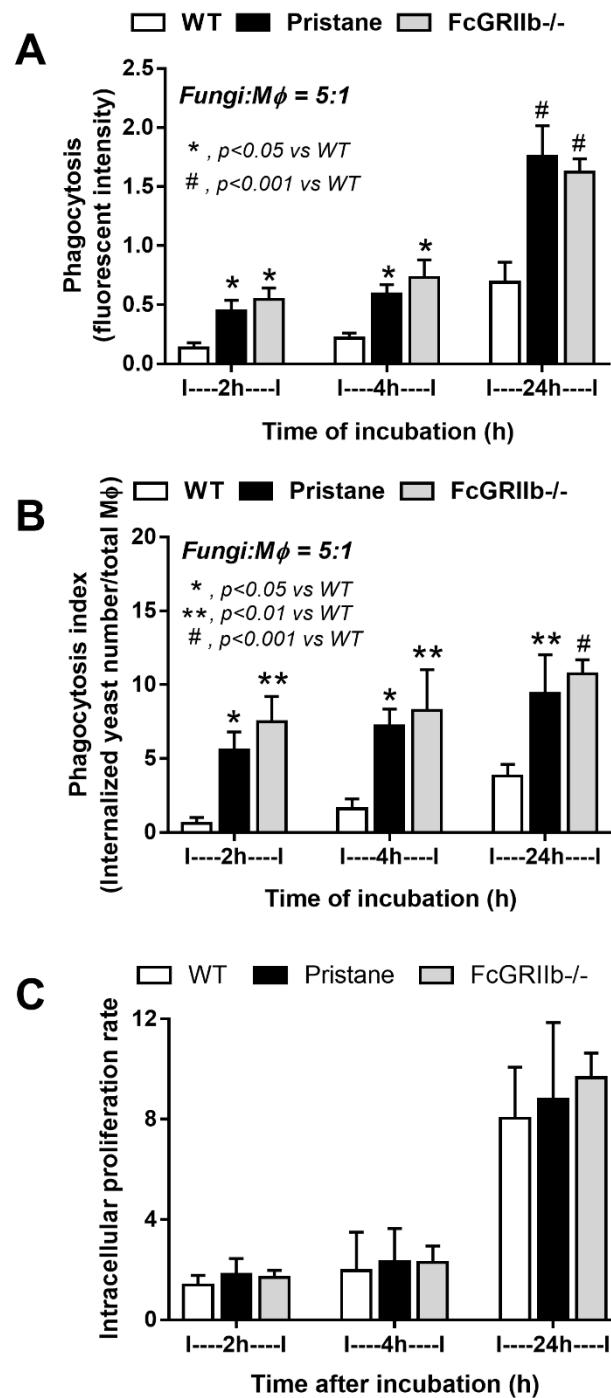
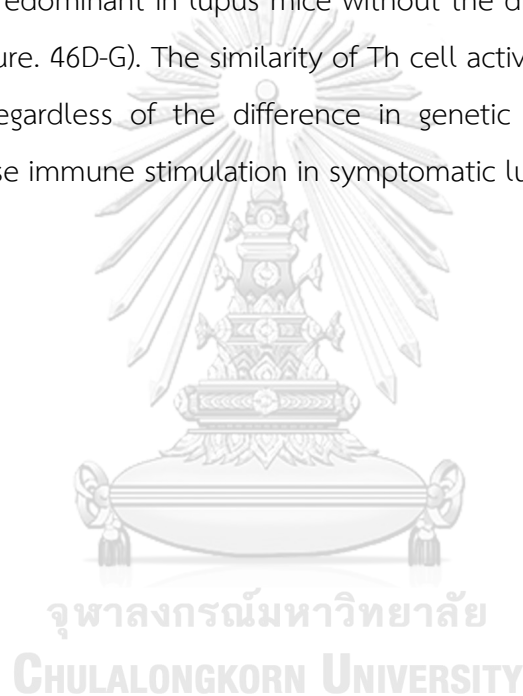


Figure 45. The phagocytosis as determined by fluorescent-conjugated fungi (A) and live-fungi (B) with the killing activity (B) of macrophage in the response against *C. neoformans* were demonstrated (experiments were performed in triplicate).

Because of the *in vivo* association between macrophage and T cell, we analyzed T cells from spleen of 6-month-old mice in all experimental groups. The total number of Th cell in spleen was more predominant in FcγRIIb<sup>-/-</sup> mice than the mice with normal group and pristane treatment (Figure 46A). On contrary, the naïve Th cell and the central memory Th cell of wild-type were higher than pristane implying the role of immune stimulation of pristane model (Figure 46B, C). More importantly, the populations of active Th cell (effector Th cell, activated Th cell and Th cell with ICOS expression) and the Th cell with intracellular IFN-γ (a cytokine of macrophage activation) were predominant in lupus mice without the difference between pristane and FcγRIIb<sup>-/-</sup> (Figure. 46D-G). The similarity of Th cell activities between pristane and FcγRIIb<sup>-/-</sup> mice, regardless of the difference in genetic backgrounds, implied the influence of intense immune stimulation in symptomatic lupus.



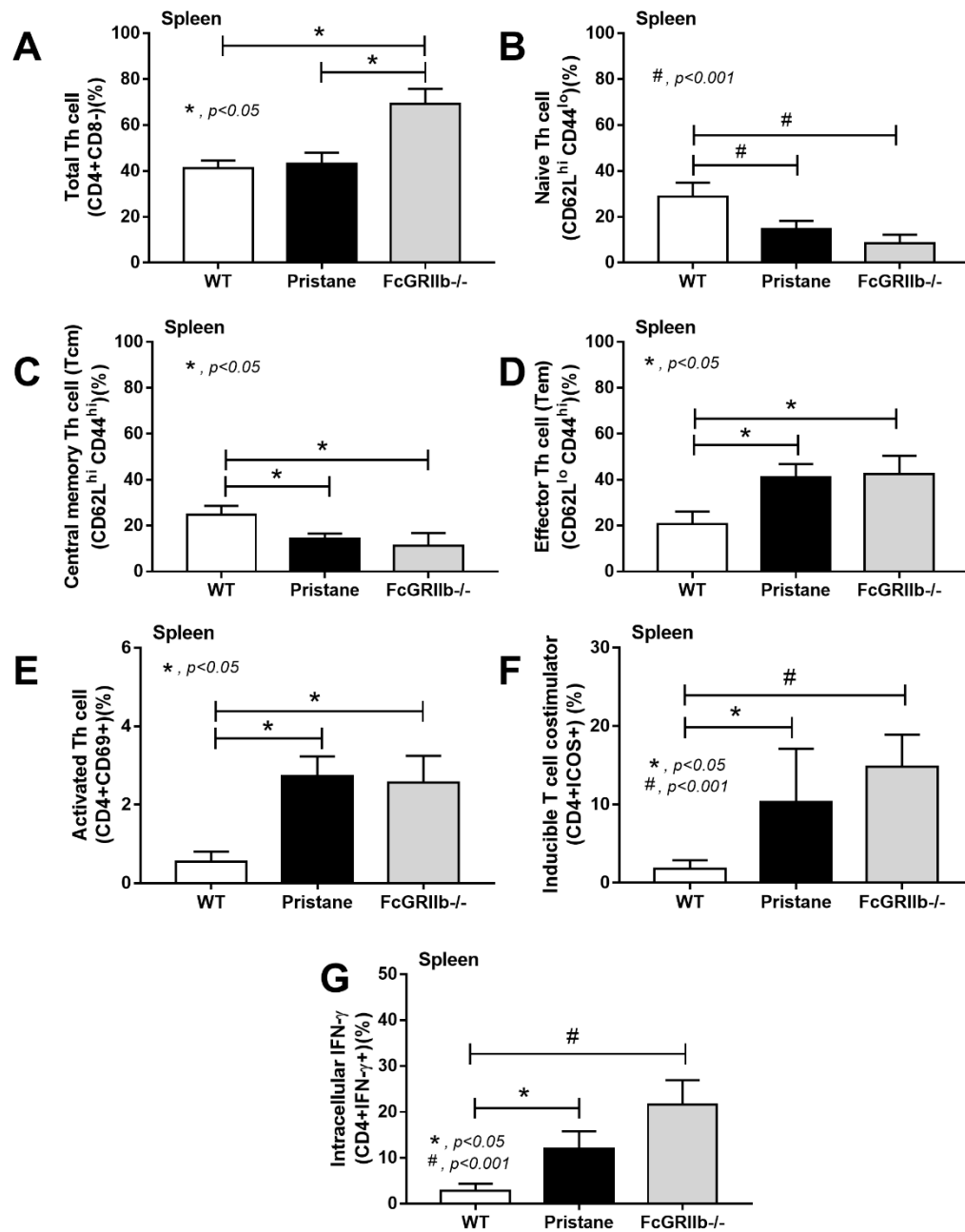


Figure 46. The analysis of spleen from wild-type, pristane and Fc $\gamma$ RIIb<sup>-/-</sup> mice by flow cytometry demonstrated total Th cell (CD3<sup>+</sup>CD4<sup>+</sup>CD8<sup>-</sup>) (A), naive Th cell (CD44<sup>+</sup>CD62L<sup>+</sup>) (B), central memory Th cell (CD44<sup>+</sup>CD62L<sup>+</sup>) (C), effector Th cell (CD44<sup>+</sup>CD62L<sup>-</sup>) (D), activated Th cell (CD4<sup>+</sup>CD69<sup>+</sup>) (E) and Th cell with inducible T cell co-stimulator (CD4<sup>+</sup>ICOS<sup>+</sup>) (F) (n=4-6/group). In addition, the intra-cellular IFN- $\gamma$  of Th cell was also demonstrated (G) (n=4-6/group). IFN, interferon

In order to support the prominent immune stimulation in lupus models, several serum cytokines were measured. Indeed, the pro-inflammatory cytokines (IL-1 $\alpha$  and IL-1 $\beta$ ), the cytokines of macrophage-activation (IL-12p70, IL-27, MCP-1 and GM-CSF), the Th cell-cytokines (IL-17, IFN- $\gamma$ ) and the cytokine of lupus pathogenesis (type I interferon: IFN- $\beta$ ) were higher in lupus mice without the difference between Fc $\gamma$ R11b-/- and pristane (Figure. 47). These results supported the prominent pro-inflammation and the enhanced macrophage-Th cell activation of lupus mice over the wild-types.

Moreover, *C. neoformans* infection activated active Th cells (activated Th cell, Th cell with ICOS and Th cell with IFN- $\gamma$ ) more extensively in Fc $\gamma$ R11b-/- and pristane than the wild-type (Figure 48). While *C. neoformans* induced all subtype of the selected active Th cell in both pristane mice and Fc $\gamma$ R11b-/-, the fungi activated only Th cell with ICOS in the wild-type (Figure 48). In addition, Th cell with ICOS and IFN- $\gamma$  in spleen in Fc $\gamma$ R11b-/- mice were higher than pristane implying an impact of the gene deficiency on top of the infection (Figure 48B, C).

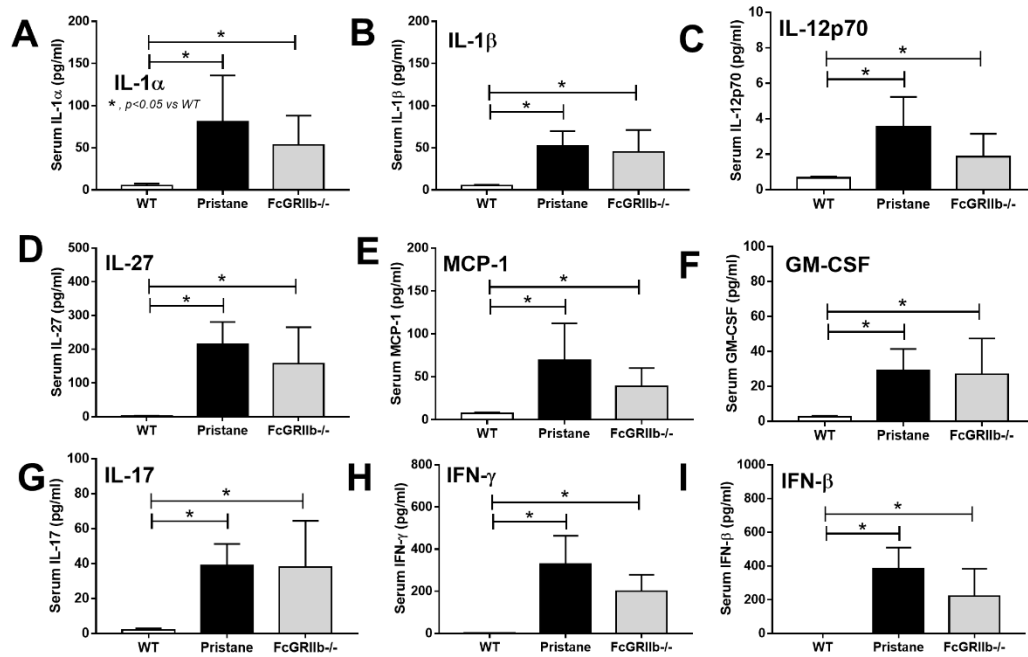


Figure 47. The analysis of serum cytokines, in panels, from wild-type, pristane and FcγRIIb<sup>-/-</sup> mice by a Luminex-based multiplex method was demonstrated (n=5-7/group). IL, interleukin; MCP-1, monocyte chemoattractant protein-1; GM-CSF, granulocyte-macrophage colony stimulating factor; IFN, interferon

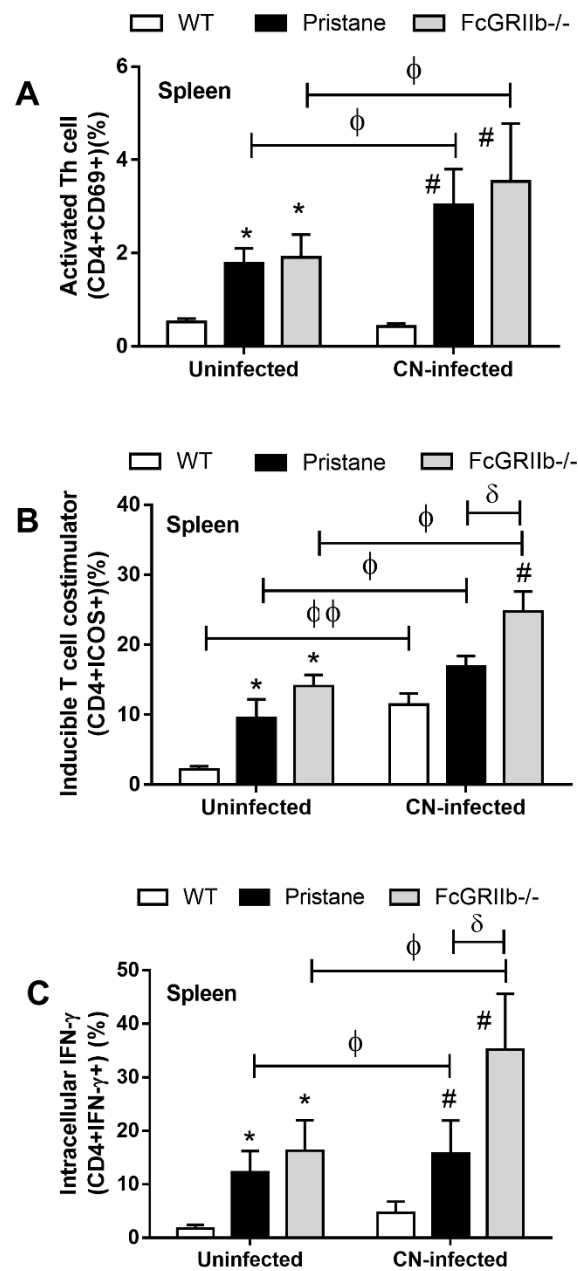


Figure 48. The analysis of spleen from wild-type, pristane and *FcγRIIb*<sup>-/-</sup> mice after 2 week of the administration by phosphate buffer saline control (uninfected) or *C. neoformans* (CN-infected) with flow cytometry demonstrated activated Th cell ( $CD4^+CD69^+$ ) (A), Th cell with inducible T cell co-stimulator ( $CD4^+ICOS^+$ ) (B) and Th cell with intra-cellular  $IFN-\gamma$  ( $n=5-7/group$ ).  $IFN$ , interferon; \*,  $p<0.05$  vs. wild-type; #,  $p<0.001$  vs. wild-type;  $\Phi$ ,  $p<0.05$ ;  $\Phi\Phi$ ,  $p<0.01$ ;  $\delta$ ,  $p<0.05$ .



## CHAPTER VI

### DISCUSSION

Fc $\gamma$ R polymorphisms have previously found an association with increased susceptibility to some infectious disease, including cryptococcosis (15-17). An association between Fc $\gamma$ R11b polymorphism and cryptococcal meningitis was found (17). We demonstrated that the increased severity of cryptococcosis in Fc $\gamma$ R11b $^{-/-}$  mice is, at least in part, due to the unique properties of Fc $\gamma$ R11b $^{-/-}$  macrophages include enhanced phagocytosis and elevated pro-inflammatory cytokine responses.

Although inhalation of cryptococcal spores is the common route of infection, however cryptococcosis mouse model with intravenous administration is appropriate for a proof model to demonstrate the difference between the Fc $\gamma$ R11b $^{-/-}$  and wild-type counterparts. Indeed, Fc $\gamma$ R11b $^{-/-}$  mice showed more severe cryptococcosis than wild-type mice.

The cell-mediated immunity is predominantly control fungal infection. The defunctioning of Fc $\gamma$ R11b, the only inhibitory receptor in the Fc $\gamma$ R family, result in lack of inhibitory signal to control immune response by these Fc $\gamma$ R family. Therefore, defect in Fc $\gamma$ R11b enhance immune response and effectively controls several infectious organisms (21, 23, 25).

Because Fc $\gamma$ R11b $^{-/-}$  mice are prone to spontaneous lupus manifestations with age dependent characteristics, the study in different age of mice allow the experiment on symptomatic and asymptomatic lupus. To study the role of Fc $\gamma$ R11b function without effect of symptomatic lupus characteristics, we used Fc $\gamma$ R11b $^{-/-}$  mice at 2-month-old mice which were asymptomatic lupus as determined by negative proteinuria and non-elevated anti-dsDNA. In this study, we were shown that Fc $\gamma$ R11b $^{-/-}$  mice were more susceptible to cryptococcosis compared to wild-type counterparts. There was difference in survival rate between the Fc $\gamma$ R11b $^{-/-}$  and wild-type. The severity of cryptococcosis in Fc $\gamma$ R11b $^{-/-}$  mice was independent of amount of CD4 $^{+}$  T cell. These result support the susceptibility to cryptococcosis of patients with Fc $\gamma$ R11b polymorphisms (17, 198, 199). Subsequently, the severity of cryptococcosis was

evaluated with different parameters at 2 weeks, the earlier stage of infection, and in the moribund stage. Disseminated cryptococcosis, including fungal organisms found in several internal organs, which was observed in FcγRIIb<sup>-/-</sup> mice, was similar to the disseminated cryptococcosis observed in patients with compromised immune systems (218). However, the lesions were limited mostly to the brain in wild-type mice, a major target organ (219), as usually observed in the immunocompetent human host.

Surprisingly, despite the absence of generalized lesions in wild-type mice, the brain lesions were larger than in FcγRIIb<sup>-/-</sup> mice. This difference remains to be investigated. It seems that the neurotropism characteristic of *C. neoformans* is not apparent in the infection in FcγRIIb<sup>-/-</sup> mice because the organism could survive in any organ. However, in wild-type mice, *C. neoformans* may prefer to grow in the brain because of more suitable nutritional conditions (220-222).

FcγRIIb<sup>-/-</sup> mice was also more severe liver injury with enhanced pathogenesis result in cryptococcal disseminated disease and enhanced cryptococcal dissemination in the FcγRIIb<sup>-/-</sup> mice underscores the role of this genetic lesion in pathogenesis. Additionally, the inflammatory cytokines, TNF- $\alpha$  and IL-6, but not IL-10, were higher in FcγRIIb<sup>-/-</sup> than wild-type mice. This is a response to the higher fungal burden, in addition to the anti-inflammatory defect. Serum IL-10 is too low to balance out the pro-inflammatory immune responses, leading to more severe organ histopathology and symptoms.

Macrophages and T helper cells are the main immune cells responsible for the immune response to cryptococcosis(148, 217). FcγRIIb is present in macrophages but not in T cells(167) and the study on T cell subpopulation in FcγRIIb<sup>-/-</sup> mice found that these mice were not CD4<sup>+</sup> T cell deficiency. Therefore, the higher fungal burdens in FcγRIIb<sup>-/-</sup> mice may be due to the primary defect in macrophages. Accordingly, we evaluated the phagocytosis activity, killing activity and cytokine responses of macrophages after exposure to *C. neoformans*. Interestingly, the phagocytosis of FcγRIIb<sup>-/-</sup> macrophages in response to cryptococci was elevated compared with wild-type cells, as reported for other organisms(21, 25). In FcγRIIb<sup>-/-</sup> mice, nearly all of the macrophages incubated with heat-killed *C. neoformans* phagocytosed approximately 6-7 yeasts per cell at 4 h (phagocytosis index). In contrast, approximately only 50-60%

of wild-type macrophages phagocytosed yeast, and they did so with a reduced activity of 2-3 yeasts per cell. On the other hand, the total killing capacity and the intracellular proliferation activity of FcγRIIb<sup>-/-</sup> macrophages was not different from wild-type macrophages, unlike the responses to other organisms(25), perhaps due to the immune evasion properties of *C. neoformans*(148).

*Cryptococcus* is a facultative intracellular pathogen, which can utilize host macrophages to spread within the body, via the Trojan horse mechanism(214). Moreover, the recent study found that *C. neoformans*-infected phagocyte transported from post-capillary venules across the endothelium into the perivascular space, subsequently, passed to the cerebral parenchyma and lead to development of meningitis. Therefore, this is an evidence supported the association of phagocyte-dependent entry with *C. neoformans* (223). Cryptococci typically escape extracellular immune responses, survive and replicate intracellularly, transfer laterally between macrophages, and eventually invade tissue and organs(214). They can use macrophages as trafficking vehicles for dissemination, particularly to pass through the blood-brain barrier into the central nervous system(9). Interestingly, the depletion of macrophages, at least in certain situations, is associated with less severe pathogenesis(8). We hypothesized that the elevated phagocytosis of FcγRIIb<sup>-/-</sup> macrophages and the immune evasion properties of *C. neoformans* enhanced the Trojan horse mechanism, resulting in more severe cryptococcosis *in vivo*. We tested cryptococcosis severity in a macrophage depletion model with daily liposomal clodronate injection in FcγRIIb<sup>-/-</sup> and wild-type mice. As expected, at 1 week after fungal administration, macrophage depletion led to lower fungal burdens in the liver, lung and spleen of FcγRIIb<sup>-/-</sup> mice, but not of wild-type mice. Nevertheless, liposomal clodronate not only depleted monocytes/macrophages but also reduced the numbers of dendritic cells and regulatory T cells (224, 225). Although loss of dendritic cells after liposomal clodronate injection might be responsible for the less severe cryptococcosis, the enhanced cryptococcosis severity after *Cryptococcus*-infected macrophage injection supports the greater pathogenic role of macrophages compared to dendritic cells. The inoculation of fungi-containing FcγRIIb<sup>-/-</sup> macrophages increased the fungal burdens in the brains and livers of wild-type mice at 24 h after administration. These

results support the high phagocytosis capacity of FcγRIIb<sup>-/-</sup> macrophages and the enhancement of fungal transmission by macrophages, particularly through the blood-brain barrier. Together, these results support the importance of macrophages in cryptococcosis pathogenesis in FcγRIIb<sup>-/-</sup> mice and in patients with FcγRIIb loss-of-function polymorphisms.

In addition, the prominent pro-inflammatory cytokine response (TNF-α and IL-6), but not the anti-inflammatory cytokine (IL-10) response, was demonstrated in the FcγRIIb<sup>-/-</sup> groups, both *in vivo* and *in vitro*. This might be because glucuronoxylomannan (GXM), an important cryptococcal capsular polysaccharide, induces potent immunosuppression by direct engagement of FcγRIIb, an immunoinhibitory receptor, and stimulates greater IL-10 production (226, 227). In FcγRIIb<sup>-/-</sup> mice, perhaps GXM was unable to induce IL-10, resulting in the more severe pro-inflammatory cytokine storm and fungal sepsis (226, 227). More studies on this topic are needed to explain the underlying mechanism.

Indeed, cryptococcosis is one of the common systemic fungal infections in patients with lupus (199, 228, 229). We demonstrated the similar increased susceptibility against cryptococcosis between the lupus model of FcγRIIb<sup>-/-</sup> (a model with gene deficiency) and pristane (a model with normal genetic background), at least in part, due to the macrophage activation.

Because of the heterogeneity of lupus pathogenesis (32), we used 2 lupus models of the genetic-prone mouse strain, FcγRIIb<sup>-/-</sup>, and the chemical induction, pristane injection, as the representatives of lupus caused by genetic- and environmental- factors, respectively. While FcγRIIb<sup>-/-</sup> mice develop the autoimmunity because of the loss of the inhibitory signaling (20, 31), pristane injection induced lupus by the enhanced immune responses from chronic peritoneal inflammation (37, 230). Because the lupus manifestations in FcγRIIb<sup>-/-</sup> and pristane mice depends on age (31, 231) and the duration after pristane administration (232, 233), respectively, cryptococcosis was induced in symptomatic lupus mice of both models. At the time of cryptococcal challenge, the severity of lupus nephritis (proteinuria and serum creatinine) of both lupus models was not different despite the higher anti-dsDNA in FcγRIIb<sup>-/-</sup> group. Interestingly, the severity of cryptococcosis in pristane mice was

similar to Fc $\gamma$ R11b $^{-/-}$  mice as determined by the mortality rate, fungal burdens and serum cytokines. The prominent serum cytokines in lupus mice of both models implied the responses against the higher fungal burdens in these mice and/or the enhanced immune responses of lupus against cryptococcosis. In addition, the cryptococcal lesions in both lupus models were detected in several organs in contrast to the limited lesions mostly in brain in the wild-types (9, 231) implying the organism-control defect in lupus mice (234-237).

Subsequently, we explored macrophage phagocytosis and killing activity, the main mechanism of organism-control in cryptococcosis (206, 207, 231). Indeed, phagocytosis function of macrophages from pristane and Fc $\gamma$ R11b $^{-/-}$  groups was higher than the wild-type cells supported our previous report on Fc $\gamma$ R11b $^{-/-}$  (231). The prominent macrophage phagocytosis in pristane, despite normal genetic background, supports the strong immune activation in this model as previously reported (37, 230, 238). But, the macrophage killing activity was not different among experimental groups, possibly due to the immune evasion properties of *Cryptococci* (148). The enhanced phagocytosis with limited killing activity of macrophage against cryptococcosis in both lupus models suggested the similar hyper-immune responses in lupus regardless of the genetic background.

Because of the prominent influence of Th cell on macrophage activation (234, 239) and hyper-function of Th cell in patients with lupus (184), Th cell analysis in spleen was explored in these mice. Interestingly, the total number of Th cell in Fc $\gamma$ R11b $^{-/-}$  mice is more prominent than pristane and wild-type. The lesser Th cell number in pristane mice compared with Fc $\gamma$ R11b $^{-/-}$ , despite the similar lupus characteristics, suggested the influence of hyper-immune response in Fc $\gamma$ R11b $^{-/-}$  mice. In addition, the similar prominent proportion of active Th cells, as examined by CD69 $^{+}$ , ICOS $^{+}$ , IFN- $\gamma$  $^{+}$  and low CD62L expression, in spleen of both lupus models implied the higher impact of lupus hyper-immune stimulation on Th cell and the lesser influence of the genetic background. Moreover, lupus mice demonstrated several groups of active cytokines in serum, including; the pro-inflammation (IL-1 $\alpha$  and IL-1 $\beta$ ), the macrophage-Th cell activation (eg. IL-12, IL-17 and IFN- $\gamma$ ) and the cytokine of lupus-pathogenesis (type I interferon). The similar prominent cytokines in pristane and Fc $\gamma$ R11b $^{-/-}$  also implied the

limited influence of genetic background in active lupus. Furthermore, the percentage of active Th cells was even higher after cryptococcal infection in lupus mice (more prominently in Fc $\gamma$ R11b<sup>-/-</sup> mice over pristane group) in comparison with the wild-type. These data supported the influence of infection in the acceleration of immune responses in lupus (35).

Hence, the increased IFN- $\gamma$  from Th cell and other serum cytokines possibly induced the prominent cryptococcal phagocytosis of macrophage in lupus models. Despite the prominent phagocytosis, the natural resistance of *Cryptococci* against macrophage killing activity possibly lead to the intracellular parasitism and enhanced cryptococcal dissemination. Indeed, the intracellular parasitism is one of the well-known mechanism of the cryptococcal dissemination (148) and is a possible mechanism of increased cryptococcal susceptibility in Fc $\gamma$ R11b<sup>-/-</sup> mice (231). Here, we proposed that enhanced phagocytosis and limited killing activity of macrophage in pristane lupus models increased cryptococcal susceptibility similar to a previous report on Fc $\gamma$ R11b<sup>-/-</sup> mice (231). Translationally, the prevention of cryptococcosis in patients with lupus, especially in the endemic area of cryptococcosis, should be concerned regardless of the genetic background of the patients.

## CHAPTER VII

### CONCLUSION

In this study, we compared the disease severity of cryptococcosis between FcγRIIb-/- mice and wild-type mice. The FcγRIIb-/- mice show more severity cryptococcosis with lower percent survival, higher fungal burdens and histopathology with cryptococcoma-like lesions when compared with wild-type counterparts. The protective immunity against cryptococcosis was associated with macrophage and T helper cell functions. The role of macrophage against *Cryptococcus neoformans* appear to be involved in the live fungal containment within the macrophages that explained by Trojan horse mechanism. The macrophage that lack FcγRIIb (FcγRIIb-/- macrophages) challenged with *C. neoformans* found that these macrophages shown prominent phagocytic activity with the more intracellular fungal cells per macrophage in comparison with wildtype cell. Although more fungal cells contained within FcγRIIb-/- macrophages than wild-type but the killing activity of FcγRIIb-/- macrophages did not different from wild-type macrophages as determined by the higher viability of intracellular yeast in FcγRIIb-/- macrophages. To see if prominent phagocytosis and more live fungal containment in FcγRIIb-/- macrophages play an important role in fungal dissemination and cryptococcosis severity in FcγRIIb-/- mice, an *in vivo* macrophage depletion model was performed. The FcγRIIb-/- and wild-type mice with clodronate induced macrophage depletion were infected with *C. neoformans*. Indeed, the macrophage-depleted FcγRIIb-/- mice show the reduction in fungal burdens. Moreover, the role of macrophage function was confirmed by either fungal contained-FcγRIIb-/- or wild-type macrophage (infected macrophage) was transferred to wild-type mice. Indeed, the wild-type mice administered with infected FcγRIIb-/- macrophage shown the higher fungal burden. Additionally, the cytokine secretion from macrophage *in vitro* and *in vivo* model after *C. neoformans* administration found that pro-inflammatory cytokine, TNF-α, IL-6 but not IL-10 significantly different between FcγRIIb-/- and wild-type counterpart. The role of T helper cell also examined by T cell

subpopulation analysis and IFN- $\gamma$  intracellular staining suggesting that the severity of cryptococcosis in Fc $\gamma$ R11b $^{-/-}$  mice did not depend on T helper cell deficiency.

Therefore, we conclude that more severe cryptococcosis in Fc $\gamma$ R11b $^{-/-}$  mice was due to enhanced dissemination, possibly through the Trojan horse mechanism, and the hyper-responsiveness of pro-inflammatory cytokine production during sepsis. This is the first report of the disadvantage of the prominent macrophage function of Fc $\gamma$ R11b $^{-/-}$  mice in cryptococcosis. In clinical translation, we propose Fc $\gamma$ R11b loss-of-function-polymorphisms as a new risk factor for cryptococcosis. Moreover, we demonstrated the similarity of symptomatic lupus from pristane induction and Fc $\gamma$ R11b $^{-/-}$  in i) the susceptibility against cryptococcosis, ii) the macrophage activities and iii) the Th cell activation in spleen. These suggested the higher impact of the hyper-immune responsiveness over the genetic background on cryptococcosis susceptibility in symptomatic lupus condition. The prevention for cryptococcosis, especially in the endemic area, is possibly beneficial for patients with symptomatic lupus, regardless of the lupus genetic background.



## REFERENCES

1. Jarvis JN, Harrison TS. HIV-associated cryptococcal meningitis. *AIDS*. 2007;21(16):2119-29.
2. Park BJ, Wannemuehler KA, Marston BJ, Govender N, Pappas PG, Chiller TM. Estimation of the current global burden of cryptococcal meningitis among persons living with HIV/AIDS. *AIDS*. 2009;23(4):525-30.
3. Garcia-Hermoso D, Janbon G, Dromer F. Epidemiological evidence for dormant *Cryptococcus neoformans* infection. *J Clin Microbiol*. 1999;37(10):3204-9.
4. Vecchiarelli A, Pericolini E, Gabrielli E, Kenno S, Perito S, Cenci E, et al. Elucidating the immunological function of the *Cryptococcus neoformans* capsule. *Future Microbiol*. 2013;8(9):1107-16.
5. Del Poeta M. Role of phagocytosis in the virulence of *Cryptococcus neoformans*. *Eukaryot Cell*. 2004;3(5):1067-75.
6. Alvarez M, Casadevall A. Phagosome extrusion and host-cell survival after *Cryptococcus neoformans* phagocytosis by macrophages. *Curr Biol*. 2006;16(21):2161-5.
7. Tucker SC, Casadevall A. Replication of *Cryptococcus neoformans* in macrophages is accompanied by phagosomal permeabilization and accumulation of vesicles containing polysaccharide in the cytoplasm. *Proc Natl Acad Sci U S A*. 2002;99(5):3165-70.
8. Kechichian TB, Shea J, Del Poeta M. Depletion of alveolar macrophages decreases the dissemination of a glucosylceramide-deficient mutant of *Cryptococcus neoformans* in immunodeficient mice. *Infect Immun*. 2007;75(10):4792-8.
9. Charlier C, Nielsen K, Daou S, Brigitte M, Chretien F, Dromer F. Evidence of a role for monocytes in dissemination and brain invasion by *Cryptococcus neoformans*. *Infect Immun*. 2009;77(1):120-7.
10. Pappas PG. Cryptococcal infections in non-HIV-infected patients. *Trans Am Clin Climatol Assoc*. 2013;124:61-79.

11. Kidd SE, Hagen F, Tscharke RL, Huynh M, Bartlett KH, Fyfe M, et al. A rare genotype of *Cryptococcus gattii* caused the cryptococcosis outbreak on Vancouver Island (British Columbia, Canada). *Proc Natl Acad Sci U S A*. 2004;101(49):17258-63.
12. Day JN, Hoang TN, Duong AV, Hong CT, Diep PT, Campbell JI, et al. Most cases of cryptococcal meningitis in HIV-uninfected patients in Vietnam are due to a distinct amplified fragment length polymorphism-defined cluster of *Cryptococcus neoformans* var. *grubii* VN1. *J Clin Microbiol*. 2011;49(2):658-64.
13. Chau TT, Mai NH, Phu NH, Nghia HD, Chuong LV, Sinh DX, et al. A prospective descriptive study of cryptococcal meningitis in HIV uninfected patients in Vietnam - high prevalence of *Cryptococcus neoformans* var *grubii* in the absence of underlying disease. *BMC Infect Dis*. 2010;10:199.
14. Netea MG. Toward identification of the genetic risk profile for cryptococcal disease in HIV-infected patients. *MBio*. 2013;4(5):e00798-13.
15. Rohatgi S, Gohil S, Kuniholm MH, Schultz H, Dufaud C, Armour KL, et al. Fc gamma receptor 3A polymorphism and risk for HIV-associated cryptococcal disease. *MBio*. 2013;4(5):e00573-13.
16. Meletiadis J, Walsh TJ, Choi EH, Pappas PG, Ennis D, Douglas J, et al. Study of common functional genetic polymorphisms of FCGR2A, 3A and 3B genes and the risk for cryptococcosis in HIV-uninfected patients. *Med Mycol*. 2007;45(6):513-8.
17. Hu XP, Wu JQ, Zhu LP, Wang X, Xu B, Wang RY, et al. Association of Fc gamma receptor IIB polymorphism with cryptococcal meningitis in HIV-uninfected Chinese patients. *PLoS One*. 2012;7(8):e42439.
18. Parren PW, Warmerdam PA, Boeije LC, Arts J, Westerdaal NA, Vlug A, et al. On the interaction of IgG subclasses with the low affinity Fc gamma RIla (CD32) on human monocytes, neutrophils, and platelets. Analysis of a functional polymorphism to human IgG2. *J Clin Invest*. 1992;90(4):1537-46.
19. Salmon JE, Edberg JC, Brogle NL, Kimberly RP. Allelic polymorphisms of human Fc gamma receptor IIA and Fc gamma receptor IIIB. Independent mechanisms for differences in human phagocyte function. *J Clin Invest*. 1992;89(4):1274-81.
20. Smith KG, Clatworthy MR. Fc gamma RIIB in autoimmunity and infection: evolutionary and therapeutic implications. *Nat Rev Immunol*. 2010;10(5):328-43.

21. Clatworthy MR, Willcocks L, Urban B, Langhorne J, Williams TN, Peshu N, et al. Systemic lupus erythematosus-associated defects in the inhibitory receptor FcγRIIb reduce susceptibility to malaria. *Proc Natl Acad Sci U S A*. 2007;104(17):7169-74.
22. Gjertsson I, Kleinau S, Tarkowski A. The impact of Fcγ receptors on *Staphylococcus aureus* infection. *Microb Pathog*. 2002;33(4):145-52.
23. Maglione PJ, Xu J, Casadevall A, Chan J. Fc γ receptors regulate immune activation and susceptibility during *Mycobacterium tuberculosis* infection. *J Immunol*. 2008;180(5):3329-38.
24. Franz BJ, Li Y, Bitsaktsis C, Iglesias BV, Pham G, Sunagar R, et al. Downmodulation of vaccine-induced immunity and protection against the intracellular bacterium *Francisella tularensis* by the inhibitory receptor FcγRIIb. *J Immunol Res*. 2015;2015:840842.
25. Clatworthy MR, Smith KG. FcγRIIb balances efficient pathogen clearance and the cytokine-mediated consequences of sepsis. *J Exp Med*. 2004;199(5):717-23.
26. Uppington H, Menager N, Boross P, Wood J, Sheppard M, Verbeek S, et al. Effect of immune serum and role of individual Fcγ receptors on the intracellular distribution and survival of *Salmonella enterica* serovar Typhimurium in murine macrophages. *Immunology*. 2006;119(2):147-58.
27. Goodman AL, Forbes EK, Williams AR, Douglas AD, de Cassan SC, Bauza K, et al. The utility of *Plasmodium berghei* as a rodent model for anti-merozoite malaria vaccine assessment. *Sci Rep*. 2013;3:1706.
28. Da Silva DM, Fausch SC, Verbeek JS, Kast WM. Uptake of human papillomavirus virus-like particles by dendritic cells is mediated by Fcγ receptors and contributes to acquisition of T cell immunity. *J Immunol*. 2007;178(12):7587-97.
29. Chan KR, Zhang SL, Tan HC, Chan YK, Chow A, Lim AP, et al. Ligation of Fc γ receptor IIB inhibits antibody-dependent enhancement of dengue virus infection. *Proc Natl Acad Sci U S A*. 2011;108(30):12479-84.
30. Zhang Y, Zhou Y, Yang Q, Mu C, Duan E, Chen J, et al. Ligation of Fc γ receptor IIB enhances levels of antiviral cytokine in response to PRRSV infection in vitro. *Vet Microbiol*. 2012;160(3-4):473-80.

31. Bolland S, Ravetch JV. Spontaneous autoimmune disease in Fc(gamma)RIIB-deficient mice results from strain-specific epistasis. *Immunity*. 2000;13(2):277-85.
32. Tsokos GC. Systemic lupus erythematosus. *N Engl J Med*. 2011;365(22):2110-21.
33. Crispin JC, Hedrich CM, Tsokos GC. Gene-function studies in systemic lupus erythematosus. *Nat Rev Rheumatol*. 2013;9(8):476-84.
34. Ropes MW. Observations on the Natural Course of Disseminated Lupus Erythematosus. *Medicine (Baltimore)*. 1964;43:387-91.
35. Zandman-Goddard G, Shoenfeld Y. Infections and SLE. *Autoimmunity*. 2005;38(7):473-85.
36. Ondee T, Surawut S, Taratummarat S, Hirankarn N, Palaga T, Pisitkun P, et al. Fc Gamma Receptor IIB Deficient Mice: A Lupus Model with Increased Endotoxin Tolerance-Related Sepsis Susceptibility. *Shock*. 2017;47(6):743-52.
37. Leiss H, Niederreiter B, Bandur T, Schwarzecker B, Blüml S, Steiner G, et al. Pristane-induced lupus as a model of human lupus arthritis: evolution of autoantibodies, internal organ and joint inflammation. *Lupus*. 2013;22(8):778-92.
38. Kwon-Chung KJ, Fraser JA, Doering TL, Wang Z, Janbon G, Idnurm A, et al. *Cryptococcus neoformans* and *Cryptococcus gattii*, the etiologic agents of cryptococcosis. *Cold Spring Harb Perspect Med*. 2014;4(7):a019760.
39. Andama AO, den Boon S, Meya D, Cattamanchi A, Worodria W, Davis JL, et al. Prevalence and outcomes of cryptococcal antigenemia in HIV-seropositive patients hospitalized for suspected tuberculosis in Uganda. *J Acquir Immune Defic Syndr*. 2013;63(2):189-94.
40. Jarvis JN, Harrison TS, Govender N, Lawn SD, Longley N, Bicanic T, et al. Routine cryptococcal antigen screening for HIV-infected patients with low CD4+ T-lymphocyte counts--time to implement in South Africa? *S Afr Med J*. 2011;101(4):232-4.
41. Liu Y, Kang M, Wu SY, Ma Y, Chen ZX, Xie Y, et al. Different characteristics of cryptococcal meningitis between HIV-infected and HIV-uninfected patients in the Southwest of China. *Med Mycol*. 2017;55(3):255-61.
42. Mitchell TG, Castañeda E, Nielsen K, Wanke B, Lazéra MS. Environmental Niches for *Cryptococcus neoformans* and *Cryptococcus gattii*. *Cryptococcus: American Society of Microbiology*; 2011.

43. Hajjeh RA, Brandt ME, Pinner RW. Emergence of cryptococcal disease: epidemiologic perspectives 100 years after its discovery. *Epidemiol Rev.* 1995;17(2):303-20.
44. Singh N, Dromer F, Perfect JR, Lortholary O. Cryptococcosis in solid organ transplant recipients: current state of the science. *Clin Infect Dis.* 2008;47(10):1321-7.
45. Horcajada JP, Pena JL, Martinez-Taboada VM, Pina T, Belaustegui I, Cano ME, et al. Invasive Cryptococcosis and adalimumab treatment. *Emerg Infect Dis.* 2007;13(6):953-5.
46. Ely EW, Peacock JE, Jr., Haponik EF, Washburn RG. Cryptococcal pneumonia complicating pregnancy. *Medicine (Baltimore).* 1998;77(3):153-67.
47. Singh N, Husain S, De Vera M, Gayowski T, Cacciarelli TV. Cryptococcus neoformans Infection in Patients With Cirrhosis, Including Liver Transplant Candidates. *Medicine (Baltimore).* 2004;83(3):188-92.
48. Mitchell DH, Sorrell TC, Allworth AM, Heath CH, McGregor AR, Papanoum K, et al. Cryptococcal disease of the CNS in immunocompetent hosts: influence of cryptococcal variety on clinical manifestations and outcome. *Clin Infect Dis.* 1995;20(3):611-6.
49. Lui G, Lee N, Ip M, Choi KW, Tso YK, Lam E, et al. Cryptococcosis in apparently immunocompetent patients. *QJM.* 2006;99(3):143-51.
50. Rosen LB, Freeman AF, Yang LM, Jutivorakool K, Olivier KN, Angkasekwinai N, et al. Anti-GM-CSF autoantibodies in patients with cryptococcal meningitis. *J Immunol.* 2013;190(8):3959-66.
51. Chuang YM, Ho YC, Chang HT, Yu CJ, Yang PC, Hsueh PR. Disseminated cryptococcosis in HIV-uninfected patients. *Eur J Clin Microbiol Infect Dis.* 2008;27(4):307-10.
52. Liao CH, Chi CY, Wang YJ, Tseng SW, Chou CH, Ho CM, et al. Different presentations and outcomes between HIV-infected and HIV-uninfected patients with Cryptococcal meningitis. *J Microbiol Immunol Infect.* 2012;45(4):296-304.
53. Feldmesser M, Tucker S, Casadevall A. Intracellular parasitism of macrophages by *Cryptococcus neoformans*. *Trends Microbiol.* 2001;9(6):273-8.

54. Garcia-Solache MA, Casadevall A. Global warming will bring new fungal diseases for mammals. *MBio*. 2010;1(1).
55. Casadevall A. Fungi and the rise of mammals. *PLoS Pathog*. 2012;8(8):e1002808.
56. Goldman DL, Khine H, Abadi J, Lindenberg DJ, Pirofski L, Niang R, et al. Serologic evidence for *Cryptococcus neoformans* infection in early childhood. *Pediatrics*. 2001;107(5):E66.
57. Chen LC, Goldman DL, Doering TL, Pirofski L, Casadevall A. Antibody response to *Cryptococcus neoformans* proteins in rodents and humans. *Infect Immun*. 1999;67(5):2218-24.
58. Giles SS, Dagenais TR, Botts MR, Keller NP, Hull CM. Elucidating the pathogenesis of spores from the human fungal pathogen *Cryptococcus neoformans*. *Infect Immun*. 2009;77(8):3491-500.
59. Shibuya K, Hirata A, Omuta J, Sugamata M, Katori S, Saito N, et al. Granuloma and cryptococcosis. *J Infect Chemother*. 2005;11(3):115-22.
60. Lindell DM, Ballinger MN, McDonald RA, Toews GB, Huffnagle GB. Diversity of the T-cell response to pulmonary *Cryptococcus neoformans* infection. *Infect Immun*. 2006;74(8):4538-48.
61. Lim TS, Murphy JW. Transfer of immunity to cryptococcosis by T-enriched splenic lymphocytes from *Cryptococcus neoformans*-sensitized mice. *Infect Immun*. 1980;30(1):5-11.
62. Huffnagle GB, Yates JL, Lipscomb MF. Immunity to a pulmonary *Cryptococcus neoformans* infection requires both CD4+ and CD8+ T cells. *J Exp Med*. 1991;173(4):793-800.
63. Zaragoza O, Alvarez M, Telzak A, Rivera J, Casadevall A. The relative susceptibility of mouse strains to pulmonary *Cryptococcus neoformans* infection is associated with pleiotropic differences in the immune response. *Infect Immun*. 2007;75(6):2729-39.
64. Rhodes JC. Contribution of complement component C5 to the pathogenesis of experimental murine cryptococcosis. *Sabouraudia*. 1985;23(3):225-34.

65. Hoag KA, Lipscomb MF, Izzo AA, Street NE. IL-12 and IFN-gamma are required for initiating the protective Th1 response to pulmonary cryptococcosis in resistant C.B-17 mice. *Am J Respir Cell Mol Biol.* 1997;17(6):733-9.
66. Chen GH, McDonald RA, Wells JC, Huffnagle GB, Lukacs NW, Toews GB. The gamma interferon receptor is required for the protective pulmonary inflammatory response to *Cryptococcus neoformans*. *Infect Immun.* 2005;73(3):1788-96.
67. Decken K, Kohler G, Palmer-Lehmann K, Wunderlin A, Mattner F, Magram J, et al. Interleukin-12 is essential for a protective Th1 response in mice infected with *Cryptococcus neoformans*. *Infect Immun.* 1998;66(10):4994-5000.
68. Kobayashi M, Ito M, Sano K, Koyama M. Granulomatous and cytokine responses to pulmonary *Cryptococcus neoformans* in two strains of rats. *Mycopathologia.* 2001;151(3):121-30.
69. Arora S, Olszewski MA, Tsang TM, McDonald RA, Toews GB, Huffnagle GB. Effect of cytokine interplay on macrophage polarization during chronic pulmonary infection with *Cryptococcus neoformans*. *Infect Immun.* 2011;79(5):1915-26.
70. Jain AV, Zhang Y, Fields WB, McNamara DA, Choe MY, Chen GH, et al. Th2 but not Th1 immune bias results in altered lung functions in a murine model of pulmonary *Cryptococcus neoformans* infection. *Infect Immun.* 2009;77(12):5389-99.
71. Zhang Y, Wang F, Tompkins KC, McNamara A, Jain AV, Moore BB, et al. Robust Th1 and Th17 immunity supports pulmonary clearance but cannot prevent systemic dissemination of highly virulent *Cryptococcus neoformans* H99. *Am J Pathol.* 2009;175(6):2489-500.
72. Stenzel W, Muller U, Kohler G, Heppner FL, Blessing M, McKenzie AN, et al. IL-4/IL-13-dependent alternative activation of macrophages but not microglial cells is associated with uncontrolled cerebral cryptococcosis. *Am J Pathol.* 2009;174(2):486-96.
73. Kawakami K, Qifeng X, Tohyama M, Qureshi MH, Saito A. Contribution of tumour necrosis factor-alpha (TNF-alpha) in host defence mechanism against *Cryptococcus neoformans*. *Clin Exp Immunol.* 1996;106(3):468-74.
74. Conti HR, Gaffen SL. Host responses to *Candida albicans*: Th17 cells and mucosal candidiasis. *Microbes Infect.* 2010;12(7):518-27.

75. Wozniak KL, Young ML, Wormley FL, Jr. Protective immunity against experimental pulmonary cryptococcosis in T cell-depleted mice. *Clin Vaccine Immunol.* 2011;18(5):717-23.
76. Shao X, Mednick A, Alvarez M, van Rooijen N, Casadevall A, Goldman DL. An innate immune system cell is a major determinant of species-related susceptibility differences to fungal pneumonia. *J Immunol.* 2005;175(5):3244-51.
77. Feldmesser M, Casadevall A, Kress Y, Spira G, Orlofsky A. Eosinophil-Cryptococcus neoformans interactions in vivo and in vitro. *Infect Immun.* 1997;65(5):1899-907.
78. Mednick AJ, Feldmesser M, Rivera J, Casadevall A. Neutropenia alters lung cytokine production in mice and reduces their susceptibility to pulmonary cryptococcosis. *Eur J Immunol.* 2003;33(6):1744-53.
79. Piehler D, Stenzel W, Grahnert A, Held J, Richter L, Kohler G, et al. Eosinophils contribute to IL-4 production and shape the T-helper cytokine profile and inflammatory response in pulmonary cryptococcosis. *Am J Pathol.* 2011;179(2):733-44.
80. Casadevall A. Amoeba provide insight into the origin of virulence in pathogenic fungi. *Adv Exp Med Biol.* 2012;710:1-10.
81. Mansour MK, Yauch LE, Rottman JB, Levitz SM. Protective efficacy of antigenic fractions in mouse models of cryptococcosis. *Infect Immun.* 2004;72(3):1746-54.
82. Kawakami K. Regulation by innate immune T lymphocytes in the host defense against pulmonary infection with *Cryptococcus neoformans*. *Jpn J Infect Dis.* 2004;57(4):137-45.
83. Osterholzer JJ, Milam JE, Chen GH, Toews GB, Huffnagle GB, Olszewski MA. Role of dendritic cells and alveolar macrophages in regulating early host defense against pulmonary infection with *Cryptococcus neoformans*. *Infect Immun.* 2009;77(9):3749-58.
84. Hardison SE, Wozniak KL, Kolls JK, Wormley FL, Jr. Interleukin-17 is not required for classical macrophage activation in a pulmonary mouse model of *Cryptococcus neoformans* infection. *Infect Immun.* 2010;78(12):5341-51.
85. Hardison SE, Herrera G, Young ML, Hole CR, Wozniak KL, Wormley FL, Jr. Protective immunity against pulmonary cryptococcosis is associated with STAT1-mediated classical macrophage activation. *J Immunol.* 2012;189(8):4060-8.



86. Hardison SE, Ravi S, Wozniak KL, Young ML, Olszewski MA, Wormley FL, Jr. Pulmonary infection with an interferon-gamma-producing *Cryptococcus neoformans* strain results in classical macrophage activation and protection. *Am J Pathol*. 2010;176(2):774-85.
87. Kozel TR, Gotschlich EC. The capsule of *cryptococcus neoformans* passively inhibits phagocytosis of the yeast by macrophages. *J Immunol*. 1982;129(4):1675-80.
88. Small JM, Mitchell TG. Strain variation in antiphagocytic activity of capsular polysaccharides from *Cryptococcus neoformans* serotype A. *Infect Immun*. 1989;57(12):3751-6.
89. Shoham S, Huang C, Chen JM, Golenbock DT, Levitz SM. Toll-like receptor 4 mediates intracellular signaling without TNF-alpha release in response to *Cryptococcus neoformans* polysaccharide capsule. *J Immunol*. 2001;166(7):4620-6.
90. Monari C, Bistoni F, Casadevall A, Pericolini E, Pietrella D, Kozel TR, et al. Glucuronoxylomannan, a microbial compound, regulates expression of costimulatory molecules and production of cytokines in macrophages. *J Infect Dis*. 2005;191(1):127-37.
91. Stano P, Williams V, Villani M, Cymbalyuk ES, Qureshi A, Huang Y, et al. App1: an antiphagocytic protein that binds to complement receptors 3 and 2. *J Immunol*. 2009;182(1):84-91.
92. Biondo C, Midiri A, Messina L, Tomasello F, Garufi G, Catania MR, et al. MyD88 and TLR2, but not TLR4, are required for host defense against *Cryptococcus neoformans*. *Eur J Immunol*. 2005;35(3):870-8.
93. Nakamura K, Miyagi K, Koguchi Y, Kinjo Y, Uezu K, Kinjo T, et al. Limited contribution of Toll-like receptor 2 and 4 to the host response to a fungal infectious pathogen, *Cryptococcus neoformans*. *FEMS Immunol Med Microbiol*. 2006;47(1):148-54.
94. Wang JP, Lee CK, Akalin A, Finberg RW, Levitz SM. Contributions of the MyD88-dependent receptors IL-18R, IL-1R, and TLR9 to host defenses following pulmonary challenge with *Cryptococcus neoformans*. *PLoS One*. 2011;6(10):e26232.
95. Shapiro S, Beenhouwer DO, Feldmesser M, Taborda C, Carroll MC, Casadevall A, et al. Immunoglobulin G monoclonal antibodies to *Cryptococcus neoformans* protect mice deficient in complement component C3. *Infect Immun*. 2002;70(5):2598-604.

96. Means TK, Mylonakis E, Tampakakis E, Colvin RA, Seung E, Puckett L, et al. Evolutionarily conserved recognition and innate immunity to fungal pathogens by the scavenger receptors SCARF1 and CD36. *J Exp Med*. 2009;206(3):637-53.
97. Nakamura K, Kinjo T, Saijo S, Miyazato A, Adachi Y, Ohno N, et al. Dectin-1 is not required for the host defense to *Cryptococcus neoformans*. *Microbiol Immunol*. 2007;51(11):1115-9.
98. Dan JM, Kelly RM, Lee CK, Levitz SM. Role of the mannose receptor in a murine model of *Cryptococcus neoformans* infection. *Infect Immun*. 2008;76(6):2362-7.
99. Monga DP, Kumar R, Mohapatra LN, Malaviya AN. Experimental cryptococcosis in normal and B-cell-deficient mice. *Infect Immun*. 1979;26(1):1-3.
100. Monga DP. Role of macrophages in resistance of mice to experimental cryptococcosis. *Infect Immun*. 1981;32(3):975-8.
101. Hill JO, Aguirre KM. CD4+ T cell-dependent acquired state of immunity that protects the brain against *Cryptococcus neoformans*. *J Immunol*. 1994;152(5):2344-50.
102. Yuan RR, Casadevall A, Oh J, Scharff MD. T cells cooperate with passive antibody to modify *Cryptococcus neoformans* infection in mice. *Proc Natl Acad Sci U S A*. 1997;94(6):2483-8.
103. Kawakami K, Koguchi Y, Qureshi MH, Kinjo Y, Yara S, Miyazato A, et al. Reduced host resistance and Th1 response to *Cryptococcus neoformans* in interleukin-18 deficient mice. *FEMS Microbiol Lett*. 2000;186(1):121-6.
104. Muller U, Stenzel W, Kohler G, Werner C, Polte T, Hansen G, et al. IL-13 induces disease-promoting type 2 cytokines, alternatively activated macrophages and allergic inflammation during pulmonary infection of mice with *Cryptococcus neoformans*. *J Immunol*. 2007;179(8):5367-77.
105. Beenhouwer DO, Shapiro S, Feldmesser M, Casadevall A, Scharff MD. Both Th1 and Th2 cytokines affect the ability of monoclonal antibodies to protect mice against *Cryptococcus neoformans*. *Infect Immun*. 2001;69(10):6445-55.
106. Baker RD, Haugen RK. Tissue changes and tissue diagnosis in cryptococcosis; a study of 26 cases. *Am J Clin Pathol*. 1955;25(1):14-24.

107. Schwartz DA. Characterization of the biological activity of *Cryptococcus* infections in surgical pathology. The Budding Index and Carminophilic Index. *Ann Clin Lab Sci.* 1988;18(5):388-97.
108. Shibuya K, Coulson WF, Wollman JS, Wakayama M, Ando T, Oharaseki T, et al. Histopathology of cryptococcosis and other fungal infections in patients with acquired immunodeficiency syndrome. *Int J Infect Dis.* 2001;5(2):78-85.
109. Goldman DL, Lee SC, Mednick AJ, Montella L, Casadevall A. Persistent *Cryptococcus neoformans* pulmonary infection in the rat is associated with intracellular parasitism, decreased inducible nitric oxide synthase expression, and altered antibody responsiveness to cryptococcal polysaccharide. *Infect Immun.* 2000;68(2):832-8.
110. Lindell DM, Ballinger MN, McDonald RA, Toews GB, Huffnagle GB. Immunologic homeostasis during infection: coexistence of strong pulmonary cell-mediated immunity to secondary *Cryptococcus neoformans* infection while the primary infection still persists at low levels in the lungs. *J Immunol.* 2006;177(7):4652-61.
111. Feldmesser M, Kress Y, Novikoff P, Casadevall A. *Cryptococcus neoformans* is a facultative intracellular pathogen in murine pulmonary infection. *Infect Immun.* 2000;68(7):4225-37.
112. Nessa K, Gross NT, Jarstrand C, Johansson A, Camner P. In vivo interaction between alveolar macrophages and *Cryptococcus neoformans*. *Mycopathologia.* 1997;139(1):1-7.
113. Goldman D, Lee SC, Casadevall A. Pathogenesis of pulmonary *Cryptococcus neoformans* infection in the rat. *Infect Immun.* 1994;62(11):4755-61.
114. Cross CE, Bancroft GJ. Ingestion of acapsular *Cryptococcus neoformans* occurs via mannose and beta-glucan receptors, resulting in cytokine production and increased phagocytosis of the encapsulated form. *Infect Immun.* 1995;63(7):2604-11.
115. Giles SS, Zaas AK, Reidy MF, Perfect JR, Wright JR. *Cryptococcus neoformans* is resistant to surfactant protein A mediated host defense mechanisms. *PLoS One.* 2007;2(12):e1370.
116. Coelho C, Bocca AL, Casadevall A. The intracellular life of *Cryptococcus neoformans*. *Annu Rev Pathol.* 2014;9:219-38.

117. Taborda CP, Casadevall A. CR3 (CD11b/CD18) and CR4 (CD11c/CD18) are involved in complement-independent antibody-mediated phagocytosis of *Cryptococcus neoformans*. *Immunity*. 2002;16(6):791-802.
118. Guillot L, Carroll SF, Badawy M, Qureshi ST. *Cryptococcus neoformans* induces IL-8 secretion and CXCL1 expression by human bronchial epithelial cells. *Respir Res*. 2008;9:9.
119. Nussbaum G, Cleare W, Casadevall A, Scharff MD, Valadon P. Epitope location in the *Cryptococcus neoformans* capsule is a determinant of antibody efficacy. *J Exp Med*. 1997;185(4):685-94.
120. Cleare W, Casadevall A. The different binding patterns of two immunoglobulin M monoclonal antibodies to *Cryptococcus neoformans* serotype A and D strains correlate with serotype classification and differences in functional assays. *Clin Diagn Lab Immunol*. 1998;5(2):125-9.
121. Cleare W, Cherniak R, Casadevall A. In vitro and in vivo stability of a *Cryptococcus neoformans* [corrected] glucuronoxylomannan epitope that elicits protective antibodies. *Infect Immun*. 1999;67(6):3096-107.
122. Kozel TR, Pfrommer GS. Activation of the complement system by *Cryptococcus neoformans* leads to binding of iC3b to the yeast. *Infect Immun*. 1986;52(1):1-5.
123. Kozel TR, Wilson MA, Farrell TP, Levitz SM. Activation of C3 and binding to *Aspergillus fumigatus* conidia and hyphae. *Infect Immun*. 1989;57(11):3412-7.
124. Zaragoza O, Taborda CP, Casadevall A. The efficacy of complement-mediated phagocytosis of *Cryptococcus neoformans* is dependent on the location of C3 in the polysaccharide capsule and involves both direct and indirect C3-mediated interactions. *Eur J Immunol*. 2003;33(7):1957-67.
125. Blackstock R, Murphy JW. Secretion of the C3 component of complement by peritoneal cells cultured with encapsulated *Cryptococcus neoformans*. *Infect Immun*. 1997;65(10):4114-21.
126. Zaragoza O, Rodrigues ML, De Jesus M, Frases S, Dadachova E, Casadevall A. The capsule of the fungal pathogen *Cryptococcus neoformans*. *Adv Appl Microbiol*. 2009;68:133-216.

127. Netski D, Kozel TR. Fc-dependent and Fc-independent opsonization of *Cryptococcus neoformans* by anticapsular monoclonal antibodies: importance of epitope specificity. *Infect Immun.* 2002;70(6):2812-9.
128. Syme RM, Spurrell JC, Amankwah EK, Green FH, Mody CH. Primary dendritic cells phagocytose *Cryptococcus neoformans* via mannose receptors and Fc $\gamma$  receptor II for presentation to T lymphocytes. *Infect Immun.* 2002;70(11):5972-81.
129. Yauch LE, Mansour MK, Shoham S, Rottman JB, Levitz SM. Involvement of CD14, toll-like receptors 2 and 4, and MyD88 in the host response to the fungal pathogen *Cryptococcus neoformans* in vivo. *Infect Immun.* 2004;72(9):5373-82.
130. Chretien F, Lortholary O, Kansau I, Neuville S, Gray F, Dromer F. Pathogenesis of cerebral *Cryptococcus neoformans* infection after fungemia. *J Infect Dis.* 2002;186(4):522-30.
131. Diamond RD, Bennett JE. Growth of *Cryptococcus neoformans* within human macrophages in vitro. *Infect Immun.* 1973;7(2):231-6.
132. Levitz SM, Nong SH, Seetoo KF, Harrison TS, Speizer RA, Simons ER. *Cryptococcus neoformans* resides in an acidic phagolysosome of human macrophages. *Infect Immun.* 1999;67(2):885-90.
133. Luberto C, Toffaletti DL, Wills EA, Tucker SC, Casadevall A, Perfect JR, et al. Roles for inositol-phosphoryl ceramide synthase 1 (IPC1) in pathogenesis of *C. neoformans*. *Genes Dev.* 2001;15(2):201-12.
134. Lee SC, Kress Y, Zhao ML, Dickson DW, Casadevall A. *Cryptococcus neoformans* survive and replicate in human microglia. *Lab Invest.* 1995;73(6):871-9.
135. Alvarez M, Burn T, Luo Y, Pirofski LA, Casadevall A. The outcome of *Cryptococcus neoformans* intracellular pathogenesis in human monocytes. *BMC Microbiol.* 2009;9:51.
136. Naslund PK, Miller WC, Granger DL. *Cryptococcus neoformans* fails to induce nitric oxide synthase in primed murine macrophage-like cells. *Infect Immun.* 1995;63(4):1298-304.
137. Williamson PR. Biochemical and molecular characterization of the diphenol oxidase of *Cryptococcus neoformans*: identification as a laccase. *J Bacteriol.* 1994;176(3):656-64.

138. Doering TL, Nosanchuk JD, Roberts WK, Casadevall A. Melanin as a potential cryptococcal defence against microbicidal proteins. *Med Mycol.* 1999;37(3):175-81.
139. van Duin D, Casadevall A, Nosanchuk JD. Melanization of *Cryptococcus neoformans* and *Histoplasma capsulatum* reduces their susceptibilities to amphotericin B and caspofungin. *Antimicrob Agents Chemother.* 2002;46(11):3394-400.
140. Gomez BL, Nosanchuk JD. Melanin and fungi. *Curr Opin Infect Dis.* 2003;16(2):91-6.
141. Giles SS, Stajich JE, Nichols C, Gerrald QD, Alspaugh JA, Dietrich F, et al. The *Cryptococcus neoformans* catalase gene family and its role in antioxidant defense. *Eukaryot Cell.* 2006;5(9):1447-59.
142. Forbes IJ, Mackaness GB. Mitosis in Macrophages. *Lancet.* 1963;2(7319):1203-4.
143. Cinatl J, Paluska E, Chudomel V, Malaskova V, Elleder M. Culture of macrophage cell lines from normal mouse bone marrow. *Nature.* 1982;298(5872):388-9.
144. Westermann J, Ronneberg S, Fritz FJ, Pabst R. Proliferation of macrophage subpopulations in the adult rat: comparison of various lymphoid organs. *J Leukoc Biol.* 1989;46(3):263-9.
145. Luo Y, Alvarez M, Xia L, Casadevall A. The outcome of phagocytic cell division with infectious cargo depends on single phagosome formation. *PLoS One.* 2008;3(9):e3219.
146. Ma H, Croudace JE, Lammas DA, May RC. Expulsion of live pathogenic yeast by macrophages. *Curr Biol.* 2006;16(21):2156-60.
147. Voelz K, Lammas DA, May RC. Cytokine signaling regulates the outcome of intracellular macrophage parasitism by *Cryptococcus neoformans*. *Infect Immun.* 2009;77(8):3450-7.
148. Garcia-Rodas R, Zaragoza O. Catch me if you can: phagocytosis and killing avoidance by *Cryptococcus neoformans*. *FEMS Immunol Med Microbiol.* 2012;64(2):147-61.
149. Nicola AM, Robertson EJ, Albuquerque P, Derengowski Lda S, Casadevall A. Nonlytic exocytosis of *Cryptococcus neoformans* from macrophages occurs in vivo and is influenced by phagosomal pH. *MBio.* 2011;2(4).

150. Alvarez M, Casadevall A. Cell-to-cell spread and massive vacuole formation after *Cryptococcus neoformans* infection of murine macrophages. *BMC Immunol.* 2007;8:16.
151. Ma H, Croudace JE, Lammas DA, May RC. Direct cell-to-cell spread of a pathogenic yeast. *BMC Immunol.* 2007;8:15.
152. Alanio A, Desnos-Ollivier M, Dromer F. Dynamics of *Cryptococcus neoformans*-macrophage interactions reveal that fungal background influences outcome during cryptococcal meningoencephalitis in humans. *MBio.* 2011;2(4).
153. Mansour MK, Vyas JM, Levitz SM. Dynamic virulence: real-time assessment of intracellular pathogenesis links *Cryptococcus neoformans* phenotype with clinical outcome. *MBio.* 2011;2(5).
154. Shi M, Li SS, Zheng C, Jones GJ, Kim KS, Zhou H, et al. Real-time imaging of trapping and urease-dependent transmigration of *Cryptococcus neoformans* in mouse brain. *J Clin Invest.* 2010;120(5):1683-93.
155. Chang YC, Stins MF, McCaffery MJ, Miller GF, Pare DR, Dam T, et al. Cryptococcal yeast cells invade the central nervous system via transcellular penetration of the blood-brain barrier. *Infect Immun.* 2004;72(9):4985-95.
156. Luberto C, Martinez-Marino B, Taraskiewicz D, Bolanos B, Chitano P, Toffaletti DL, et al. Identification of App1 as a regulator of phagocytosis and virulence of *Cryptococcus neoformans*. *J Clin Invest.* 2003;112(7):1080-94.
157. Drevets DA, Leenen PJ. Leukocyte-facilitated entry of intracellular pathogens into the central nervous system. *Microbes Infect.* 2000;2(13):1609-18.
158. Kronstad JW, Attarian R, Cadieux B, Choi J, D'Souza CA, Griffiths EJ, et al. Expanding fungal pathogenesis: *Cryptococcus* breaks out of the opportunistic box. *Nat Rev Microbiol.* 2011;9(3):193-203.
159. Okagaki LH, Strain AK, Nielsen JN, Charlier C, Baltés NJ, Chretien F, et al. Cryptococcal cell morphology affects host cell interactions and pathogenicity. *PLoS Pathog.* 2010;6(6):e1000953.
160. Zaragoza O, Garcia-Rodas R, Nosanchuk JD, Cuenca-Estrella M, Rodriguez-Tudela JL, Casadevall A. Fungal cell gigantism during mammalian infection. *PLoS Pathog.* 2010;6(6):e1000945.

161. Ou XT, Wu JQ, Zhu LP, Guan M, Xu B, Hu XP, et al. Genotypes coding for mannose-binding lectin deficiency correlated with cryptococcal meningitis in HIV-uninfected Chinese patients. *J Infect Dis.* 2011;203(11):1686-91.
162. van Sorge NM, van der Pol WL, van de Winkel JG. FcγR polymorphisms: Implications for function, disease susceptibility and immunotherapy. *Tissue Antigens.* 2003;61(3):189-202.
163. van der Pol W, van de Winkel JG. IgG receptor polymorphisms: risk factors for disease. *Immunogenetics.* 1998;48(3):222-32.
164. Gillis C, Gouel-Cheron A, Jonsson F, Bruhns P. Contribution of Human FcγR to Disease with Evidence from Human Polymorphisms and Transgenic Animal Studies. *Front Immunol.* 2014;5:254.
165. Nimmerjahn F, Ravetch JV. Fc-receptors as regulators of immunity. *Adv Immunol.* 2007;96:179-204.
166. Tarasenko T, Dean JA, Bolland S. FcγRIIB as a modulator of autoimmune disease susceptibility. *Autoimmunity.* 2007;40(6):409-17.
167. Ravetch JV, Bolland S. IgG Fc receptors. *Annu Rev Immunol.* 2001;19:275-90.
168. Brownlie RJ, Lawlor KE, Niederer HA, Cutler AJ, Xiang Z, Clatworthy MR, et al. Distinct cell-specific control of autoimmunity and infection by FcγRIIb. *J Exp Med.* 2008;205(4):883-95.
169. Noel V, Lortholary O, Casassus P, Cohen P, Genereau T, Andre MH, et al. Risk factors and prognostic influence of infection in a single cohort of 87 adults with systemic lupus erythematosus. *Ann Rheum Dis.* 2001;60(12):1141-4.
170. Cervera R, Khamashta MA, Font J, Sebastiani GD, Gil A, Lavilla P, et al. Morbidity and mortality in systemic lupus erythematosus during a 10-year period: a comparison of early and late manifestations in a cohort of 1,000 patients. *Medicine (Baltimore).* 2003;82(5):299-308.
171. Bosch X, Guilabert A, Pallares L, Cervera R, Ramos-Casals M, Bove A, et al. Infections in systemic lupus erythematosus: a prospective and controlled study of 110 patients. *Lupus.* 2006;15(9):584-9.



172. Navarro-Zarza JE, Alvarez-Hernandez E, Casasola-Vargas JC, Estrada-Castro E, Burgos-Vargas R. Prevalence of community-acquired and nosocomial infections in hospitalized patients with systemic lupus erythematosus. *Lupus*. 2010;19(1):43-8.
173. Kim WU, Min JK, Lee SH, Park SH, Cho CS, Kim HY. Causes of death in Korean patients with systemic lupus erythematosus: a single center retrospective study. *Clin Exp Rheumatol*. 1999;17(5):539-45.
174. Petri M. Infection in systemic lupus erythematosus. *Rheumatic diseases clinics of North America*. 1998;24(2):423-56.
175. Gladman DD, Hussain F, Ibanez D, Urowitz MB. The nature and outcome of infection in systemic lupus erythematosus. *Lupus*. 2002;11(4):234-9.
176. Ginzler E, Diamond H, Kaplan D, Weiner M, Schlesinger M, Seleznick M. Computer analysis of factors influencing frequency of infection in systemic lupus erythematosus. *Arthritis Rheum*. 1978;21(1):37-44.
177. Cervera R, Khamashta MA, Font J, Sebastiani GD, Gil A, Lavilla P, et al. Morbidity and mortality in systemic lupus erythematosus during a 5-year period. A multicenter prospective study of 1,000 patients. *European Working Party on Systemic Lupus Erythematosus. Medicine (Baltimore)*. 1999;78(3):167-75.
178. Fessler BJ. Infectious diseases in systemic lupus erythematosus: risk factors, management and prophylaxis. *Best practice & research Clinical rheumatology*. 2002;16(2):281-91.
179. Bouza E, Moya JG, Munoz P. Infections in systemic lupus erythematosus and rheumatoid arthritis. *Infectious disease clinics of North America*. 2001;15(2):335-61, vii.
180. Iriya SM, Capelozzi VL, Calich I, Martins MA, Lichtenstein A. Causes of death in patients with systemic lupus erythematosus in Sao Paulo, Brazil: a study of 113 autopsies. *Arch Intern Med*. 2001;161(12):1557.
181. Hellmann DB, Petri M, Whiting-O'Keefe Q. Fatal infections in systemic lupus erythematosus: the role of opportunistic organisms. *Medicine (Baltimore)*. 1987;66(5):341-8.
182. Shayakul C, Ong-aj-yooth L, Chirawong P, Nimmannit S, Parichatikanond P, Laohapand T, et al. Lupus nephritis in Thailand: clinicopathologic findings and outcome

in 569 patients. *American journal of kidney diseases : the official journal of the National Kidney Foundation*. 1995;26(2):300-7.

183. Al-Hadithy H, Isenberg DA, Addison IE, Goldstone AH, Snaith ML. Neutrophil function in systemic lupus erythematosus and other collagen diseases. *Ann Rheum Dis*. 1982;41(1):33-8.

184. Bermas BL, Petri M, Goldman D, Mittleman B, Miller MW, Stocks NI, et al. T helper cell dysfunction in systemic lupus erythematosus (SLE): relation to disease activity. *J Clin Immunol*. 1994;14(3):169-77.

185. Cronin ME, Balow JE, Tsokos GC. Immunoglobulin deficiency in patients with systemic lupus erythematosus. *Clin Exp Rheumatol*. 1989;7(4):359-64.

186. Cunha BA. Infections in nonleukopenic compromised hosts (diabetes mellitus, SLE, steroids, and asplenia) in critical care. *Critical care clinics*. 1998;14(2):263-82.

187. Piliero P, Furie R. Functional asplenia in systemic lupus erythematosus. *Semin Arthritis Rheum*. 1990;20(3):185-9.

188. Iliopoulos AG, Tsokos GC. Immunopathogenesis and spectrum of infections in systemic lupus erythematosus. *Semin Arthritis Rheum*. 1996;25(5):318-36.

189. Duffy KN, Duffy CM, Gladman DD. Infection and disease activity in systemic lupus erythematosus: a review of hospitalized patients. *J Rheumatol*. 1991;18(8):1180-4.

190. Zonana-Nacach A, Camargo-Coronel A, Yanez P, Sanchez L, Jimenez-Balderas FJ, Fraga A. Infections in outpatients with systemic lupus erythematosus: a prospective study. *Lupus*. 2001;10(7):505-10.

191. Danza A, Ruiz-Irastorza G. Infection risk in systemic lupus erythematosus patients: susceptibility factors and preventive strategies. *Lupus*. 2013;22(12):1286-94.

192. Mohamed DF, Habeeb RA, Hosny SM, Ebrahim SE. Incidence and risk of infection in egyptian patients with systemic lupus erythematosus. *Clin Med Insights Arthritis Musculoskelet Disord*. 2014;7:41-8.

193. Niederer HA, Willcocks LC, Rayner TF, Yang W, Lau YL, Williams TN, et al. Copy number, linkage disequilibrium and disease association in the FCGR locus. *Hum Mol Genet*. 2010;19(16):3282-94.

194. Schwarting A. Genetic predisposition--is lupus nephritis a question of copy numbers? *Nephrol Dial Transplant*. 2006;21(9):2378-9.

195. Siriboonrit U, Tsuchiya N, Sirikong M, Kyogoku C, Bejrachandra S, Suthipinittharm P, et al. Association of Fc $\gamma$  receptor IIb and IIIb polymorphisms with susceptibility to systemic lupus erythematosus in Thais. *Tissue Antigens*. 2003;61(5):374-83.
196. Jakes RW, Bae SC, Louthrenoo W, Mok CC, Navarra SV, Kwon N. Systematic review of the epidemiology of systemic lupus erythematosus in the Asia-Pacific region: prevalence, incidence, clinical features, and mortality. *Arthritis Care Res (Hoboken)*. 2012;64(2):159-68.
197. Tsuchiya N, Kyogoku C. Role of Fc  $\gamma$  receptor IIb polymorphism in the genetic background of systemic lupus erythematosus: insights from Asia. *Autoimmunity*. 2005;38(5):347-52.
198. Chu ZT, Tsuchiya N, Kyogoku C, Ohashi J, Qian YP, Xu SB, et al. Association of Fc $\gamma$  receptor IIb polymorphism with susceptibility to systemic lupus erythematosus in Chinese: a common susceptibility gene in the Asian populations. *Tissue Antigens*. 2004;63(1):21-7.
199. Chen HS, Tsai WP, Leu HS, Ho HH, Liou LB. Invasive fungal infection in systemic lupus erythematosus: an analysis of 15 cases and a literature review. *Rheumatology (Oxford)*. 2007;46(3):539-44.
200. Yang CD, Wang XD, Ye S, Gu YY, Bao CD, Wang Y, et al. Clinical features, prognostic and risk factors of central nervous system infections in patients with systemic lupus erythematosus. *Clinical rheumatology*. 2007;26(6):895-901.
201. Hamilton KJ, Satoh M, Swartz J, Richards HB, Reeves WH. Influence of microbial stimulation on hypergammaglobulinemia and autoantibody production in pristane-induced lupus. *Clin Immunol Immunopathol*. 1998;86(3):271-9.
202. Crampton SP, Deane JA, Feigenbaum L, Bolland S. Ifih1 gene dose effect reveals MDA5-mediated chronic type I IFN gene signature, viral resistance, and accelerated autoimmunity. *J Immunol*. 2012;188(3):1451-9.
203. Mihara M, Tan I, Chuzhin Y, Reddy B, Budhai L, Holzer A, et al. CTLA4Ig inhibits T cell-dependent B-cell maturation in murine systemic lupus erythematosus. *J Clin Invest*. 2000;106(1):91-101.

204. Boonyatecha N, Sangphech N, Wongchana W, Kueanjinda P, Palaga T. Involvement of Notch signaling pathway in regulating IL-12 expression via c-Rel in activated macrophages. *Mol Immunol*. 2012;51(3-4):255-62.
205. Ray A, Dittel BN. Isolation of mouse peritoneal cavity cells. *J Vis Exp*. 2010(35).
206. Nicola AM, Casadevall A. In vitro measurement of phagocytosis and killing of *Cryptococcus neoformans* by macrophages. *Methods Mol Biol*. 2012;844:189-97.
207. Vonk AG, Wieland CW, Netea MG, Kullberg BJ. Phagocytosis and intracellular killing of *Candida albicans* blastoconidia by neutrophils and macrophages: a comparison of different microbiological test systems. *J Microbiol Methods*. 2002;49(1):55-62.
208. Walenkamp AM, Scharringa J, Schramel FM, Coenjaerts FE, Hoepelman IM. Quantitative analysis of phagocytosis of *Cryptococcus neoformans* by adherent phagocytic cells by fluorescence multi-well plate reader. *J Microbiol Methods*. 2000;40(1):39-45.
209. Sabiiti W, Robertson E, Beale MA, Johnston SA, Brouwer AE, Loyse A, et al. Efficient phagocytosis and laccase activity affect the outcome of HIV-associated cryptococcosis. *J Clin Invest*. 2014;124(5):2000-8.
210. Redlich S, Ribes S, Schutze S, Eiffert H, Nau R. Toll-like receptor stimulation increases phagocytosis of *Cryptococcus neoformans* by microglial cells. *J Neuroinflammation*. 2013;10:71.
211. Guillot L, Carroll SF, Homer R, Qureshi ST. Enhanced innate immune responsiveness to pulmonary *Cryptococcus neoformans* infection is associated with resistance to progressive infection. *Infect Immun*. 2008;76(10):4745-56.
212. Lee HS, Lee GS, Kim SH, Kim HK, Suk DH, Lee DS. Anti-oxidizing effect of the dichloromethane and hexane fractions from *Orostachys japonicus* in LPS-stimulated RAW 264.7 cells via upregulation of Nrf2 expression and activation of MAPK signaling pathway. *BMB Rep*. 2014;47(2):98-103.
213. Kasagi S, Kawano S, Okazaki T, Honjo T, Morinobu A, Hatachi S, et al. Anti-programmed cell death 1 antibody reduces CD4+PD-1+ T cells and relieves the lupus-like nephritis of NZB/W F1 mice. *J Immunol*. 2010;184(5):2337-47.

214. Voelz K, May RC. Cryptococcal interactions with the host immune system. *Eukaryot Cell*. 2010;9(6):835-46.
215. Buchanan KL, Doyle HA. Requirement for CD4(+) T lymphocytes in host resistance against *Cryptococcus neoformans* in the central nervous system of immunized mice. *Infect Immun*. 2000;68(2):456-62.
216. Mody CH, Lipscomb MF, Street NE, Toews GB. Depletion of CD4+ (L3T4+) lymphocytes in vivo impairs murine host defense to *Cryptococcus neoformans*. *J Immunol*. 1990;144(4):1472-7.
217. Koguchi Y, Kawakami K. Cryptococcal infection and Th1-Th2 cytokine balance. *Int Rev Immunol*. 2002;21(4-5):423-38.
218. Meesing A, Jittjareon A, Pornpetchpracha A, Tassaneetrithep B, Phuphuakrat A, Kiertiburanakul S. Disseminated cryptococcosis in an HIV-seronegative pregnant woman with transient T-lymphocytopenia: a case report and review of the literature. *Southeast Asian J Trop Med Public Health*. 2014;45(3):647-53.
219. Srikanta D, Santiago-Tirado FH, Doering TL. *Cryptococcus neoformans*: historical curiosity to modern pathogen. *Yeast*. 2014;31(2):47-60.
220. Zhu X, Williamson PR. Role of laccase in the biology and virulence of *Cryptococcus neoformans*. *FEMS Yeast Res*. 2004;5(1):1-10.
221. Nosanchuk JD, Valadon P, Feldmesser M, Casadevall A. Melanization of *Cryptococcus neoformans* in murine infection. *Mol Cell Biol*. 1999;19(1):745-50.
222. Nosanchuk JD, Rosas AL, Lee SC, Casadevall A. Melanisation of *Cryptococcus neoformans* in human brain tissue. *Lancet*. 2000;355(9220):2049-50.
223. Kaufman-Francis K, Djordjevic JT, Juillard PG, Lev S, Desmarini D, Grau GER, et al. The Early Innate Immune Response to, and Phagocyte-Dependent Entry of, *Cryptococcus neoformans* Map to the Perivascular Space of Cortical Post-Capillary Venules in Neurocryptococcosis. *Am J Pathol*. 2018;188(7):1653-65.
224. Weaver KF, Stokes JV, Gunnoe SA, Follows JS, Shafer L, Ammari MG, et al. Effect of Liposomal Clodronate-Dependent Depletion of Professional Antigen Presenting Cells on Numbers and Phenotype of Canine Cd4+Cd25+Foxp3+ Regulatory T Cells. *J Vet Med Res*. 2014;1(1).

225. Ward NL, Loyd CM, Wolfram JA, Diaconu D, Michaels CM, McCormick TS. Depletion of antigen-presenting cells by clodronate liposomes reverses the psoriatic skin phenotype in KC-Tie2 mice. *Br J Dermatol.* 2011;164(4):750-8.
226. Monari C, Kozel TR, Paganelli F, Pericolini E, Perito S, Bistoni F, et al. Microbial immune suppression mediated by direct engagement of inhibitory Fc receptor. *J Immunol.* 2006;177(10):6842-51.
227. Feldmesser M, Casadevall A. Mechanism of action of antibody to capsular polysaccharide in *Cryptococcus neoformans* infection. *Front Biosci.* 1998;3:d136-51.
228. Wang LR, Barber CE, Johnson AS, Barnabe C. Invasive fungal disease in systemic lupus erythematosus: a systematic review of disease characteristics, risk factors, and prognosis. *Semin Arthritis Rheum.* 2014;44(3):325-30.
229. Zhong Y, Li M, Liu J, Zhang W, Peng F. Cryptococcal meningitis in Chinese patients with systemic lupus erythematosus. *Clin Neurol Neurosurg.* 2015;131:59-63.
230. Reeves WH, Lee PY, Weinstein JS, Satoh M, Lu L. Induction of autoimmunity by pristane and other naturally occurring hydrocarbons. *Trends Immunol.* 2009;30(9):455-64.
231. Surawut S, Ondee T, Taratummarat S, Palaga T, Pisitkun P, Chindamporn A, et al. The role of macrophages in the susceptibility of Fc gamma receptor IIb deficient mice to *Cryptococcus neoformans*. *Sci Rep.* 2017;7:40006.
232. Satoh M, Reeves WH. Induction of lupus-associated autoantibodies in BALB/c mice by intraperitoneal injection of pristane. *J Exp Med.* 1994;180(6):2341-6.
233. Satoh M, Kumar A, Kanwar YS, Reeves WH. Anti-nuclear antibody production and immune-complex glomerulonephritis in BALB/c mice treated with pristane. *Proc Natl Acad Sci U S A.* 1995;92(24):10934-8.
234. Rohatgi S, Pirofski LA. Host immunity to *Cryptococcus neoformans*. *Future Microbiol.* 2015;10(4):565-81.
235. Liu TB, Perlin DS, Xue C. Molecular mechanisms of cryptococcal meningitis. *Virulence.* 2012;3(2):173-81.
236. Ngamskulrungraj P, Chang Y, Sionov E, Kwon-Chung KJ. The primary target organ of *Cryptococcus gattii* is different from that of *Cryptococcus neoformans* in a murine model. *MBio.* 2012;3(3).

237. Li Q, You C, Liu Q, Liu Y. Central nervous system cryptococcoma in immunocompetent patients: a short review illustrated by a new case. *Acta Neurochir (Wien)*. 2010;152(1):129-36.
238. Rottman JB, Willis CR. Mouse models of systemic lupus erythematosus reveal a complex pathogenesis. *Vet Pathol*. 2010;47(4):664-76.
239. Romani L. Immunity to fungal infections. *Nat Rev Immunol*. 2004;4(1):1-23.



## APPENDIX

### APPENDIX A

#### MATERIALS AND EQUIPMENT

##### Material

0.1% gold chloride (Merck, Germany)

0.22  $\mu\text{m}$  Surfactant-free cellulose acetate membrane filters (Minisart, Sartorius Stedim Biotech GmbH, Germany)

0.25% Trypsin in 1 mM EDTA (Hyclone, USA)

0.4% Trypan blue solution (Hyclone, USA)

1X GolgiPlug (Biolegend, USA)

2x Master Mix (Invitrogen, USA).

95% alcohol (Liquor distillery organization excise department, Thailand)

96-Well Flat-bottom tissue culture plates (Nunclon D, Denmark)

Absolute alcohol (Merck, Germany)

Agarose

anti-F4/80, anti-CD11b, anti-CD4, anti-CD8, anti-CD69, anti-CD44, anti-CD62L, anti-IFN- $\gamma$  (Biolegend, USA)

Ammonium chloride ( $\text{NH}_4\text{Cl}$ ) (Sigma-Aldrich, USA)

Barrier tips; 20, 100, 200, and 1,000  $\mu\text{l}$  (Neptune, Mexico)

Beta-mercaptoethane (Sigma-Aldrich, USA)

Bovine serum albumin (BSA) (Sigma-Aldrich, USA)

Bradford protein assay (Thermo Scientific, USA).

Calf Thymus DNA (Invitrogen, USA).

CD4<sup>+</sup> T Cell Isolation Kit, (Miltenyi biotec, Auburn, CA, USA).

Cell strainer (Nylon 70  $\mu\text{m}$ , Falcon)

Conical centrifuge tube; 15, 50 mL (Nunc, USA)

Clodronate-liposome (Encapsula Nanoscience, USA)

Cryovial (Nunc, Denmark)

DMEM medium (Hyclone, USA)

Diff-Quick stain (Life Science Dynamic Division, Nonthaburi, Thailand).

Dimethyl sulfoxide (DMSO) (Sigma-Aldrich, USA)

Disodium hydrogen phosphate ( $\text{Na}_2\text{HPO}_4$ ) (Sigma-Aldrich, Germany)

EDTA (Merck, Germany)



EnzyChrom ALT assay (BioAssay, USA)  
Eosin (Merck, Germany)  
Fetal bovine serum (Hyclone, USA)  
Glycerol (Merck, Germany)  
Hemocytometer (Bright line) (BOECO, Germany)  
Hematoxylin (Merck, Germany)  
HEPES (Hyclone, USA)  
Horse serum (Hyclone, USA)  
L-3, 4-dihydroxyphenylalanine or DOPA (Sigma-Aldrich, USA)  
Methenamine silver solution (Merck, Germany)  
Mouse TNF- $\alpha$ , IL-6, IL-10, IL-12p70 ELISA kit (eBioscience, USA)  
HRP conjugated goat anti-mouse isotype specific antibodies (BioLegend, USA)  
IFN- $\gamma$  (10 ng/ml final concentration; BioLegend, USA)  
Ionomycin (Sigma-Aldrich, USA)  
LPS (100 ng/ml final concentration; Sigma-Aldrich)  
Microcentrifuge tube (Eppendorf, USA)  
MTS assay (Promega Corporation, USA)  
Peroxidase-conjugated goat anti-mouse antibodies (BioLegend, USA)  
PMA (Sigma-Aldrich, USA)  
Proteinase K (Invitrogen, USA).  
Potassium hydrogen carbonate (KHCO<sub>3</sub>) (Sigma-Aldrich, USA)  
QuantiChrom Creatinine Assay (BioAssay, USA)  
Sabouraud Dextrose Agar (Difco, USA)  
Sodium dodecyl sulfate (SDS) (Sigma-Aldrich, USA)  
Serological pipettes; 5, 10, and 25 mL (Corning, USA)  
Sodium bicarbonate (NaHCO<sub>3</sub>) (Sigma-Aldrich, Germany)  
Sodium carbonate (Na<sub>2</sub>CO<sub>3</sub>) (Sigma-Aldrich, Germany)  
Sodium chloride (NaCl) (Sigma-Aldrich, Germany)  
Sodium dihydrogen phosphate (NaH<sub>2</sub>PO<sub>4</sub>) (Sigma-Aldrich, Germany)  
Sodium Pyruvate (Hyclone, USA)  
Streptomycin/Penicillin G (Hyclone, USA)  
Sulfuric acid (H<sub>2</sub>SO<sub>4</sub>) (Sigma-Aldrich, Germany)  
Syringe (Nipro, Thailand)  
Tissue culture flask; 25, 75 cm<sup>2</sup> (Nunc, Denmark)  
Tissue culture plates; 6, 12, 24 and 96 wells (Nunc, Denmark)  
TMB Substrate Set (BioLegend, USA)

Tris (Sigma-Aldrich, Germany)

Tween20 (Merck, Germany)

Urea agar (Difco, USA)

Xylene (Merck, Germany)

### Equipments

CytoSpin chamber (Thermo Scientific, USA)

-20°C Freezer (Sanyo, Japan)

-80 °C Freezer (Sanyo, Japan)

Autoclave (Hirayama, Japan)

Auto pipette: P-20, P-100, P-200, P-1000 (Gilson, France)

Auto pipette: P-10, P-1000 (Socorex, Switzerland)

Biological safety cabinet (Astec-Microflow, Bioquell UK Ltd, UK)

Bio Rad Trans-Blot SD Semi Dry Transfer (Bio-Rad, PA, USA)

ChemiDoc™XRS (Bio-Rad Laboratories, Inc, USA)

CO<sub>2</sub>incubator (BINDER GmbH, Germany)

Electrophoresis (Wealtec, Taiwan)

Eppendorf Master Cycler Gradient Thermal Cycler (Germany)

Equipment gel electrophoresis apparatus (Bio-Rad Laboratories)

Fireboy (IBS, Switzerland)

Hemocytometer (Boeco, Germany)

Heat block (Scientific Industries, Inc, USA)

Hotplate (Stuart, Germany)

Incubator (Mettler GmbH, Germany)

Inverted microscope (Olympus, Japan)

LightCycler 2.0 Instrument (Roche, Germany)

Micropipettes (Gilson, France)

Multi-channel pipette (Socorex, Switzerland)

NanoDrop™ 1000 Spectrophotometer (Thermo Fisher Scientific, Inc, USA)

pH meter (Thermo Fisher Scientific, Inc, USA)

Refrigerated centrifuge (Sanyo, Japan)

Safety cabinet (Augustin, Thailand)

Spectrophotometer (Bio-Rad Smart Spec™ Plus, Bio-Rad Laboratories, Inc,USA)

Vertical Laminar Flow workstation (Microflow, UK)

Ultrasonic water bath (GEN-PROBE, Germany)

Water bath (MemMert GmbH, Germany)

UV Transilluminator (Bio-Rad, USA)

### Software and programs

EndNote X7.7.1

Flow Jo v.10

GraphPad Prism 6.0

SPSS 11.5 software

G-power 3.0.10

Adobe Illustrator CS3



**APPENDIX B**  
**MOUSE GENOTYPING**

**1. DNA extraction**

**1.1 Reagent**

Lysis solution: 20mM NaCl, 20mM EDTA, 40mM Tris-HCl pH 8.0, 0.5% SDS, 0.5% Beta-mercaptone

5M NaCl	20 ml
0.5M EDTA	20 ml
1M Tris	20 ml
10% SDS	25 ml
Beta-mercaptone*	2.5 ml
Distilled water	412.5 ml

\* Beta-mercaptone should be added to solution prior to use

Proteinase K: 20 mg/ml in H<sub>2</sub>O

Saturated NaCl (approximately 6 M)

**1.2 Protocol**

- (1) Lyse the cells or mouse tail or ear piece in 500  $\mu$ l of lysis solution. Add 20  $\mu$ l of proteinase K (20mg/ml).
- (2) Incubate at least 4-6 hours at 55°C. (prefer overnight)
- (Optional; Add 250  $\mu$ l of saturated NaCl shake well for 10 secs and let it stand for 15 min on ice)
- (3) Centrifuge 10 to 15 min at 13,000 rpm, room temperature.
- (4) Transfer the clear DNA solution (supernatant) into a clean tube and precipitate it with 750  $\mu$ l of ethanol.
- (5) Pellet gently by spinning at room temp (13,000 rpm, 15 min).
- (6) Wash the DNA precipitate with 70% ethanol and air dry.
- (7) Dissolve it in 100  $\mu$ l TE or DW. DNA can be put into solution rapidly by soaking tubes at 55°C for 15 min.

## 2. PCR for FcγRIIb<sup>-/-</sup> genotyping

### 2.1 PCR mixture preparation

Calculation and aliquot PCR composition as following table in 1.5 ml microcentrifuge tube

PCR Mixture	μl/samples
2x Master Mix (μl)	7.5
dH <sub>2</sub> O	4.5
10 μM FcREC1	0.38
10 μM OL4143	0.38
10 μM OL4080	0.75
	13μl/sample
Mouse DNA	2

Primer:

FcREC1-Forward: 5'-AAGGCTGTGGTCAAACCTCGAGCC-3'

OL4143: 5'-CTCGTGCTTTACGGTATCGCC -3'

OL4080: 5'-TTGACTGTGGCCTTAAACGTGTAG -3'

### 2.2 PCR condition

Set Thermal cycler machine as show in table

Table 1. PCR condition for mouse genotyping

Step	Temperature (C°)	Time	Cycles
1.	98	3 min	
2.	98	30 sec	35 cycles
3.	60	30 sec	
4.	72	60 sec	
5.	72	5 min	
6.	4	forever	

### 3. Gel electrophoresis

The PCR products were run on agarose gel by using 4 $\mu$ l PCR product with 1  $\mu$ l loading dye and run on 2% agarose gel with 80V for 60 min. The Fc $\gamma$ R11b+/+ or wildtype mice should give 173 bp only, Fc $\gamma$ R11b+/- or heterogenous mice should give 173 bp and 232 bp products. However, Fc $\gamma$ R11b-/- or knockout mice should give only 232 bp as show in figure1.

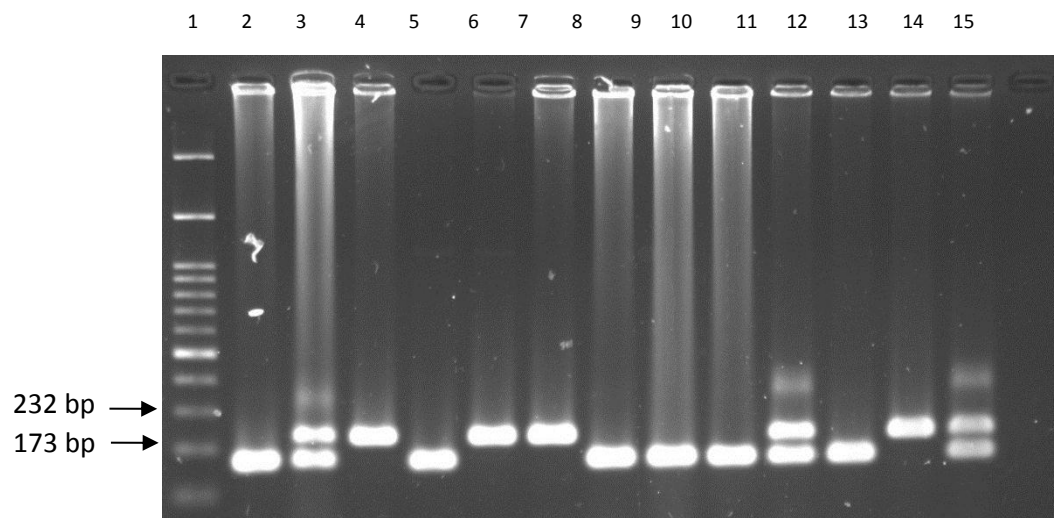


Figure 1. Representative result from Fc $\gamma$ R11b genotyping

Lane 1: DNA ladder; 2: Fc $\gamma$ R11b+/+ or wildtype mouse; 3: Fc $\gamma$ R11b+/- or heterogenous mouse; 4: Fc $\gamma$ R11b-/- or knockout mouse; 5: Fc $\gamma$ R11b+/+; 6: Fc $\gamma$ R11b-/-; 7: Fc $\gamma$ R11b-/-; 8: Fc $\gamma$ R11b+/+; 9: Fc $\gamma$ R11b+/+; 10: Fc $\gamma$ R11b+/+; 11: Fc $\gamma$ R11b+/-; 12: Fc $\gamma$ R11b+/+ positive control; 13: Fc $\gamma$ R11b-/- positive control; 14: Fc $\gamma$ R11b+/- positive control; 15: Distilled water negative control

(Saiworn W, et al. Calcif Tissue Int. 2018;103(6):686-97.)

## APPENDIX C

### ANTI-DOUBLE STAND DNA PRODUCTION IN MICE

#### ELISA to measure serum levels of murine anti-dsDNA antibodies

##### 1.Reagent

###### 1.1 Coating solution pH 9.5

Na<sub>2</sub>CO<sub>3</sub> 0.356g

NaHCO<sub>3</sub> 0.84g

Distilled water 100 ml

###### 1.2 Washing solution

0.05% Tween-20 in PBS

###### 1.3 Blocking solution

5%FBS and 3%BSA in PBS+0.1% Tween-20

##### 2.Protocol

- (1) Dilute antigen using coating buffer (from stock Calf Thymus DNA solution 10mg/ml, Invitrogen, lot no.1508585, ref no.15633-019).
- (2) Add 100 µg/ml calf DNA (10mg/ml) to a 96-well microtest assay plate.
- (3) Wrap the plate with plastic wrap and incubate at 4 C for overnight.
- (4) Discard the coating antibody solution and wash the plate with washing solution 5 times.
- (5) Dry the plate and add 100 µl of blocking solution per well to the plate.
- (6) Incubate the plate at room temperature (RT) for 1.5 h with shaking.
- (7) Discard the blocking solution and wash the plate with washing solution 5 time.
- (8) Dilute the mouse serum in blocking solution (dilute1:100, if mice age of 6m use 1:400).
- (9) Add 100 µl/well of diluted serum in duplicates to the plate. Serum should be diluted in 1%BSA in PBS and titration is required to achieve optimal detection (1:100)
- (10) Incubate the plate at RT for 1 h with shaking.
- (11) Discard the diluted serum and wash the plate with washing solution 5 times.

(12) Add 100  $\mu\text{L}$ /well of HRP conjugated goat anti-mouse isotype specific antibodies (Cat.405306, 500  $\mu\text{L}$ , BioLegend) (1/4,000 in blocking solution) to the plate and incubate at RT for 1 h with shaking.

(13) Discard the secondary antibodies and wash the plate with washing solution 5 times.

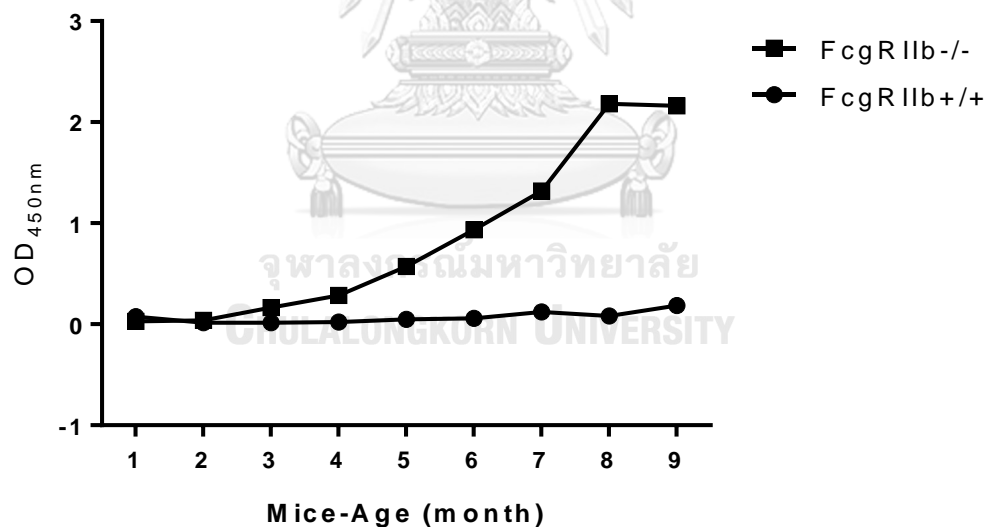
(14) Add 100  $\mu\text{L}$ /well of 1:1 mix of ABTS Peroxidase Substrate Solution A and B (TMB Substrate Set, Cat.421101, BioLegend) to the plate.

(15) Develop the plate at RT in dark. Incubation times will vary depending on your assay (10minutes).

(16) Stop the reaction by adding 100  $\mu\text{L}$ /well of ABTS Peroxidase Stop Solution (2N H<sub>2</sub>SO<sub>4</sub>)

(17) Read the plate using an ELISA reader with a wavelength of 450nm

### 3. Determination of anti-dsDNA production by Fc $\gamma$ R IIb<sup>+/+</sup> and Fc $\gamma$ R IIb<sup>-/-</sup>





**APPENDIX D**  
**THE HISTOLOGY STAINING**

**1. Hematoxylin and Eosin staining**

- (1) Deparaffin by add slide in xylene jar for 3 jars, each jar for 10 min.
- (2) Add slide in 95% alcohol for 3 jars, each jar for 20 second.
- (3) Soak in bowl with water running for 2-3 min (Beware slide drying)
- (4) Staining step, add slide in hematoxylin jar for 3 min.
- (5) Running water for 3 min.
- (6) Dip slide in 95% alcohol for 10 dip.
- (7) Add slide in eosin jar for 3 min.
- (8) Dip in 95% alcohol for 10 dip.
- (9) Dip in 95% alcohol for 10 dip.
- (10) Dip in absolute alcohol for 10 dip.
- (11) Dip in absolute alcohol for 10 dip.
- (12) Dip in xylene for 10 dip.
- (13) Dip in xylene for 10 dip.

**2. Microwave G.M.S. staining (Grocott-Gomori's or Gömöri methenamine silver)**

- (1) Deparaffin by add slide in xylene jar for 3 jars, each jar for 10 min
- (2) Add silde in 95% alcohol for 3 jars, each jar for 20 second.
- (3) Soak in bowl with water running for 2-3 min (Beware slide drying)
- (4) Add slide in 5% chromic acid, heat for 10 sec. wait at RT for 30 sec.
- (5) Running water 1 min.
- (6) Wash with distilled water.
- (7) Add slide in methenamine silver solution (fresh prepare).  
Heat for 10 sec. wait at RT for 30 sec.  
Heat for 20 sec. wait at RT for 30 sec.  
Heat for 10 sec. wait at RT for 30 sec.
- (8) Slide present black-brown color and rised with distilled water
- (9) Dip slide in 0.1% gold choride 1-2 dip

- (10) Wash with distilled water
- (11) Add slide in light green for 5 min
- (12) Wash with distilled water
- (13) Dehydrate slide (95%alcohol, absolute alcohol, absolute alcohol, xylene, xylene)
- (14) Mounting slide and examine slide by fungi present gray to black; background present green color.



**APPENDIX E**  
**BONE MARROW DERIVED MACROPHAGE**

**1. Media preparation**

\*All media ingredients using Hyclone, USA

**1.1 DMEM completed media**

DMEM serum free media (high glucose)	100 ml
FBS	10 ml
HEPES	1 ml
Sodium Pyruvate	1 ml
Step/PenG	1 ml

**1.2 BMM media**

DMEM completed media	80 ml
L929 culture supernatant	20 ml
Horse serum	5 ml

**1.3 Preparation of BM macrophage freezing media**

- DMEM (without serum) + 20% FBS
- DMEM (without serum) + 20% FBS+ 20%DMSO
- Add 500 ul of (1) and follow by adding 500 µl of (2)

**2. L929 culture supernatant preparation**

NCTC clone 929 (L cell, L929, derivative of Strain L) (ATCC)

(1) Thaw cells by using DMEM serum free media and plate cells on TC culture flask

Pass cells by using Trpsin-EDTA

(2) Culture cells in 8 ml of DMEM completed media in 5% CO<sub>2</sub>, 37°C

(3) Cells should be grown at 70-80% confluent before passage or collection of supernatant

- (4) Filtrate supernatant using 0.2  $\mu\text{m}$  filter
- (5) Freeze cells by using 10%DMSO in DMEM completed media, keep in  $-80^{\circ}\text{C}$  for overnight before transferring to liquid  $\text{N}_2$  for long storage

### 3. Ammonium chloride lysis (Red Blood Cell lysis buffer)

$\text{KHCO}_3$	0.5	g
$\text{NH}_4\text{Cl}$	4.15	g
EDTA	0.018	g

Made up to 500 ml in distilled water

Autoclave before use.

Resuspend cell in 1 ml media and add to 9 ml lysis buffer (1:10)

Stand for 3 min (red cell lysis will be visible) and pellet cell.

### 4. Protocol

- (1) Mice were sacrificed for femur bone.
- (2) Bone were suspended in DMEM serum free on petri dish and use gaze to eliminate the remaining muscle
- (3) Bone were resuspended in DMEM serum free in 15 ml centrifuge tube on ice to transfer to tissue culture room
- (4) Pour all bones and media on petri dish in laminar flow
- (5) Prepare 0.5 ml microcentrifuge (small) tube with a pore at the bottom of tube and then put this tube in 1.5 ml microcentrifuge (big) tube (all is steriled before use). All tubes are on ice.
- (6) Use scissors to cut the bone on header and footer of bone and put a piece of bones in microcentrifuge tube with pore
- (7) Centrifuge at 6,000 rpm, 10 min,  $4^{\circ}\text{C}$ . Bone marrow cells will be pelleted on bottom of 1.5 ml microcentrifuge tube with red color (red blood cell)
- (8) Add 1ml of DMEM in cell pellet and dispersed by pipette up and down.
- (9) To eliminate red blood cell, prepare 9ml Red Blood Cell lysis (RBC lysis or  $\text{NH}_4\text{Cl}$  solution) in 15 ml centrifuge tube

- (10) Add 1 ml of cell suspension in 9ml RBC lysis and incubate for 5 min on ice
- (11) Centrifuge 1,000 rpm, 10min, 4°C and discard supernatant (cell pellet should be no red color of RBC, if see some red should be treat again)
- (12) Add BMM media 1ml/pellet and dispersed by pipette up and down and pool cell suspension in 50 ml centrifuge tube on ice
- (13) Count bone marrow (BM) cell with 0.4% trypan blue (cell 4 in trypan 16 µl, dilution factor is 5)
- (14) Plate cell on petri dish at  $5 \times 10^6$  cells/plate in 8 ml BMM media
- (15) Incubate at 37°C, 5%CO<sub>2</sub>
- (16) Add fresh BMM 3ml on day 4 of incubation
- (17) Harvest bone marrow derived macrophage on day7 of incubation by using cold-PBS
- (18) Count the cell and feed into tissue culture well plate for your experimental design.



## APPENDIX F

### SPLENOCYTES ISOLATION

#### Splenocytes isolation

##### 1. Preparation of ACK lysis buffer (RBC lysis buffer)

NH <sub>4</sub> Cl	8.26 g
KHCO <sub>3</sub>	1 g
EDTA	0.037 g
Distilled water	1000 ml

Mix well and autoclave. Store up to 6 months at room temperature or 4°C. RBC lysis buffer should always be used at room temperature.

##### 2. Protocol (no enzymatic digestion)

- (1) Take a 6-well plate and add 10ml of ice-cold PBS into individual well. (one well per one tissue)
- (2) Place a strainer (Nylon 70 um, Falcon) into each well.
- (3) Clip the spleen into several pieces with scissors.
- (4) Use the plunger to gently mesh the tissue over the strainer.
- (5) Remove the strainer and transfer cell sample into 15 ml conical tube.
- (6) Centrifuge 1200 rpm, 5 min, 4°C
- (7) Aspirate out the supernatant, and flick the bottom of the tube to disperse cells.
- (8) Resuspend cells in ACK lysis buffer. Normally use 4 ml for regular sized spleen (70-100 mg), 4 ml for BM, and 2 ml for the thymus.
- (9) Incubate cells in ACK for 5 min, RT
- (10) Add 10 ml of PBS or medium to stop the lysis.
- (11) Spin 1200 rpm, 5 min, 4°C
- (12) Remove the supernatant.
- (13) Flick the bottom of the tube to disperse cells.
- (14) Resuspend cells in 10 ml of appropriate buffer and count it.

\*Tissues and cells should be processed at 4°C if not indicated

**APPENDIX G**  
**CULTURE MEDIA**

**1. Sabouraud Dextrose Agar**

Pancreatic digest of casein	5.0 g
Peptic digest of animal tissue.	5.0 g
Dextrose	40.0 g
Agar	15.0 g
Distilled water	1000 ml

**2. Urea Agar Slants**

Digest of gelatin	1.0 g
Dextrose	1.0 g
Sodium chloride	5.0 g
Potassium phosphate	2.0 g
Urea	20.0 g
Phenol red	0.012g
Agar	15.0 g
Distilled water	1000 ml

**3. L-3, 4-dihydroxyphenylalanine or DOPA medium**

Flask I	
Sabouraud dextrose agar	4 g
Potato dextrose agar	4 g
Agar power	6 g
Tween 80	80 $\mu$ l
Distilled water	280 ml
Flask II	
Caffeic acid (avoid light)	0.2 g
Distilled water	120 ml

Autoclaved flask I and II, mix together, pour plate and wrap plate with aluminum foil to avoid light

## APPENDIX H

### CELL VIABILITY BY MTT ASSAY

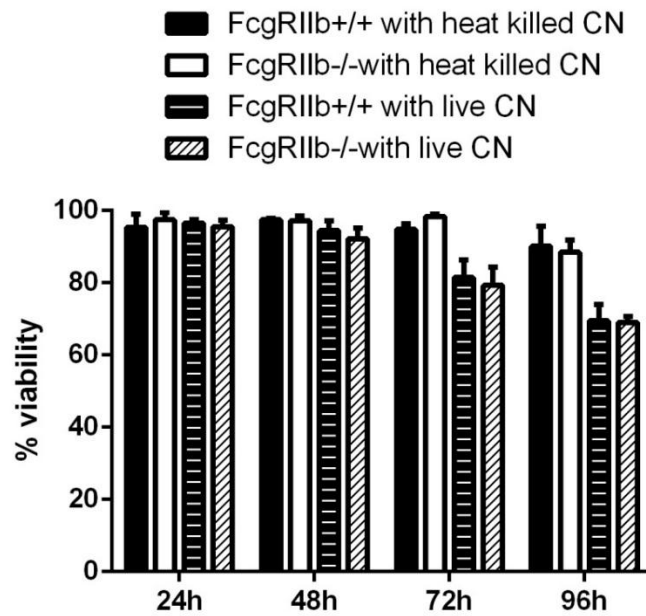


Figure H1. Percent cell viability by MTT assay. Bone marrow derived macrophages were generated from FcγRIIb+/+ and FcγRIIb-/- mice, the macrophages were challenged with *C. neoformans* MOI 5:1 for 24-96 h.



## VITA

**NAME** Saowapha Surawut

**DATE OF BIRTH** 9 July 1983

**PLACE OF BIRTH** Bangkok, Thailand

**HOME ADDRESS** 5/99 Moo.9, Thachang, Mueng, Chanthaburi, 22000

**PUBLICATION** Surawut S, Ondee T, Taratummarat S, Palaga T, Pisitkun P, Chindamporn A, et al. The role of macrophages in the susceptibility of Fc gamma receptor IIb deficient mice to *Cryptococcus neoformans*. *Sci Rep.* 2017;7:40006.

Surawut S, Makjaroen J, Thim-Uam A, Wongphoom J, Palaga T, Pisitkun P, et al. Increased susceptibility against *Cryptococcus neoformans* of lupus mouse models (pristane-induction and FcGR11b deficiency) is associated with activated macrophage, regardless of genetic background. *J Microbiol.* 2018.